DEVELOPMENT OF NEW DYE SENSITIZED MATERIALS FOR SOLAR CELL APPLICATIONS

BY

Umer Mehmood

A Dissertation Presented to the

DEANSHIP OF GRADUATE STUDIES

KING FAHD UNIVERSITY OF PETROLEUM & MINERALS

DHAHRAN, SAUDI ARABIA

In Partial Fulfillment of the
Requirements for the Degree of

DOCTOR OF PHILOSOPHY

In

CHEMICAL ENGINEERING

May, 2015

KING FAHD UNIVERSITY OF PETROLEUM & MINERALS

DHAHRAN- 31261, SAUDI ARABIA

DEANSHIP OF GRADUATE STUDIES

This thesis, written by **Umer Mehmood** under the direction his thesis advisor and approved by his thesis committee, has been presented and accepted by the Dean of Graduate Studies, in partial fulfillment of the requirements for the degree of **DOCTOR OF PHILOSOPHY IN CHEMICAL ENGINEERING.**

Dr. Ibnelwaleed Ali Hussein
(Advisor)

Dr. Mohammded Ba-Shammakh
Department Chairman

Dr. Khalil Harrabi
(Co-Advisor)

Dr. Salam A. Zummo
Dean of Graduate Studies

15/6/15
Date

Dr. Mohammded Ba-Shammakh
(Member)

Dr. Reyad A. Shawabkeh
(Member)

Dr. Shakeel Ahmed
(Member)

DEVELOPMENT OF NEW DYE SENSITIZED MATERIALS FOR SOLAR CELL APPLICATIONS

Umer Mehmood

CHEMICAL ENGINEERING DEPARTMENT

May 2015

KING FAHD UNIVERSITY OF PETROLEUM & MINERALS

DHAHRAN- 31261, SAUDI ARABIA

DEANSHIP OF GRADUATE STUDIES

This thesis, written by **Umer Mehmood** under the direction his thesis advisor and approved by his thesis committee, has been presented and accepted by the Dean of Graduate Studies, in partial fulfillment of the requirements for the degree of **DOCTOR OF PHILOSOPHY IN CHEMICAL ENGINEERING.**

_____

Dr. TYPE NAME
(Advisor)

_____

Dr. TYPE NAME
Department Chairman

_____

Dr. TYPE NAME
(Co-Advisor)

_____

Dr. Salam A. Zummo
Dean of Graduate Studies

_____

Dr. TYPE NAME
(Member)

_____
Date

_____

Dr. TYPE NAME
(Member)

_____

Dr. TYPE NAME
(Member)

Dedicated to my beloved parents

Mrs. & Mr. Mehmood Ahmed

Dedicated to my beloved brothers and sisters

Dedicated to my friends and those who love me more than anything

ACKNOWLEDGMENTS

I express my gratitude and praise to ALMIGHTY ALLAH, the creator of universe, who is beneficent and merciful, guided us in difficult and congeal circumstance, who endowed us with the will to complete this project. Great respect our Holy Prophet Hazrat Muhammad (PBUH), who taught us to learn till lap of grave.

I am highly thankful to Department of chemical Engineering, King Fahad University of Petroleum and Minerals (KFUPM), Saudi Arabia for awarding me scholarship to pursue my PhD. Special thanks to King Abdul-Aziz City for Science and Technology (KACST) through the Science & Technology Unit at King Fahd University of Petroleum & Minerals (KFUPM) for funding this work through project # 11-ENE1635-04 as part of the National Science, Technology and Innovation Plan (NSTIP).

I express my sincere thanks to my advisor Prof. Ibnelwaleed Ali Hussein for supervising my research. Without his technical and moral support I would not have been able to complete my work. My hearties thanks to my committee members: Dr.Shakeel Ahmed, Dr. Khalil Harrabi, Dr. **Reyad A. Shawabkeh and Dr. Mohammded Ba-Shammakh for their useful comments and suggestion. I am thankful to** Dr. Amir Al Ahmed and Mr. Mogtaba B. Mekki for helping me in the experimentation. I would also like to thank to Dr. Saleem (former advisor) and Dr. Nouar tabet for their helpful suggestions. Special thanks to Dr.Ghulam Mustafa Mamoor from University of Engineering and Technology (UET), Lahore, Pakistan for guiding me in my research. I would also like to acknowledge the Center of Research Excellence for Renewable Energy at KFUPM for providing me the laboratory facility.

Last but not least, thanks to my parents, brothers, sisters and friends in my country prayed day and night for my success

TABLE OF CONTENTS

LIST OF TABLES

LIST OF FIGURES

ABSTRACT

Full Name : [UMER MEHMOOD]

Thesis Title : [DEVELOPMENT OF NEW DYE SENSITIZED MATERIALS FOR SOLAR CELL APPLICATIONS]

Major Field : [CHEMICAL ENGINEERING]

Date of Degree : May, 2015]

Solar cells based on organic materials are among the promising candidates for the implementation of the next generation of solar cells. For their advantage, to be flexible compared to the counterpart based on silicon. Its synthesis might be achieved with low cost; however its efficiency remains a challenging issue to be deeply studied and improved. It becomes the focus of optimizing many parameters as: the adequate use of the polymer, the efficient way of collecting the generated electron-hole; which is the aim of this proposal.

Dye-sensitized solar cells (DSCs) constitute a novel class of hybrid organic solar cells. Organic donor-π-acceptor dyes are an interesting alternative to the standard metal-organic complexes used in DSCs. This provides the solar cell flexibility and may make them inexpensive. The aim is to design and synthesize novel Donor- π-Acceptor molecules in order to increase the efficiency of organic solar cells. Efficient photovoltaic conversion and stable performance could be demonstrated with few classes of donor systems, such as diphenylamine, diuorenylaminophenyl, coumarin etc. It has been concluded that Cyano Acrylic acid is one of the best acceptor group. Therefore, to synthesize a novel series of Donor Acceptor Based Organic molecules to screen their efficiency in solar applications we couple few different donor and π-conjugated bridges to cyano acrylic acid in a different fashion. After the synthesis of the organic molecules, solar cells will be fabricated, tested and compared with the existing commercial solar cells. After the synthesis of the organic molecules by our collaborators in India, systematic studies and characterization of the molecules are going to be carried out by our team at KFUPM Laboratories. Results will be published and presented in international conferences..

Keywords: Dye-sensitized solar cells; solar cell performance, organic solar cells

ملخص الرسالة

الاسم الكامل: عمر محمود

عنوان الرسالة: تطوير مواد صباغة توعية جديدة لتطبيقات الخلايا الشمسية

التخصص: هندسة كيميائية

تاريخ الدرجة العلمية: : مايو 2015

. من مزاياها أنها مرنه مقارنة مع نظيراتها المبنية من السيلكون. كما يمكن تصنيعها بتكلفه اقل، ولكن تبقى كفاءتها وطرق تحسينها مسألة تحتاج لمزيد البحث و الدراسة. أصبح تحسين الكفاءة يعتمد على عدة محاور منها: الاستخدام الملائم للمواد العضوية (اللبوليمر) ، وإيجاد وسائل فعالة لجمع الشحنات المولدة، الذي هو الهدف من هذا المشروع.

الخلايا الشمسية الصبغية (DSSCs) تشكل فئة جديدة من الخلايا الشمسية العضوية المختلطة. المواد العضوية المانحة-π- المتقبلة الأصباغ تعتبر من البدائل المهمة للمركبات المعدنية-العضوية المستخدمة في الخلايا الشمسية الصبغية (DSSCs) . وهذا يوفر مرونة الخلايا الشمسية، ويجعل إنتاجها غير مكلف. الهدف من هذا المشروع هو تصميم وتركيب جزيئات مانحة-π- متقبلة جديدة من أجل زيادة كفاءة الخلايا الشمسية العضوية.

كفاءة التحويل الكهروضوئية العالية والأداء المستقرة يمكن الحصول عليها مع فئات قليلة من النظم المانحة مثل (diphenylamine) ، (diuorenylaminophenyl) ، (coumarin) الخ... وقد خلصت الدراسة إلى أن حمض الاكريليك , (Cyano Acrylic Acid) هو واحد من أفضل المجموعة المتقبلة. لذلك ، لتركيب سلسلة جديدة من الجزيئات العضوية المانحة- المتقبلة لمعرفه كفاءتها في تطبيقات الطاقة الشمسية، سنعمل على مزاوجة أعداد مختلفة من المانحة و π - الجسور المترافق لحمض الاكريليك (Cyano Acrylic Acid) بطرق مختلفة.

بعد تركيب الجزيئات العضوية ، سيتم تصنيع الخلايا الشمسية واختبار كفاءتها ومقارنتها مع الخلايا الشمسية التجارية القائمة. بعد تركيب الجزيئات العضوية من قبل المتعاونين لدينا في الهند، الدراسة المنهجية لهذه الجزيئات العضوية و معرفة خصائصها سوف تنفذ من قبل فريقنا في مختبرات جامعة الملك فهد. وسيتم نشر النتائج وتقديمها في المؤتمرات الدولية.

كلمات البحث: صبغ الخلايا الشمسية؛ أداء خلايا الطاقة الشمسية, خلايا الطاقة الشمسية العضوي

CHAPTER 1

INTRODUCTION

1.1.Energy

Energy is the driving force for development, economic growth, automation, and modernization. Energy usage and demand are increasing globally and researchers have taken this seriously to fulfill future energy demands [1,2]. At present global energy sources are mainly dependent on fossil fuels and the use of fossil fuel is the main reason for global increases of CO_2 amount [3]. According to global carbon emissions sources [4], carbon dioxide emissions from coal, oil, natural gas, cement, and gas flaring were 43%, 33%, 18%, 5.3%, and 0.6%, respectively in 2012. Emissions of greenhouse gases grew 2.2% per year between 2000 and 2010, compared with 1.3% per year from 1970 to 2000 [5].The world is not capable of absorbing large amounts of CO_2 at the rate it is produced by fossil fuels. As a result, increasing the volume of CO_2 in the environment has increased global warming and further climate change. Global warming and climate changes are challenging all over the world. The use of renewable energy provides benefits that reduce emissions of air pollutants as well as greenhouse gases.Therefore, alternative sources of energy are needed so that mankind can survive on the earth without depending on fossil fuels. Solar energy is one of the renewable energy sources that will contribute to the security of future energy supplies [6,7] . Today, only 13% of energy comes from renewable sources (biofuel and waste 10%, hydro 2.3% and others: solar,

wind, geothermal, heat, among others 0.9%), 81% fossil fuels (oil 32.4%, natural gas 21.4%, and coal 27.3%), and 5.7% nuclear power. Fig. 1 shows the worldwide sources of total primary energy supply in 2010 [5].

1.2.Solar energy distribution in Saudi Arabia

It is common knowledge that solar radiation is unevenly distributed, and that it varies in intensity from one geographic location to another depending upon the latitude, season, and time of day.Saudi Arabia lies between latitudes 31^{o} N and 17.5^{o} N and longitudes 50^{o} E and 36.6^{o} E. The land elevation varies between 0 and 2600 m above the mean sea level. Complex terrain is found in the southwest region of the Kingdom. The East and the West coasts of the Kingdom are located on the Arabian Gulf and Red Sea, respectively. Mainly two seasons, winter and summer, are observed during the year. The vast open land experiences high intensities of solar radiation and long hours of sunshine duration [8]. The seasonal variation of global solar radiation over Saudi Arabia is shown in Fig-2. Solar radiation from the sun is approximately 3×10^{24} J per year, which is ten times the current energy demands [9]. Light from the sun can be harvested by dye-sensitized solar cells (DSSCs). DSSCs have attracted considerable attention due to an ideal compromise between efficiency and cost-performance [10–12]. The major component of the DSSCs is a dye. Its function is to absorb incoming sunlight and produce excitons. It is chemically bonded to the porous surface of the semiconductor.

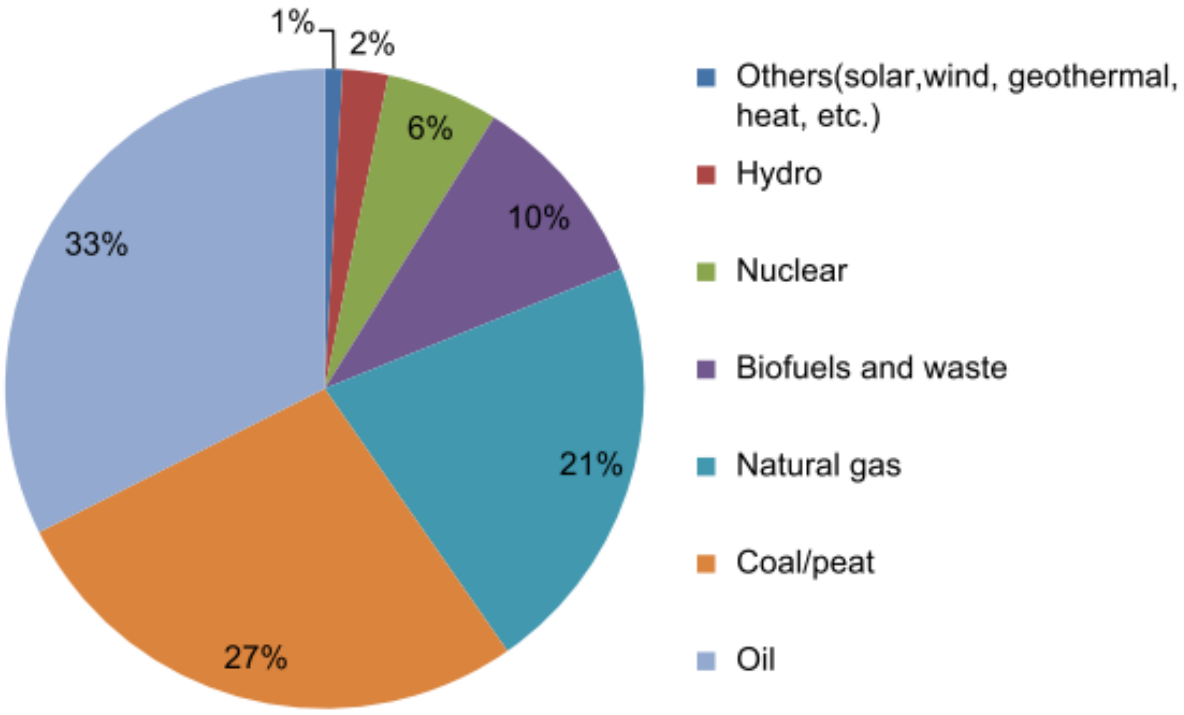

Fig 1.1: Shows the sources of world total primary energy supply 2010

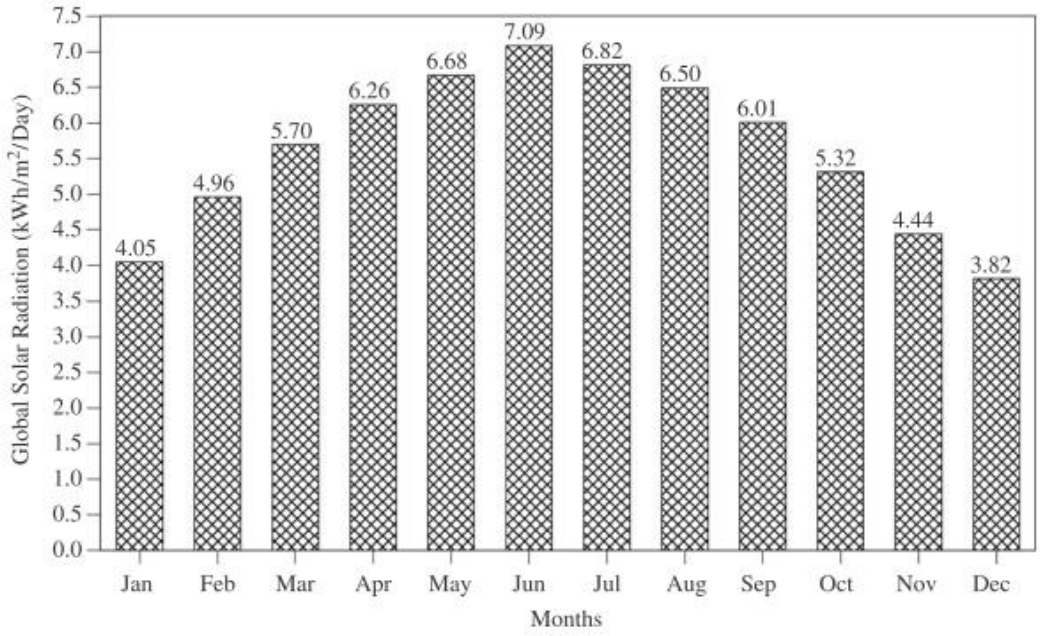

Fig 1.2:Seasonal variation of global solar radiation over Saudi Arabia [8]

1.3.Quantum Mechanical Modeling

We used density functional theory (DFT) and time dependent DFT quantum mechanical techniques to simulate the complex photosensitizers. For the past 30 years density functional theory has been the dominant method for the quantum mechanical simulation of periodic systems. In recent years, it has also been adopted by quantum chemists and is now very widely used for the simulation of energy surfaces in molecules [13]. The reasons for its popularity and success are

1) The DFT approach is in principle exact [14].
2) It preserves at all levels of approximation the appealing one-electron molecular orbital (MO) view on chemical reactions and properties. The computed orbitals are suitable for the typical MO-theoretical analyses and easy to understand [15].
3) It is a relatively efficient computational method, and its fundamental scaling properties do not deteriorate when methodological precision is increased, in particular, when a more accurate XC functional is applied [16].

1.3.1.The Khon-Sham molecular orbital (MO) model

The fundamental assumption in Kohn–Sham density functional theory (KS-DFT) is that we can use a single electron calculation to "n" interacting electrons. It can be done by applying appropriate local potential V_{XC} (r), external potentials Vext (r) and the Coulomb potential of the electron cloud V_C(r), then using Eq. (1)

$$\left(-\frac{1}{2}\nabla^2 + V_{ext}(r) + V_C(r) + V_{XC}(r)\right)\varphi_i(r) = \varepsilon_i\phi_i(r) \qquad (1)$$

The potential V_{XC} is the functional derivative with respect to the density (ρ) of the exchange–and–correlation energy functional E_{XC} [ρ]. The one-electron molecular orbitals (MOs) ϕ_i with corresponding orbital energies ε_i define the exact electronic charge density and give access to all properties. The (first) derivatives of the energy with respect to nuclear displacements at the end of the self consistent field (SCF) method are used to find stationary points in the energy surface, particularly for the geometry optimization of molecules [13].

According to Runge-Gross theorem [17] , the external potential individually finds out the density for a given interaction potential. While according to Kohn-Sham assumption the density of the non-interacting system is equal to the density of an interacting system. The benefit of this assumption is that, the wave function of a non-interacting system can be represented as a Slater determinant of single-particle orbitals, each of which are determined by a single partial differential equation in three variable. Then, the time-dependent (TD) Kohn–Sham equations are:

$$i\frac{\partial}{\partial \mathrm{t}}\varphi_{\mathrm{i}}(\mathrm{r},\mathrm{t}) = \left(-\frac{\nabla^2}{2} + \mathrm{V}[\rho](\mathrm{r},\mathrm{t})\right)\varphi_{\mathrm{i}}(\mathrm{r},\mathrm{t}) \qquad (2)$$

$$\rho(r,t) = \Sigma n_j |\varphi_i(r,t)|^2 \qquad (3)$$

The potential (V) includes the V_C(r), the nuclear potential ,Vext(r) and (X_C), all are functions of time KS-TDDFT technique with solvent effect is used to calculate the excitation energies (E_{ex}) in DFT.

1.4. Thesis Summary

This section will highlight the summary of each chapter. Each chapter will be discussed in the manuscript format.

Chapter-2

Chapter-2 describes the comprehensive review on importance of solar energy and superiority of dye sensitized solar cells (DSSCs) over silicon solae cells. Solar energy is an abundant and accessible source of renewable energy available on earth, and many types of photovoltaic (PV) devices like organic, inorganic, and hybrid cells have been developed to harness the energy. PV cells directly convert solar radiation into electricity without affecting the environment. Although silicon based solar cells (inorganic cells) are widely used because of their high efficiency, they are rigid and manufacturing costs are high. Researchers have focused on organic solar cells to overcome these disadvantages, . DSSCs comprise of a sensitized semiconductor (Photoelectrode) and a catalytic electrode (counter electrode) with an electrolyte sandwiched between them and their efficiency depends on many factors. The maximum electrical conversion efficiency of DSSCs attained so far is 11.1%, which is still low for commercial applications. This chapter examines the working principle, factors affecting the efficiency and key challenges facing DSSCs.

Chapter-3

This chapter describes the synthesis of 1,3,4-Oxadiazol based photosensitizers for solar cell applications. In this work, four oxadiazol based photosensitizers were synthesized by

introducing biphenyl, naphthalene, anthracene and triphenyl amin as electron-donating moieties. The electrochemical and optical properties of these sensitizers were investigated .These photosensitizers were then employed in solar cells. The UV-Visible absorption spectroscopy, photocurrent–voltage (*I–V*) characteristic and electrochemical impedance spectroscopy (EIS) measurements were carried out to characterize the solar cells. The results indicate that 1,3,4-Oxadiazo pi-spacer with anthracene moiety shows the highest efficiency of 2.58%. Density functional theory and time dependent density functional theory DFT/TD-DFT modeling techniques were used to compute the electronic and optical properties of sensitizers.

Chapter-4

Chapter-4 describes the fabrication of DSSCs using hybrid photoanode and N_3 (cis-diisothiocyanato-bis(2,2'-bipyridyl-4,4'-dicarboxylic acid) ruthenium(II)) sensitizer. CNTs suppress the charge recombination with electrolyte and improves the charge transport process in DSSCs. Titanium oxide/multi-walled carbon nanotubes (TiO_2/MWCNTs) photoanodes were prepared using mixing technique. Dye sensitized solar cells (DSSCs) based on TiO_2/MWCNTs composite with different concentrations of CNTs (0, 0.03. 0.06, 0.09, 0.15, 0.21 wt. %) were fabricated using N_3 dye as a sensitizer. Transmission electron microscope (TEM) was used to confirm the dispersion of carbon nanotubes in TiO_2. The UV-Visible absorption spectroscopy, photocurrent–voltage (*I–V*) characteristic and electrochemical impedance spectroscopy (EIS) measurements were carried out to characterize device. The results show that the photo conversion efficiency is highly dependent on the concentration of CNTs in the photoanode. The solar cell based on photoanode containing 0.03 wt. % MWCNTs, has a

power conversion efficiency, which is about 30% greater than that of the unmodified photoanode.

Chapter-5

This chapter describes the co-sensitization technique to enhance the efficiency of DSSCs. Co-sensitization of two or more dyes on hybrid TiO_2- MWCNTs photoanode is an effective approach to enhance the performance of a dye-sensitized solar cell (DSSC). In this work, N719 sensitizer is co-sensitized with N3. It was found that the co-sensitized device showed significantly enhanced V_{OC} and J_{SC} relative to its individual single-dye sensitized devices. Upon optimization, the device made of the 0.1Mm N_3 + 0.4mM N719 system yielded J_{SC} = 12.5 mA cm^{-2}, V_{oc} =0.73V, FF= 0.45 and η = 4.1 %; this performance is superior to that of either individual device made from N_3 (3.69%) and N719 (3.59 %) under the same conditions of fabrication. The overall efficiency of DSSCs was further improved to 4.46% by the incorporation of MWCNTs in TiO_2. The hybrid TiO_2/MWCNTs photoanodes with different concentrations of CNTs (0.04. 0.08, 0.12, 0.16 wt. %) were prepared using mixing technique. The optimized composition of N3+N719 was selected for the co-sensitization of hybrid photonodes.

Chapter-6

This chapter highlights the applications of graphene in DSSCs. Composite photoanodes for dye sensitized solar cells (DSSCs) were prepared by simple addition of graphene (GR) micro-platelets to TiO_2 nanoparticulate paste. Transmission electron microscopy (TEM) was used to confirm the presence of graphene in composite films after heating at 450 C for 30 minutes. TiO_2/graphene based DSSCs with different concentrations of

gaphene were fabricated using N749 photosensitizer. The UV-Visible absorption spectroscopy, photocurrent–voltage (*I–V*) characteristic and electrochemical impedance spectroscopy (EIS) measurements were carried out to characterize the cells. The results indicate that graphene/TiO2 photoanode improves the performance of of solar cell. This is because the graphene/titania electrode accelerates electronic transportation and suppresses the charge recombination. Under an optimal conditions, solar cell based on graphene/TiO2 shows power conversion efficiency (PCE) of 4.1 %, which is about 30% greater than the cell based on pristine TiO_2 electrode (3.16%). The objective of this study is to develop a fast, cheap, and an effective means to increase the photo conversion efficiency (PCE) of DSSCs.

Chapter-7

This chapter further describes the applications of DFT/D-DFT in optimizing the complex structures of photosensitizers. Complex organic compounds with benzene/thiophene as pi-segments are inspected as photosensitizers for applications in dye sensitized solar cells. To better understand the charge transport process involved in the dye sensitized solar cells, we used the results of Kohn–Sham density functional theory and time-dependent density functional theory (DFT) studies of benzene/thiophene based sensitizers as well as the dye bound to a TiO_2 nano cluster. We investigated the electronic structures and UV-Vis spectra of the sensitizers alone and linked to the cluster. We also showed energy level diagrams, the major transitions of molecular orbitals and free energy calculation of the electron transfer from the sensitizer to the conduction band of the TiO_2. The objective of this study is to explore the applications of DFT and time dependent DFT in the field of dye designing for solar cells.

Chapter-8

These chapters describe the computational study of geometry and electronic structure properties of novel oxadiazole based organic sensitizers using density functional theory (DFT) and time dependent DFT (TD-DFT) modeling techniques. In this study, four photosensitizers were designed by introducing oxadiazole isomers as π-conjugated bridges between donor and acceptor moieties. The computational analysis was performed to investigate the key parameters of light harvesting efficiency (LHE), free energy for electron injection (ΔG^{inject}), excitation energies and frontier molecular orbitals (FMOs). The results suggest that the system with 1,2,3-oxadiazole shows a balance among the different crucial factors and may result in the highest incident photon to charge carrier efficiency of dye-sensitized solar cells. The dye/$(TiO_2)8$ anatase clusters were also simulated to illustrate the electron injection efficiency at the interface. Similarly, the N_3 (ruthenium based sensitizer) dye was simulated under the same conditions. The computation results were compared with experimental values to validate the simulation basis/assumptions.

Chapter-9

Brief summary of the conclusion and recommendations will be presented in this chapter.

1.5.References

[1] Hasanuzzaman M, Rahim NA, Saidur R, Kazi SN. Energy savings and emissions reductions for rewinding and replacement of industrial motor. Energy 2011;36:233–40. doi:10.1016/j.energy.2010.10.046.

[2] Hasanuzzaman M, Rahim NA, Hosenuzzaman M, Saidur R, Mahbubul IM, Rashid MM. Energy savings in the combustion based process heating in industrial sector. Renew Sustain Energy Rev 2012;16:4527–36. doi:10.1016/j.rser.2012.05.027.

[3] Timilsina GR, Csordás S, Mevel S. When does a carbon tax on fossil fuels stimulate biofuels? Ecol Econ 2011;70:2400–15. doi:10.1016/j.ecolecon.2011.07.022.

[4] Canadell JG, Le Quéré C, Raupach MR, Field CB, Buitenhuis ET, Ciais P, et al. Contributions to accelerating atmospheric CO2 growth from economic activity, carbon intensity, and efficiency of natural sinks. Proc Natl Acad Sci U S A 2007;104:18866–70. doi:10.1073/pnas.0702737104.

[5] Hosenuzzaman M, Rahim NA, Selvaraj J, Hasanuzzaman M, Malek ABMA, Nahar A. Global prospects, progress, policies, and environmental impact of solar photovoltaic power generation. Renew Sustain Energy Rev 2015;41:284–97. doi:10.1016/j.rser.2014.08.046.

[6] Barnham KWJ, Mazzer M, Clive B. Resolving the energy crisis: nuclear or photovoltaics? Nat Mater 2006;5:161–4. doi:10.1038/nmat1604.

[7] Bredas J-L, Durrant JR. Organic photovoltaics. Acc Chem Res 2009;42:1689–90. doi:10.1021/ar900238j.

[8] Rehman S, Bader MA, Al-Moallem SA. Cost of solar energy generated using PV panels. Renew Sustain Energy Rev 2007;11:1843–57. doi:10.1016/j.rser.2006.03.005.

[9] Millington KR. Encyclopedia of Electrochemical Power Sources. Elsevier; 2009. doi:10.1016/B978-044452745-5.00317-8.

[10] Robertson N. Optimizing dyes for dye-sensitized solar cells. Angew Chem Int Ed Engl 2006;45:2338–45. doi:10.1002/anie.200503083.

[11] Hagfeldt A, Boschloo G, Sun L, Kloo L, Pettersson H. Dye-sensitized solar cells. Chem Rev 2010;110:6595–663. doi:10.1021/cr900356p.

[12] Klein C, Nazeeruddin MK, Liska P, Di Censo D, Hirata N, Palomares E, et al. Engineering of a novel ruthenium sensitizer and its application in dye-sensitized solar cells for conversion of sunlight into electricity. Inorg Chem 2005;44:178–80. doi:10.1021/ic048810p.

[13] Te Velde G, Bickelhaupt FM, Baerends EJ, Fonseca Guerra C, van Gisbergen SJA, Snijders JG, et al. Chemistry with ADF. J Comput Chem 2001;22:931–67. doi:10.1002/jcc.1056.

[14] Ziegler T. Approximate density functional theory as a practical tool in molecular energetics and dynamics. Chem Rev 1991;91:651–67. doi:10.1021/cr00005a001.

[15] Baerends EJ, Gritsenko O V. A Quantum Chemical View of Density Functional Theory. J Phys Chem A 1997;101:5383–403. doi:10.1021/jp9703768.

[16] The Journal of Chemical Physics n.d.

[17] Runge E, Gross EKU. Density-Functional Theory for Time-Dependent Systems. Phys Rev Lett 1984;52:997–1000. doi:10.1103/PhysRevLett.52.997.

CHAPTER 2

RECENT ADVANCES IN DYE SENSITIZED SOLAR CELLS

Umer Mehmood [a], Saleem-ur-Rehman [a], Khalil Harrabi [b], Ibnelwaleed A. Hussein* [a], BVS Reddy [c]

[a] Department of Chemical Engineering, King Fahd University of Petroleum & Minerals (KFUPM), P. O. Box 5050, Dhahran 31261, Kingdom of Saudi Arabia

[b] Department of physics, (KFUPM), P. O. Box 5050, Dhahran 31261, Kingdom of Saudi Arabia

[c] Indian Institute of Chemical Technology, Hyderabad, India

*Corresponding Author: Ibnelwaleed A. Hussein , E-mail address: ihussein@kfupm.edu.sa

This chapter has been published in "Advances in Materials Science and Engineering" on 17 April 2014

Abstract

The solar energy is an abundant and accessible source of renewable energy available on earth. To bring this energy in use, many types of photovoltaic (PV) devices like organic, inorganic and hybrid cells have been developed. These PV cells directly convert the solar radiation into electricity, leaving no environmental effect. Silicon based solar cells (inorganic cells) are being widely used because of their high efficiency. But silicon PV cells are rigid and their manufacturing cost is high. To address these problems, research has focused on the organic solar cells. Dye sensitized solar cells (DSSCs) are proficient and low cost photovoltaic devices among all the organic solar cells. They consist of an electrolyte sandwiched between a sensitized semiconductor (Photoelectrode) and a catalytic electrode (counter electrode). The efficiency of DSSC depends on many factors. The electrical conversion efficiency of DSSCs has been attained to 11.1% so far. But it is still low for commercial applications. This review examines working principle, factors affecting the efficiency and key challenges of DSSCs.

Keywords: Solar radiation**,** DSSC, Photovoltaic, Semiconductor, electrolyte.

2.1. Introduction

The world energy demand is increasing day by day. It is expected that world power consumption will be about 23 TW (terawatts) in 2050, which is currently 13 TW [1]. Fossil fuels meet 80% of the energy requirement of the whole world. But fossil fuels are depleting rapidly [2]. Moreover, the burning of fossil fuels also raises the amount of carbon dioxide in the atmosphere. Owing to growing energy demand, exhaustion of oil resources and global warming issues, there is a need for clean and renewable energy technologies. The photovoltaic technology employing solar energy is regarded as most efficient technology among all the sustainable energy technologies such as tidal power, solar thermal, hydropower and biomass [3].

The solar radiation from the sun is approximately 3×10^{24} J per year, which is ten times more than current energy demands [4]. To bring solar energy in use, the first practical photovoltaic cell was designed in 1954 at Bell laboratories. They used a diffused silicon p–n junction and 6% efficiency was found [5] . But now the light to electricity conversion efficiency of silicon based solar cells is between 15% and 20% [6]. Though need of high decontamination of silicon, use of toxic chemicals in their manufacturing and high cost has restricted their worldwide use. These constraints encouraged the search for environmentally friendly and low cost solar cells. In 1991, Michael Gratzel developed a new photovoltaic cell and the principle was similar to that of plant photosynthesis. This PV cell became known as DSSC. The efficiency of this cell was 7.1-7.9% [7]. DSSCs consist of an electrolyte inserted between a photoelectrode and a catalytic-electrode. The measuring parameters of DSSCs like electrical conversion efficiency (η), Open circuit voltage (Voc), close circuit current density (J_{sc}), fill factor (FF), interface charge

resistance and an incident photon to current efficiency (IPCE) depend on the morphological, spectroscopic and electrical properties of semiconductors, dyes and electrolytes respectively. DSSCs are an important type of thin film photovoltaic technology because of their low cost of manufacturing, ease of fabrication and light weight product [8,9]. In the near future, the venture of DSSCs as a competitive technology will thus be revealed. The latest efficiency of DSSC is more than 11% [10].

2.2. Structure and Mechanism of DSSC

Structure and working principle of DSSC is shown in Fig 2-1. It consists of an electrolyte inserted between a photoelectrode and a catalytic-electrode. A charge separation process in DSSC consists of the following steps [3],

i. Dye adsorbs on a thin film of semiconductor, absorbs incident solar energy. Upon absorbing energy, dye is become exited from the ground to the excited state
ii. Due to the difference in energy levels of electronic states, electrons from the exited state are injected to the conduction band of the semiconductor. As a result dye is become oxidized.
iii. The electrolyte in contact with dye donates electrons to dye to restore its initial state.
iv. Electrolyte diffuses towards catalytic electrode where the reduction reaction takes place and electrolyte restores its initial state.

In addition to this forward charge transfer processes some backward charge transfer processes also occur in one complete cycle. These backward electron transfer processes drastically reduce the efficiency of DSSCs. These are

i. Back transfer of electrons from semiconductor to the oxidized dye.

ii. Recombination of injected electrons with electrolyte (dark current).

iii. Transfer of electrons from dye excited state to ground state.

In order to reduce backward transfer processes,

i. Charge transfer to semiconductor must occur with a quantum yield [12].

ii. Lowest unoccupied molecular orbital (LUMO) of photosensitizer should be more negative than the conduction band of the semiconductor and highest occupied molecular orbital (HOMO) should be more positive than the redox potential of electrolyte [13].

iii. Electron injection rate to semiconductor should be higher than the rate of decay of electrons from dye excited state to ground state [14].

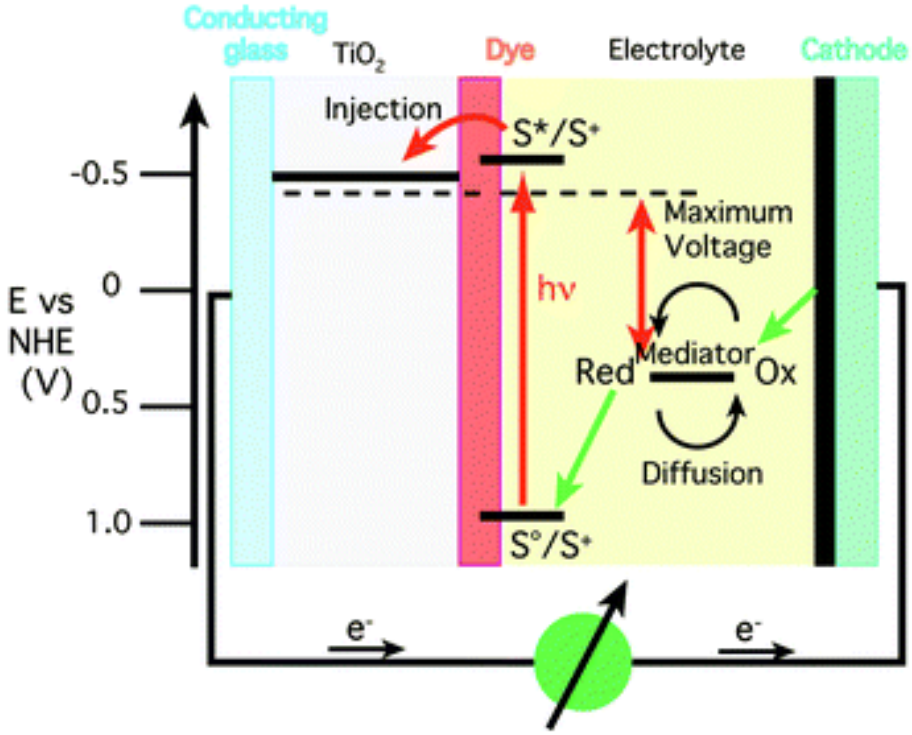

Fig 2-1:Structure and working principle of DSSC $S°/S^{+}/S*$ = sensitizer in the ground, oxidized and excited state, respectively. Red/Ox = Redox mediator [11]

2.3.Components of Dye-Sensitized Solar Cell

2.3.1. Transparent Conductive Substrate

DSSCs are normally constructed between two sheets of conductive transparent materials. These sheets provide a space for semiconductor and catalyst deposition and also act as current collector. Substrates must be highly transparent (transparency >80%) to allow the maximum passage of sunlight to the active area of the cell. Its electrical conductivity should also be high for efficient charge transfer and minimize energy loss. These two characteristics of substrate dictate the efficiency of DSSCs [3].

FTO (fluorine tin oxide, SnO_2: F) and ITO (indium tin oxide, In_2O_3: Sn) are normally being used as conductive substrate. They consist of soda lime glass coated with fluorine tin oxide and indium tin oxide layers respectively. ITO films show transmittance over 80% and sheet resistance 18Ω/sq, while FTO films exhibit transmittance about 75% in the visible region and sheet resistance of 8.5Ω/sq. Siam et al have conducted the study for the comparison of FTO and ITO based DSSCs [15]. They constructed FTO and ITO based DSSCs. Photoanodes based on FTO and ITO glass substrates were sintered at 450^{o}C for 2 hrs in oxygen atmosphere. They found that after sintering sheet resistance of FTO remained constant, while sheet resistance of ITO changed from 18Ω/sq to 52Ω/sq. The DSSC based on FTO has an overall η of 9.4% in comparison with identical cell based on ITO which has η of 2.4%. Thus, FTO is highly recommended for DSSCs because of its low and temperature-stable sheet resistance.

Polymers can also be used as an alternative to glass substrate because of their flexibility and low cost. Takurou et al. used PET (Polyethylene terephthalate) coated with ITO and found efficiency of 3.8% [16]. Polyethylene naphthalate (PEN) coated with ITO was used

by Rothenberger et al. and observed efficiency of 7.8% [17]. But temperature limitation restricts the use of polymers as substrate in DSSCs [18]. Metals that form a conducting layer like stainless steel, tungsten and titanium have also been used as substrates. Man Gu Kang. et al applied stainless steel and depicted efficiency of 6.1% [19]. However, the high cost and corrosion with electrolyte prohibit the use of metals as substrates [20].

2.3.2. Mesoporous Semiconductor

Semiconductor provides a surface area for the dye adsorption. It accepts and conducts electrons from the excited dye to the external circuit to produce electric current [21]. The electron transport rate in the semiconductor affects the efficiency of DSSCs. It highly depends on crystallinity, morphology, and the surface area of semiconductors. Metal oxides like titanium oxide (TiO_2), zinc oxide (ZnO) [22] and stannic oxide (SnO_2) [23] have been used as semiconductor materials. But experiments show that DSSCs based on ZnO and SnO_2 establish lower efficiency in comparison with nanocrystalline TiO_2 [23–25]. Therefore, it has been considered as an ideal semiconductor material for DSSCs since 1991 because of its better morphological and photovoltaic properties as compared to other semiconductors [26].

There are two crystalline forms of TiO_2, anatase and rutile. But the former is preferable because, anatase has high conduction band edge energy (3.2 eV) as compared to rutile (~3 eV). High band gap energy makes anatase chemically more stable [27]. An electron transport process in rutile is also slow as compared to anatase due to high packing density. Short circuit photo current of anatase based DSSC is 30% more than that of rutile based DSSC of the same film thickness. Owing to smaller surface area per unit volume, rutile absorbs less dye and therefore less efficient [28].

The main loss path in DSSCs is the recombination of injected electrons with electrolyte. This phenomenon is also called dark current and diminishes the efficiency of DSSCs. Dark current can be minimized by employing structural changes, use of insulating layers or surface treatments of TiO_2 [29]. Many morphologies of anatase TiO_2 from nanoparticles, nanofibers [30], nanowires [31], hollow sphere [32], hollow hemisphere [33], nanotubes [34] and hierarchical spheres to ellipsoid spheres [35] have been fruitfully fabricated *via* solvothermal reactions of titanium *n*-butoxide and acetic acid. The DSSC based on the hierarchical anatase TiO_2 sphere photoelectrode shows an overall η of 9.35% accompanying a J_{sc} of 17.94 mA cm^{-2}, V_{oc} of 803 mV and FF of 0.65, which is much higher than that of nanoparticles (7.37%), nanofibers (8.15%) and ellipsoid TiO_2 spheres (7.93%) [36]. The substantial improvement of short-J_{sc} and η for the hierarchical sphere-based DSSC compared to other nanostructure is mainly due to the larger dye loading, higher light scattering ability, faster charge transport and longer electron lifetime [36,37]. Another approach to minimize the charge recombination is deposition of the insulating layer on semiconductor electrode. Many metal oxide like ZnO [38], Niobium pentoxide (Nb_2O_5) [39], Al_2O_3 [40] and SiO_2 [41] have been used as an energy barrier for retarding the charge recombination owing to their insulating properties. These insulating layers reduce the interaction between injected electron to the semiconductor and the electrolyte solution [42]. Similarly, surface treatment of TiO_2 with $TiCl_4$ also reduces the charge recombination process by increasing interfacial charge-transfer resistance of the TCO/electrolyte interface [43,44]. Recently, Johann Boucle synthesized Nitrogen-doped TiO_2 electrode (optically active electrode) by laser pyrolysis [45]. They found that the short-circuit current density of DSSC based on an N-doped

electrode increased by more than 10% compared to that of pure anatase. This progress is found to be associated with electronic and optical properties of the starting nanopowder.

2.3.3. Dye (Photosensitizer)

The function of dye is to absorb light and transfer electrons to the conduction band of the semiconductor. It is chemically bonded to the porous surface of the semiconductor. An efficient photosensitizer should:

i. Show intense absorption in the visible region (400 nm-700 nm).
ii. Be strongly adsorbed on the surface of the semiconductor.
iii. Possess a high extinction coefficient.
iv. Be stable in its oxidized form until it is re-reduced by an electrolyte.
v. Be adequate for carrying out ~10^8 turnovers without instability, which typically corresponds to the 20 years of cell operation.
vi. LUMO of photosensitizer should be more negative than the CB of the semiconductor and redox potential of the electrolyte should be less positive than the HOMO

In addition the performance of DSSCs highly depends on a molecular structure of the sensitizers. Many chemical compounds are being used for the sensitization of semiconductor, such as the phthalocyanines [46–48], coumarin-343 [13,49,50], carboxy-lated derivatives of anthracene [51,52] and porphyrins [53–55]. But photosensitizers based on transition metals have been the best so far [56]. There are three classes of photosensitizer: metal complex sensitizers, metal-free organic sensitizers and natural sensitizers.

2.3.3.1.Metal complex sensitizers

Metal complex sensitizers consist of anchoring ligands (ACLs) and ancillary ligands (ALLs). The adhesion of photosensitizers with semiconductor is strongly dependent on the properties of ACLs. While ALLs are responsible for the tuning of the overall properties of sensitizers, the intense metal to charge transfer (MLCT) bands in the visible region is shown by polypyridinic complexes of d^6 metal ions. The modification of ACLs as well as by changing the ALLs or its substituents can alter the energies of MLCT states. Many metal complex sensitizers have been prepared by changing the ALLs. However, ruthenium(II) polypyridyl complexes show better light to electricity conversion efficiency [57] because of their good spectroscopic, photostability, redox and excited state properties in the final device [58,59] The general representation of carboxylic based sensitizers is [Ru $(dcbH_2)_2LL'$], while $dcbH_2$, and L and/or L′ represent anchoring ligands and ancillary ligands, respectively. An example of high performance carboxylic based sensitizer is *cis*-[$Ru(dcbH_2)_2(NCS)_2$] also identified as N_3 dye [60]. An efficient performance has also been perceived for the other ruthenium based photosensitizers such as $[Ru(tcterpy)(NCS)_3]^-$ also named black dye. Fig 2-2 shows that the cell based on black dye is more proficient than red dye in the near infrared region and attained efficiency of 10.4% [4]. Record efficiencies of various sizes and their structures are shown in Table 2-1 and Fig 2-3, respectively. Although the record efficiency and stability has been achieved with ruthenium based sensitizers. But due to the high cost and scarcity of ruthenium, another course of actions should also be considered.

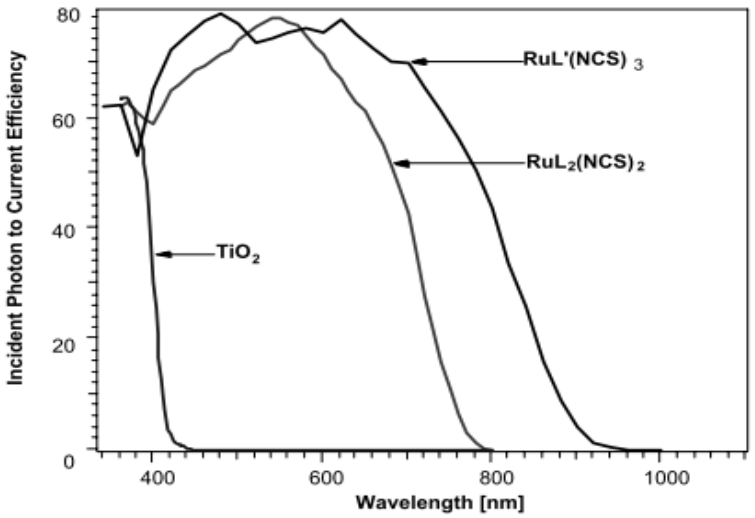

Fig 2-2: (IPCE) of an efficient dyes and their chemical structures[61]

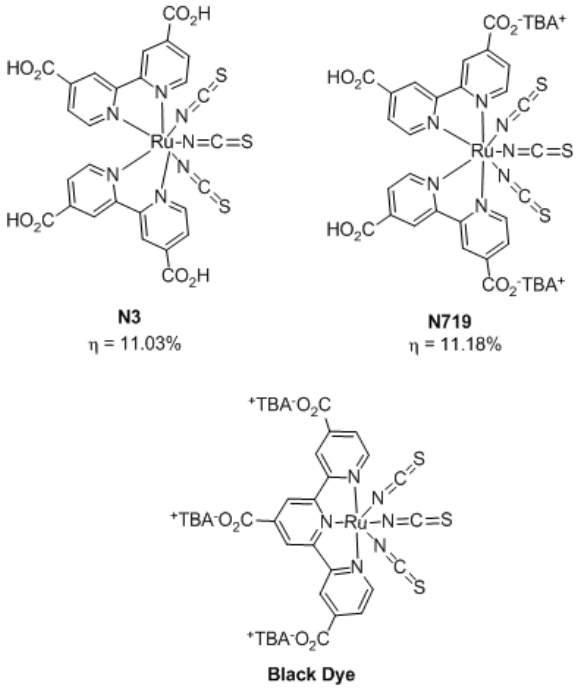

Fig 2-3: Structure of some efficient Ru-based photosensitizers [62]

Table 2-1: Record efficiencies achieved for DSSCs of varying surface area [56]

No	Dye	Surface area (cm^2)	η (%)	V_{oc} (V)	I_{sc} (mA/cm^2)	FF (%)
1	N719	<1	11.2	0.84	17.73	74
2	N749	0.219	11.1	0.736	20.9	72
3	N749	1.004	10.4	0.72	21.8	65
4	N719	1.310	10.1	0.82	17.0	72
5	N3	2.360	8.2	0.76	15.8	71

2.3.3.2.Metal-free photosensitizers

Metal-free organic sensitizers have been fabricated not only to replace the expansive ruthenium based sensitizers but also to improve the electronic properties of devices. However, the efficiency of these sensitizers is still low as compared to ruthenium based dyes. But efficiency and performance can be improved by proper selection or tuning of the designing components. The general design mechanism of metal free organic is shown in Fig.-4. Donor and acceptors substituents are separated by π-conjugated spacer. The photoelectric properties of these dyes can be tuned by altering or matching different substituents within D-π-A structure. Literature shows that efficiency of such dyes changes with the changing of the chemistry of electrolytes. For example efficiencies of metal free organic dyes in liquid, ionic and solid state electrolytes are greater than 8%, 6% and 4%, respectively [63]. These results suggest that donor groups for efficient sensitizers should be selected from the electron rich aryl amines family such as phenylamine, aminocoumarin, indoline and (difluorenyl)triphenylamine. While π-conjugated connector must be selected from thiophene units e.g. oligothiophenes, thienylenevinylenes, or dithienothiophene due to their outstanding charge transfer characteristics. While on the acceptor side acrylic acid group is considered as best acceptor moiety. However, the efficiency of DSSCs based on metal-free organic sensitizers is still low for industrial applications. Some important metal free photosensitizers and their photoelectric properties are summarized in Table 2-2.

Table 2-2: Metal free organic photosensitizers with different electrolytes.

Compound	V_{oc}	J_{sc}	FF [%]	η [%]	Electrolyte*	Ref
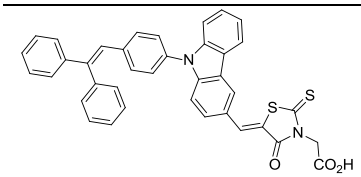	0.6	17.8	57	6.1	OE	[64]
	0.67	9.7	74	4.9	IL	[65]
	0.87	7.7	61	4.1	SS	[66]
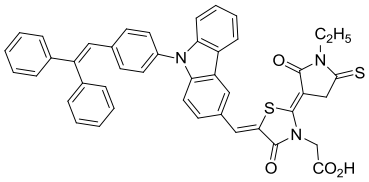	0.65	20	69.4	9	OE	[67]
	0.71	12.5	72	6.4	IL	[65]
	0.55	14.1	54	4.2	SS	[68]

Electrolyte*: O.E= Organic Electrolyte, I.E= Ionic Liquid, S.S= Solid State

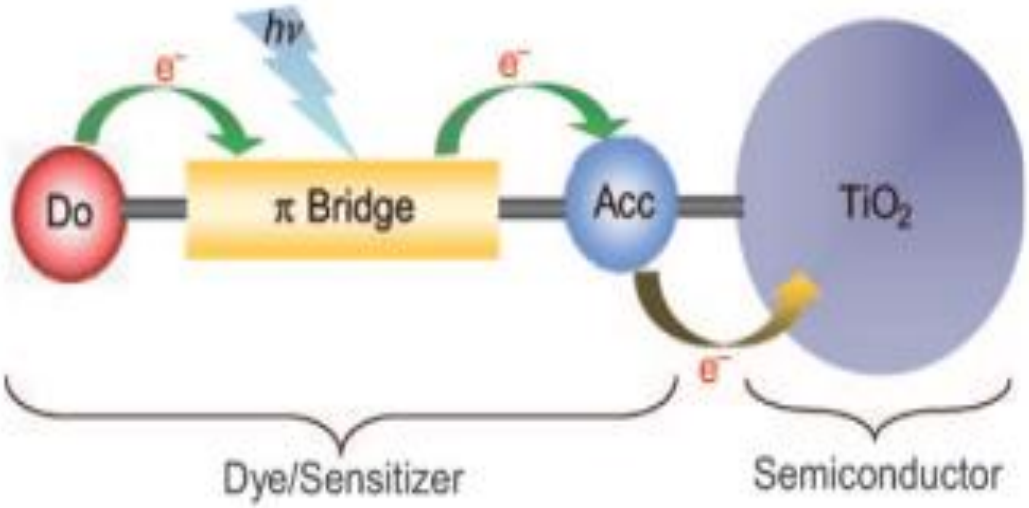

Fig 2-4: Design mechanism of an organic dye for TiO2 photoanodes in DSSCs

2.3.3.3.Natural Sensitizers

Natural dyes have also been used in DSSCs because of their low cost, easy extraction, nontoxicity and environment-free threats [69]. There are two classes of plant pigments such as carotenoids and flavonoid. In addition, there are three subclasses of flavonoid: anthocyanins, proanthocyanidins and flavonols. But only anthocyanins of flavonoid group are responsible for cyanic colors ranging from salmon pink through red and violet to dark blue of most flowers, fruits and leaves. Anthocyanins are most extensively investigated as natural sensitizers and their extracts show maximum absorption in the range of 510-548 nm depending on the fruit or solvent used [70]. The basic chemical structures of most abundant anthocyanins are shown in Fig 2-5.

The length of substituent R also affects the performance of anthocyanins. If the length of R is large then performance of the dye will be less due to the steric hindrance which restricts the transfer of electrons from dye molecules to the conduction band of the semiconductor. The efficiency of natural dyes is very low because of weak interaction between semiconductor (TiO_2) and dyes. Also, dye aggregation on nanocrystalline film is another important cause of low efficiency. Some important natural dyes and their photoelectric properties are summarized in Table 2-3. The highest efficiency has been produced by Red turnip based on the work produced by Calogero et al [71].

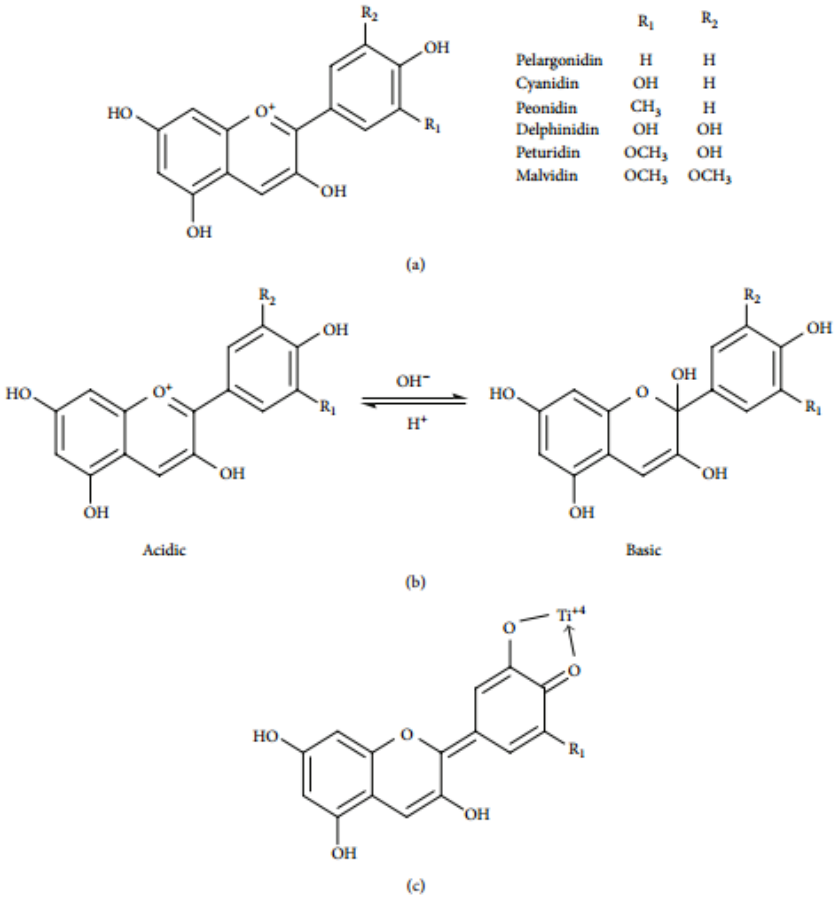

Fig 2-5: a) chemical structures of anthocyanins b) Structure in acidic and basic medium c) Chelation mechanism with TiO_2 [70]

Table 2-3: Photoelectric parameters of DSSCs based on natural dyes.

No	Dye	η(%)	V_{oc}(V)	J_{sc}(mA/cm^2)	FF(%)	Ref
1	Red Turnip	1.7	0.43	9.50	0.37	[71]
2	Rhoeo Spathacea	1.49	0.5	10.9	0.27	[72]
3	Shisonin	1.31	0.53	4.80	0.51	[73]
4	Wild Sicilian	1.19	0.38	8.2	0.38	[71]
5	Mangosteen	1.17	0.67	2.69	0.63	[74]

2.3.4. Electrolyte

The function of electrolyte is to regenerate the dye after injecting electrons into the conduction band of the semiconductor. It also acts as a charge transport medium to transfer positive charges toward the counter electrodes. The long term stability of DSSCs depends on the properties of electrolyte. Therefore, electrolyte must hold the following characteristics [75,76],

i. It should have high electrical conductivity and low viscosity for the faster diffusion of electrons.
ii. It should produce good interfacial contact with nanocrystalline semiconductor and the counter electrode.
iii. It must not cause desorption and degradation of dye from the oxidized surface.
iv. It should not absorb light in the visible region.

Electrolytes for DSSCs are classified into three types, liquid electrolytes, solid state electrolytes and quasi-solid state electrolytes.

2.3.4.1.Liquid Electrolytes

Liquid electrolytes are further classified into two types, organic solvent electrolytes and room temperature ionic liquid electrolytes (RTIL) depending on the solvent used.

2.3.4.1.1. Organic electrolytes

Each component of organic electrolytes such as redox couple, solvent and additives affect the performance of DSSCs. The major component of organic solvents is redox couple. Many kinds of redox couples such as Br^-/Br_3 [77], $SCN^-/(SCN)_2$, $SeCN^-/(SeCN)_2$ [78,79] and substituted bipyridyl cobalt(III/II) [80] have been investigated. But I_3/I^- is considered

as an ideal redox couple so far [81] because of its good solubility, rapid dye regeneration, low absorbance of light in the visible region, suitable redox potential and very slow recombination kinetics between injected electrons in semiconductor and triode (I_3) [82].

Another basic component of liquid electrolyte is organic solvent. It is responsible for the diffusion and the dissolution of the iodide/triiodide ions. Many types of solvents such as acrylonitrile (AcN), ethylenecarbonate (EC), propylenecarbonate (PC), 3-methoxypropionitrile (MePN) and N- methylpyrolidone (NMP) have been investigated with reliable performance [83,84]. The photoelectric performance of DSSCs depends on the donor number (DN) of the solvents. Using solvents with large DN increases the V_{OC} and decreases J_{sc} Values [85]. This is because high DN gives a lower concentration of triode which in turn reduces the dark current and therefore high photovolatage (V_{oc}). The photovoltaic properties of DSSCs can be optimized by employing electric additives. The most efficient additives are 4-*tert*-butylpyridine(TBP), Nmethylbenzimidazole (NMBI) and guanidinium thiocyanate (GuNCS) [86]. These additives are adsorbed onto the photoelectrode/electrolyte interface and prevent the recombination of injected electrons with tri-iodide ions. One important parameter is the concentration of I^-/I_3 in the mixture when used as redox couple. If the concentration is low, then it will be difficult to maintain the required conductivity. But if the concentration is high then it will absorb light in the visible region . Therefore, the concentration of I^-/I_3 in electrolyte must be optimized.

2.3.4.1.2. Ionic electrolytes

Although covalent electrolytes show record efficiency they have a high evaporation rate due to high volatility. High evaporation rate and leakage problem limit the long term stability of DSSCs based on covalent electrolytes. In order to minimize these problems, room temperature ionic liquids (RTIL) have been employed successfully. They are a group of organic salts consisting of cations such as pyridinium, imidazolium and anions from the halide or pseudo-halide family [87]. They act simultaneously as iodine source and as a solvent. The most commonly used IL for DSSCs applications are N, N′ bis-alkyl-substituted imidazolium iodides [88]. It has been found that the viscosity of these salts decrease with decreasing alkyl chain length due to decrease of van der Waals forces. Therefore, the conductivity of IL electrolytes decreases because an increase in viscosity limits the diffusion of charges in the liquid [89]. The preferred counter ions for alkyl imidazolium based ILs are I^-, $N(CN)_2^-$, $B(CN)_4^-$, $CF_3COO)_2N^-$, BF_4^-, PF_6^- and NCS^-. Instead of alkyl imidazolium based ILs, alkyl pyridinium and trialkylmethylsulfonium based ILs have also been developed for DSSCs applications. Some ILs and their efficiencies in DSSCs are presented in Table 2-4. However, low efficiency due to high viscosity limits their application as electrolytes in DSSCs.

Table 2-4: : ILs and their efficiencies in DSSC applications

No	Ionic Liquids	η[%]	Ref
1	1-hexyl-3-methylimidazolium iodide	5.0	[89]
2	1-methyl-3-(3,3,4,4,5,5,6,6,6,-nonaflurohexyl) imidazolium	5.1	[90]
3	1-butyl-3-methylimidazolium iodide	4.6	[90]
4	S-propyltetrahydrothiophenium iodide	3.51	[91]
5	Eutectic mixture of glycerol and choline iodide	3.88	[92]

2.3.4.2.Solid-state electrolytes

Leakage is a key problem in liquid electrolytes based DSSCs which drastically reduce the long term stability of solar cells. In order to improve the performance and stability, solid state electrolytes have been developed [2]. It is just to replace the liquid electrolyte with p-type semiconductor or hole transfer material (HTM). A band gap structure of p-type semiconductor must be compatible with the HOMO level of the photosensitizer and the conduction band of the n-type semiconductor (TiO_2) [3]. Copper based compound such as CuI, CuBr and CuSCN have been employed as an inorganic HTM because of their good conductivity [81]. Organic HTMs have advantages over inorganic HTMs because of their low cost and easy deposition. The pioneer element of this class was 2,2',7,7'-tetrakis (N,N-di-pmethoxyphenylamine) 9,9'-spirobifluorene (OMeTAD) having efficiency of 0.74% (under white-light illumination of 4mW/cm^2) only [93]. Its efficiency was increased to 3.2% by improving dye adsorption in the presence of silver ions in the dye solution [94]. Solid state electrolytes based DSSCs have very low light-to-electricity conversion efficiency due to poor intimate contact between photoelectrode–HTMs and high rate of charge recombination from semiconductor to HTM. However, light-to-electricity conversion efficiency can be improved by introducing a redox couple into solid state electrolyte as a transport medium. Some common HTMs and their efficiencies in DSSCs are presented in Table 2-5.

Table 2-5: Performance of different HTMs in DSSCs.

No	HTMs	η**[%]**	**Ref**
1	CuI	2.4	[95]
2	CuI	3.8	[96]
3	CuSCN	1.5	[97]
4	Spiro-OMeTAD	3.2	[94]
5	Polyaniline	1.15	[98]

2.3.4.3.Quasi-solid state electrolytes

Though, leakage problem is solved by solid state electrolytes. But intimate contact between mesoporous semiconductor and HTM is still a problem. Since solid-state electrolytes do not penetrate into the pores of the semiconductor. This problem has been solved by quasi-solid state electrolytes. Quasi-solid state electrolyte is a composite of polymer and liquid electrolyte [99,100]. Because of the unique network structure of polymers, quasi-solid state electrolytes show better long term stability, high electrical conductivity and good interfacial contact as compared to liquid electrolytes [99,100]. The conductivity of the quasi-solid state electrolytes depends on the molecular weight and the morphology of the polymer because the higher mobility of charges occurs in the amorphous phase of polymer than in the crystalline phase. The performance of polymer electrolytes based DSSCs strongly depends on the working temperature. This is because an increase of temperature causes the phase transformation from a gel state to solution state [81]. Some important polymer electrolytes and their performance are summarized in Table 2-6.

Table 2-6: Polymer electrolytes and their performance in DSSC applications

No	Polymer	Solvent	η [%]	Ref
1	1,3:2,4-Di-*O*-benzylidene-D-sorbitol	3-methoxypropionitrile	6.1	[100]
2	5 poly (acrylic acid)-poly(ethylene glycol)	*N*-Methyl-2-pyrrolidone+ γ-butyrolactone	6.1	[101]
3	Low molecular weight gelator	1-hexyl-methylimidazoliumiodide, iodine	5	[89]
4	poly(acrylonitrile-*co*-styrene)	4-*tert*-butylpyridine+NaI+I_2	2.75	[102]
5	poly(ethylene glycol) (PEG)	propyleneycarbonate+potassium Iodide, Iodine	7.2	[103]
6	poly(ethylene oxide-co-propylene oxide)trimethacrylate	EC +GBL	8.1	[104]
7	poly(vinylidene-fluoride-co-hexafluoropropylene)	1,2-dimethyl-3-propylimidazoliumiodide,iodine	>6	[105]

2.3.5. Counter electrode

Counter electrode is used for the regeneration of the electrolyte. The oxidized electrolyte diffuses toward the counter electrode where it accepts electron from the external circuit. A catalyst is needed to accelerate the reduction reaction. Platinum (Pt) is considered as a preferred catalyst because of its high exchange current density, good catalytic activity and transparency. The performance of CE depends on the deposition method of Pt on TCO substrate. Many deposition methods like thermal decomposition of hexachloroplatinic salt in isopropanol [106], electrodeposition [107], sputtering [108], vapor deposition and screen printing [109]. It has been found that characteristics of Pt catalyst decrease with time in the presence of iodide/tri-iodide redox couple [110]. Experiments show that two major factors are responsible for the adulteration of Pt counter electrode: alteration of its electrocatalytic properties and annihilation of Pt from the substrate [106]. Although the Pt catalyst possesses high catalytic activity, the high cost of Pt is a disadvantage. Therefore, grapheme and conductive polymers have alsobeen used as alternative materials for counter electrode .But their electrical efficiencies were very low when compared to the Pt catalyst.

2.4. Key challenges and recommendations

Low efficiency and low stability are the major challenges for the commercial growth of DSSCs. The following factors are responsible for the low efficiency and stability of DSSCs:

i. Non-optimized dark current

ii. Poor performance of dyes in the NIR region

iii. Poor contact between the electrodes

iv. High volatility and high viscosity of electrolytes

v. Degradation of electrolyte properties due to UV absorption of light

Following steps can be recommended in order to enhance the efficiency and stability of DSSCs,

i. Improvement in the morphology of semiconductors to reduce dark current

ii. Improvement in the dye design to absorb light NIR region

iii. Develop low volatile and less viscous electrolyte to improve the charge transfer rate.

iv. Improvement in mechanical contact or adhesion between the two electrodes

v. Use of additives for dyes and electrolytes that enhance their properties.

However the efficiency and stability of DSSCs do not depend on a single factor. There must be traded off among different factors to improve the performance of DSSCs.

2.5. Acknowledgments

The authors would like to acknowledge the support provided by King Abdulaziz City for Science and Technology (KACST) through the Science & Technology Unit at King Fahd University of Petroleum & Minerals (KFUPM) for funding this work through project 11-ENE1635-04 as part of the National Science, Technology, and Innovation Plan. KFUPM is also acknowledged for supporting this research. The authors would like to acknowledge the Center of Research Excellence for Renewable Energy at KFUPM.

2.6. References

[1] Hasanuzzaman M, Rahim NA, Saidur R, Kazi SN. Energy savings and emissions reductions for rewinding and replacement of industrial motor. Energy 2011;36:233–40. doi:10.1016/j.energy.2010.10.046.

[2] Li B, Wang L, Kang B, Wang P, Qiu Y. Review of recent progress in solid-state dye-sensitized solar cells. Sol Energy Mater Sol Cells 2006;90:549–73. doi:10.1016/j.solmat.2005.04.039.

[3] Gong J, Liang J, Sumathy K. Review on dye-sensitized solar cells (DSSCs): Fundamental concepts and novel materials. Renew Sustain Energy Rev 2012;16:5848–60. doi:10.1016/j.rser.2012.04.044.

[4] Millington KR. Encyclopedia of Electrochemical Power Sources. Elsevier; 2009. doi:10.1016/B978-044452745-5.00317-8.

[5] Perlin J. Silicon Solar Cell Turns 50 2004.

[6] Grant CD, Schwartzberg AM, Smestad GP, Kowalik J, Tolbert LM, Zhang JZ. Characterization of nanocrystalline and thin film TiO2 solar cells with poly(3-undecyl-2,2′-bithiophene) as a sensitizer and hole conductor. J Electroanal Chem 2002;522:40–8. doi:10.1016/S0022-0728(01)00715-X.

[7] Reagen BO, Gratzel M. A Low-Cost , High-Efficiency Solar Cell Based on Dye-Sensitized Colloidal Ti02 Films. Lett to Nat 1991;350:737–9.

[8] Robertson N. Optimizing dyes for dye-sensitized solar cells. Angew Chem Int Ed Engl 2006;45:2338–45. doi:10.1002/anie.200503083.

[9] Hagfeldt A, Boschloo G, Sun L, Kloo L, Pettersson H. Dye-sensitized solar cells. Chem Rev 2010;110:6595–663. doi:10.1021/cr900356p.

[10] Nazeeruddin MK, De Angelis F, Fantacci S, Selloni A, Viscardi G, Liska P, et al. Combined experimental and DFT-TDDFT computational study of photoelectrochemical cell ruthenium sensitizers. J Am Chem Soc 2005;127:16835–47. doi:10.1021/ja052467l.

[11] Yum J-H, Baranoff E, Wenger S, Nazeeruddin MK, Grätzel M. Panchromatic engineering for dye-sensitized solar cells. Energy Environ Sci 2011;4:842–57. doi:10.1039/C0EE00536C.

[12] Grätzel M. Conversion of sunlight to electric power by nanocrystalline dye-sensitized solar cells. J Photochem Photobiol A Chem 2004;164:3–14. doi:10.1016/j.jphotochem.2004.02.023.

[13] Hara K, Sato T, Katoh R, Furube A, Ohga Y, Shinpo A, et al. Molecular Design of Coumarin Dyes for Efficient Dye-Sensitized Solar Cells. J Phys Chem B 2003;107:597–606. doi:10.1021/jp026963x.

[14] Anderson NA, Lian T. ULTRAFAST ELECTRON TRANSFER AT THE MOLECULE-SEMICONDUCTOR NANOPARTICLE INTERFACE 2004.

[15] Sima C, Grigoriu C, Antohe S. Comparison of the dye-sensitized solar cells performances based on transparent conductive ITO and FTO. Thin Solid Films 2010;519:595–7. doi:10.1016/j.tsf.2010.07.002.

[16] Murakami TN, Kijitori Y, Kawashima N, Miyasaka T. Low temperature preparation of mesoporous TiO2 films for efficient dye-sensitized photoelectrode by chemical vapor deposition combined with UV light irradiation. J Photochem Photobiol A Chem 2004;164:187–91. doi:10.1016/j.jphotochem.2003.11.021.

[17] Ito S, Ha N-LC, Rothenberger G, Liska P, Comte P, Zakeeruddin SM, et al. High-efficiency (7.2%) flexible dye-sensitized solar cells with Ti-metal substrate for nanocrystalline-TiO2 photoanode. Chem Commun (Camb) 2006:4004–6. doi:10.1039/b608279c.

[18] Weerasinghe HC, Huang F, Cheng Y-B. Fabrication of flexible dye sensitized solar cells on plastic substrates. Nano Energy 2013;2:174–89. doi:10.1016/j.nanoen.2012.10.004.

[19] Jun Y, Kim J, Kang MG. A study of stainless steel-based dye-sensitized solar cells and modules. Sol Energy Mater Sol Cells 2007;91:779–84. doi:10.1016/j.solmat.2007.01.007.

[20] Kuppuswamy Kalyanasundaram. Dye-sensitized Solar Cells. Taylor and Francis group; 2010. doi:N10076.

[21] Hoffmann MR, Martin ST, Choi W, Bahnemann DW. Environmental Applications of Semiconductor Photocatalysis. Chem Rev 1995;95:69–96. doi:10.1021/cr00033a004.

[22] Lupan O, Guérin VM, Tiginyanu IM, Ursaki VV, Chow L, Heinrich H, et al. Well-aligned arrays of vertically oriented ZnO nanowires electrodeposited on ITO-coated glass and their integration in dye sensitized solar cells. J Photochem Photobiol A Chem 2010;211:65–73. doi:10.1016/j.jphotochem.2010.02.004.

[23] JEET-Journal of Electrical Engineering & Technology n.d. http://home.jeet.or.kr/archives/view_articles.asp?seq=132 (accessed March 18, 2015).

[24] Fukai Y, Kondo Y, Mori S, Suzuki E. Highly efficient dye-sensitized SnO2 solar cells having sufficient electron diffusion length. Electrochem Commun 2007;9:1439–43. doi:10.1016/j.elecom.2007.01.054.

[25] Christophe Bauer, Gerrit Boschloo, Emad Mukhtar and AH. ultra electron injection in Ru dye sensitized SnO2 nanocrystalline thin film. Int J Photoenergy 2002;4:17–20.

[26] O'Regan B, Grätzel M. A low-cost, high-efficiency solar cell based on dye-sensitized colloidal TiO2 films. Nature 1991;353:737–40. doi:10.1038/353737a0.

[27] King RB, Crabtree RH, Lukehart CM, Atwood DA, Scott RA, editors. Encyclopedia of Inorganic Chemistry. Chichester, UK: John Wiley & Sons, Ltd; 2006.

[28] Park N-G, van de Lagemaat J, Frank AJ. Comparison of Dye-Sensitized Rutile- and Anatase-Based TiO 2 Solar Cells. J Phys Chem B 2000;104:8989–94. doi:10.1021/jp994365l.

[29] Longo C, De Paoli M-A. Dye-sensitized solar cells: a successful combination of materials. J Braz Chem Soc 2003;14:898–901. doi:10.1590/S0103-50532003000600005.

[30] Song MY, Kim DK, Ihn KJ, Jo SM, Kim DY. Electrospun TiO 2 electrodes for dye-sensitized solar cells. Nanotechnology 2004;15:1861–5. doi:10.1088/0957-4484/15/12/030.

[31] Adachi M, Murata Y, Takao J, Jiu J, Sakamoto M, Wang F. Highly efficient dye-sensitized solar cells with a titania thin-film electrode composed of a network structure of single-crystal-like TiO2 nanowires made by the "oriented attachment" mechanism. J Am Chem Soc 2004;126:14943–9. doi:10.1021/ja048068s.

[32] Yang S-C, Yang D-J, Kim J, Hong J-M, Kim H-G, Kim I-D, et al. Hollow TiO2 Hemispheres Obtained by Colloidal Templating for Application in Dye-Sensitized Solar Cells. Adv Mater 2008;20:1059–64. doi:10.1002/adma.200701808.

[33] Koo H-J, Kim YJ, Lee YH, Lee WI, Kim K, Park N-G. Nano-embossed Hollow Spherical TiO2 as Bifunctional Material for High-Efficiency Dye-Sensitized Solar Cells. Adv Mater 2008;20:195–9. doi:10.1002/adma.200700840.

[34] Park H, Kim W-R, Jeong H-T, Lee J-J, Kim H-G, Choi W-Y. Fabrication of dye-sensitized solar cells by transplanting highly ordered TiO2 nanotube arrays. Sol Energy Mater Sol Cells 2011;95:184–9. doi:10.1016/j.solmat.2010.02.017.

[35] Wang Z-S, Kawauchi H, Kashima T, Arakawa H. Significant influence of TiO2 photoelectrode morphology on the energy conversion efficiency of N719 dye-

sensitized solar cell. Coord Chem Rev 2004;248:1381–9. doi:10.1016/j.ccr.2004.03.006.

[36] Liao J-Y, He J-W, Xu H, Kuang D-B, Su C-Y. Effect of TiO2 morphology on photovoltaic performance of dye-sensitized solar cells: nanoparticles, nanofibers, hierarchical spheres and ellipsoid spheres. J Mater Chem 2012;22:7910. doi:10.1039/c2jm16148f.

[37] Feng L, Jia J, Fang Y, Zhou X, Lin Y. TiO2 flowers and spheres for ionic liquid electrolytes based dye-sensitized solar cells. Electrochim Acta 2013;87:629–36. doi:10.1016/j.electacta.2012.09.037.

[38] Chou C-S, Chou F-C, Kang J-Y. Preparation of ZnO-coated TiO2 electrodes using dip coating and their applications in dye-sensitized solar cells. Powder Technol 2012;215-216:38–45. doi:10.1016/j.powtec.2011.09.003.

[39] Cho T-Y, Ko K-W, Yoon S-G, Sekhon SS, Kang MG, Hong Y-S, et al. Efficiency enhancement of flexible dye-sensitized solar cell with sol–gel formed Nb2O5 blocking layer. Curr Appl Phys 2013;13:1391–6. doi:10.1016/j.cap.2013.04.012.

[40] Kumara GRRA, Tennakone K, Perera VPS, Konno A, Kaneko S, Okuya M. Suppression of recombinations in a dye-sensitized photoelectrochemical cell made from a film of tin IV oxide crystallites coated with a thin layer of aluminium oxide. J Phys D Appl Phys 2001;34:868–73. doi:10.1088/0022-3727/34/6/306.

[41] Nguyen T-V, Lee H-C, Alam Khan M, Yang O-B. Electrodeposition of TiO2/SiO2 nanocomposite for dye-sensitized solar cell. Sol Energy 2007;81:529–34. doi:10.1016/j.solener.2006.07.008.

[42] Palomares E, Clifford JN, Haque SA, Lutz T, Durrant JR. Control of charge recombination dynamics in dye sensitized solar cells by the use of conformally deposited metal oxide blocking layers. J Am Chem Soc 2003;125:475–82. doi:10.1021/ja027945w.

[43] Choi H, Nahm C, Kim J, Moon J, Nam S, Jung D-R, et al. The effect of TiCl4-treated TiO2 compact layer on the performance of dye-sensitized solar cell. Curr Appl Phys 2012;12:737–41. doi:10.1016/j.cap.2011.10.011.

[44] Vesce L, Riccitelli R, Soscia G, Brown TM, Di Carlo A, Reale A. Optimization of nanostructured titania photoanodes for dye-sensitized solar cells: Study and experimentation of TiCl4 treatment. J Non Cryst Solids 2010;356:1958–61. doi:10.1016/j.jnoncrysol.2010.05.070.

[45] Melhem H, Simon P, Wang J, Di Bin C, Ratier B, Leconte Y, et al. Direct photocurrent generation from nitrogen doped TiO2 electrodes in solid-state dye-sensitized solar cells: Towards optically-active metal oxides for photovoltaic

applications. Sol Energy Mater Sol Cells 2013;117:624–31. doi:10.1016/j.solmat.2012.08.017.

[46] Giribabu L, Singh VK, Jella T, Soujanya Y, Amat A, De Angelis F, et al. Sterically demanded unsymmetrical zinc phthalocyanines for dye-sensitized solar cells. Dye Pigment 2013;98:518–29. doi:10.1016/j.dyepig.2013.04.007.

[47] Balraju P, Kumar M, Roy MS, Sharma GD. Dye sensitized solar cells (DSSCs) based on modified iron phthalocyanine nanostructured TiO2 electrode and PEDOT:PSS counter electrode. Synth Met 2009;159:1325–31. doi:10.1016/j.synthmet.2009.03.001.

[48] Huang H, Cao Z, Li X, Zhang L, Liu X, Zhao H, et al. Synthesis and photovoltaic properties of two new unsymmetrical zinc-phthalocyanine dyes. Synth Met 2012;162:2316–21. doi:10.1016/j.synthmet.2012.11.007.

[49] Seo KD, Song HM, Lee MJ, Pastore M, Anselmi C, De Angelis F, et al. Coumarin dyes containing low-band-gap chromophores for dye-sensitised solar cells. Dye Pigment 2011;90:304–10. doi:10.1016/j.dyepig.2011.01.009.

[50] Hara K, Tachibana Y, Ohga Y, Shinpo A, Suga S, Sayama K, et al. Dye-sensitized nanocrystalline TiO2 solar cells based on novel coumarin dyes. Sol Energy Mater Sol Cells 2003;77:89–103. doi:10.1016/S0927-0248(02)00460-9.

[51] Justin Thomas KR, Singh P, Baheti A, Hsu Y-C, Ho K-C, Lin JT. Electro-optical properties of new anthracene based organic dyes for dye-sensitized solar cells. Dye Pigment 2011;91:33–43. doi:10.1016/j.dyepig.2011.02.006.

[52] Mikroyannidis JA, Tsagkournos DV, Sharma SS, Kumar A, Vijay YK, Sharma GD. Efficient bulk heterojunction solar cells based on low band gap bisazo dyes containing anthracene and/or pyrrole units. Sol Energy Mater Sol Cells 2010;94:2318–27. doi:10.1016/j.solmat.2010.08.001.

[53] Xiang N, Zhou W, Jiang S, Deng L, Liu Y, Tan Z, et al. Synthesis and characterization of trivalent metal porphyrin with NCS ligand for application in dye-sensitized solar cells. Sol Energy Mater Sol Cells 2011;95:1174–81. doi:10.1016/j.solmat.2010.12.051.

[54] Panda MK, Ladomenou K, Coutsolelos AG. Porphyrins in bio-inspired transformations: Light-harvesting to solar cell. Coord Chem Rev 2012;256:2601–27. doi:10.1016/j.ccr.2012.04.041.

[55] Zhou W, Zhao B, Shen P, Jiang S, Huang H, Deng L, et al. Multi-alkylthienyl appended porphyrins for efficient dye-sensitized solar cells. Dye Pigment 2011;91:404–12. doi:10.1016/j.dyepig.2011.05.017.

[56] Kuppuswamy Kalyanasundaram MG. Efficient Dye-Sensitized Solar Cells for Direct Conversion of Sunlight to Electricity. Mater Matters n.d.;4.

[57] Polo AS, Itokazu MK, Murakami Iha NY. Metal complex sensitizers in dye-sensitized solar cells. Coord Chem Rev 2004;248:1343–61. doi:10.1016/j.ccr.2004.04.013.

[58] Takahashi Y, Arakawa H, Sugihara H, Hara K, Islam A, Katoh R, et al. Highly efficient polypyridyl-ruthenium(II) photosensitizers with chelating oxygen donor ligands: β-diketonato-bis(dicarboxybipyridine)ruthenium. Inorganica Chim Acta 2000;310:169–74. doi:10.1016/S0020-1693(00)00279-6.

[59] Yanagida M, Islam A, Tachibana Y, Fujihashi G, Katoh R, Sugihara H, et al. Dye-sensitized solar cells based on nanocrystalline TiO2 sensitized with a novel pyridylquinoline ruthenium(ii) complex. New J Chem 2002;26:963–5. doi:10.1039/b202975h.

[60] Nazeeruddin MK, Kay A, Rodicio I, Humphry-Baker R, Mueller E, Liska P, et al. Conversion of light to electricity by cis-X2bis(2,2’-bipyridyl-4,4'-dicarboxylate)ruthenium(II) charge-transfer sensitizers (X = Cl-, Br-, I-, CN-, and SCN-) on nanocrystalline titanium dioxide electrodes. J Am Chem Soc 1993;115:6382–90. doi:10.1021/ja00067a063.

[61] Grätzel M. Recent advances in sensitized mesoscopic solar cells. Acc Chem Res 2009;42:1788–98. doi:10.1021/ar900141y.

[62] Mao M, Wang J-B, Xiao Z-F, Dai S-Y, Song Q-H. New 2,6-modified BODIPY sensitizers for dye-sensitized solar cells. Dye Pigment 2012;94:224–32. doi:10.1016/j.dyepig.2012.01.011.

[63] Mishra A, Fischer MKR, Bäuerle P. Metal-free organic dyes for dye-sensitized solar cells: from structure: property relationships to design rules. Angew Chem Int Ed Engl 2009;48:2474–99. doi:10.1002/anie.200804709.

[64] Horiuchi T, Miura H, Uchida S. Highly efficient metal-free organic dyes for dye-sensitized solar cells. J Photochem Photobiol A Chem 2004;164:29–32. doi:10.1016/j.jphotochem.2003.12.018.

[65] Kuang D, Uchida S, Humphry-Baker R, Zakeeruddin SM, Grätzel M. Organic dye-sensitized ionic liquid based solar cells: remarkable enhancement in performance through molecular design of indoline sensitizers. Angew Chem Int Ed Engl 2008;47:1923–7. doi:10.1002/anie.200705225.

[66] Howie WH, Claeyssens F, Miura H, Peter LM. Characterization of solid-state dye-sensitized solar cells utilizing high absorption coefficient metal-free organic dyes. J Am Chem Soc 2008;130:1367–75. doi:10.1021/ja076525+.

[67] Horiuchi T, Miura H, Sumioka K, Uchida S. High efficiency of dye-sensitized solar cells based on metal-free indoline dyes. J Am Chem Soc 2004;126:12218–9. doi:10.1021/ja0488277.

[68] KONNO A, KUMARA GRA, KANEKO S, ONWONA-AGYEMAN B, TENNAKONE K. Solid-state solar cells sensitized with indoline dye. Chem Lett n.d.;36:716–7.

[69] Dai Q, Rabani J. Unusually efficient photosensitization of nanocrystalline TiO2 films by pomegranate pigments in aqueous medium. New J Chem 2002;26:421–6. doi:10.1039/b108390b.

[70] Narayan MR. Review: Dye sensitized solar cells based on natural photosensitizers. Renew Sustain Energy Rev 2011;16:208–15. doi:10.1016/j.rser.2011.07.148.

[71] Calogero G, Di Marco G, Cazzanti S, Caramori S, Argazzi R, Di Carlo A, et al. Efficient dye-sensitized solar cells using red turnip and purple wild sicilian prickly pear fruits. Int J Mol Sci 2010;11:254–67. doi:10.3390/ijms11010254.

[72] Lai WH, Su YH, Teoh LG, Hon MH. Commercial and natural dyes as photosensitizers for a water-based dye-sensitized solar cell loaded with gold nanoparticles. J Photochem Photobiol A Chem 2008;195:307–13. doi:10.1016/j.jphotochem.2007.10.018.

[73] Kumara GRA, Kaneko S, Okuya M, Onwona-Agyeman B, Konno A, Tennakone K. Shiso leaf pigments for dye-sensitized solid-state solar cell. Sol Energy Mater Sol Cells 2006;90:1220–6. doi:10.1016/j.solmat.2005.07.007.

[74] Zhou H, Wu L, Gao Y, Ma T. Dye-sensitized solar cells using 20 natural dyes as sensitizers. J Photochem Photobiol A Chem 2011;219:188–94. doi:10.1016/j.jphotochem.2011.02.008.

[75] Kusama H, Arakawa H. Influence of pyrazole derivatives in I−/I3− redox electrolyte solution on Ru(II)-dye-sensitized TiO2 solar cell performance. Sol Energy Mater Sol Cells 2005;85:333–44. doi:10.1016/j.solmat.2004.05.003.

[76] Nogueira AF, Longo C, De Paoli M-A. Polymers in dye sensitized solar cells: overview and perspectives. Coord Chem Rev 2004;248:1455–68. doi:10.1016/j.ccr.2004.05.018.

[77] Wang Z-S, Sayama K, Sugihara H. Efficient eosin y dye-sensitized solar cell containing Br-/Br3- electrolyte. J Phys Chem B 2005;109:22449–55. doi:10.1021/jp053260h.

[78] Bergeron B V, Marton A, Oskam G, Meyer GJ. Dye-sensitized SnO2 electrodes with iodide and pseudohalide redox mediators. J Phys Chem B 2005;109:937–43. doi:10.1021/jp0461347.

[79] Oskam G, Bergeron B V., Meyer GJ, Searson PC. Pseudohalogens for Dye-Sensitized TiO 2 Photoelectrochemical Cells. J Phys Chem B 2001;105:6867–73. doi:10.1021/jp004411d.

[80] Sapp SA, Elliott CM, Contado C, Caramori S, Bignozzi CA. Substituted Polypyridine Complexes of Cobalt(II/III) as Efficient Electron-Transfer Mediators in Dye-Sensitized Solar Cells. J Am Chem Soc 2002;124:11215–22. doi:10.1021/ja027355y.

[81] Wu J, Lan Z, Hao S, Li P, Lin J, Huang M, et al. Progress on the electrolytes for dye-sensitized solar cells. Pure Appl Chem 2008;80:2241–58. doi:10.1351/pac200880112241.

[82] Boschloo G, Hagfeldt A. Characteristics of the iodide/triiodide redox mediator in dye-sensitized solar cells. Acc Chem Res 2009;42:1819–26. doi:10.1021/ar900138m.

[83] Fukui A, Komiya R, Yamanaka R, Islam A, Han L. Effect of a redox electrolyte in mixed solvents on the photovoltaic performance of a dye-sensitized solar cell. Sol Energy Mater Sol Cells 2006;90:649–58. doi:10.1016/j.solmat.2005.01.020.

[84] Kebede Z, Lindquist S-E. Donor–acceptor interaction between non-aqueous solvents and I2 to generate I−3, and its implication in dye sensitized solar cells. Sol Energy Mater Sol Cells 1999;57:259–75. doi:10.1016/S0927-0248(98)00178-0.

[85] Wu J, Lan Z, Lin J, Huang M, Li P. Effect of solvents in liquid electrolyte on the photovoltaic performance of dye-sensitized solar cells. J Power Sources 2007;173:585–91. doi:10.1016/j.jpowsour.2007.04.085.

[86] Stergiopoulos T, Rozi E, Karagianni C-S, Falaras P. Influence of electrolyte co-additives on the performance of dye-sensitized solar cells. Nanoscale Res Lett 2011;6:307. doi:10.1186/1556-276X-6-307.

[87] Zakeeruddin SM, Grätzel M. Solvent-Free Ionic Liquid Electrolytes for Mesoscopic Dye-Sensitized Solar Cells. Adv Funct Mater 2009;19:2187–202. doi:10.1002/adfm.200900390.

[88] Wang P, Zakeeruddin SM, Moser J-E, Grätzel M. A New Ionic Liquid Electrolyte Enhances the Conversion Efficiency of Dye-Sensitized Solar Cells. J Phys Chem B 2003;107:13280–5. doi:10.1021/jp0355399.

[89] Kubo W, Kitamura T, Hanabusa K, Wada Y, Yanagida S. Quasi-solid-state dye-sensitized solar cells using room temperature molten salts and a low molecular weight gelator. Chem Commun 2002:374–5. doi:10.1039/b110019j.

[90] Abate A, Petrozza A, Roiati V, Guarnera S, Snaith H, Matteucci F, et al. A polyfluoroalkyl imidazolium ionic liquid as iodide ion source in dye sensitized solar cells. Org Electron 2012;13:2474–8. doi:10.1016/j.orgel.2012.07.009.

[91] Guo L, Pan X, Zhang C, Liu W, Wang M, Fang X, et al. Ionic liquid electrolyte based on S-propyltetrahydrothiophenium iodide for dye-sensitized solar cells. Sol Energy 2010;84:373–8. doi:10.1016/j.solener.2009.11.008.

[92] Jhong H-R, Wong DS-H, Wan C-C, Wang Y-Y, Wei T-C. A novel deep eutectic solvent-based ionic liquid used as electrolyte for dye-sensitized solar cells. Electrochem Commun 2009;11:209–11. doi:10.1016/j.elecom.2008.11.001.

[93] Bach U, Lupo D, Comte P, Moser JE, Weissortel F, Salbeck J, et al. Solid-state dye-sensitized mesoporous TiO2 solar cells with high photon-to-electron conversion efficiencies 1998;395:583–5. doi:10.1038/26936.

[94] Hao S, Wu J, Fan L, Huang Y, Lin J, Wei Y. The influence of acid treatment of TiO2 porous film electrode on photoelectric performance of dye-sensitized solar cell. Sol Energy 2004;76:745–50. doi:10.1016/j.solener.2003.12.010.

[95] Tennakone K, Perera VPS, Kottegoda IRM, Kumara GRRA. Dye-sensitized solid state photovoltaic cell based on composite zinc oxide/tin (IV) oxide films. J Phys D Appl Phys 1999;32:374–9. doi:10.1088/0022-3727/32/4/004.

[96] Meng Q-B, Takahashi K, Zhang X-T, Sutanto I, Rao TN, Sato O, et al. Fabrication of an Efficient Solid-State Dye-Sensitized Solar Cell. Langmuir 2003;19:3572–4. doi:10.1021/la026832n.

[97] O'Regan B, Schwartz DT. Large Enhancement in Photocurrent Efficiency Caused by UV Illumination of the Dye-Sensitized Heterojunction TiO 2 /RuLL'NCS/CuSCN: Initiation and Potential Mechanisms. Chem Mater 1998;10:1501–9. doi:10.1021/cm9705855.

[98] Tan S, Zhai J, Wan M, Meng Q, Li Y, Jiang L, et al. Influence of Small Molecules in Conducting Polyaniline on the Photovoltaic Properties of Solid-State Dye-Sensitized Solar Cells. J Phys Chem B 2004;108:18693–7. doi:10.1021/jp046574y.

[99] Song JY, Wang YY, Wan CC. Review of gel-type polymer electrolytes for lithium-ion batteries. J Power Sources 1999;77:183–97. doi:10.1016/S0378-7753(98)00193-1.

[100] Mohmeyer N, Wang P, Schmidt H-W, Zakeeruddin SM, Gr?tzel M. Quasi-solid-state dye sensitized solar cells with 1,3:2,4-di-O-benzylidene-d-sorbitol derivatives as low molecular weight organic gelators. J Mater Chem 2004;14:1905. doi:10.1039/b402324b.

[101] Wu JH, Lan Z, Lin JM, Huang ML, Hao SC, Sato T, et al. A Novel Thermosetting Gel Electrolyte for Stable Quasi-Solid-State Dye-Sensitized Solar Cells. Adv Mater 2007;19:4006–11. doi:10.1002/adma.200602886.

[102] Lan Z, Wu J, Wang D, Hao S, Lin J, Huang Y. Quasi-solid state dye-sensitized solar cells based on gel polymer electrolyte with poly(acrylonitrile-co-styrene)/NaI+I2. Sol Energy 2006;80:1483–8. doi:10.1016/j.solener.2005.11.007.

[103] Wu JH, Hao SC, Lan Z, Lin JM, Huang ML, Huang YF, et al. A Thermoplastic Gel Electrolyte for Stable Quasi-Solid-State Dye-Sensitized Solar Cells. Adv Funct Mater 2007;17:2645–52. doi:10.1002/adfm.200600621.

[104] Komiya R, Han L, Yamanaka R, Islam A, Mitate T. Highly efficient quasi-solid state dye-sensitized solar cell with ion conducting polymer electrolyte. J Photochem Photobiol A Chem 2004;164:123–7. doi:10.1016/j.jphotochem.2003.11.015.

[105] Wang P, Zakeeruddin SM, Moser JE, Nazeeruddin MK, Sekiguchi T, Gratzel M. A stable quasi-solid-state dye-sensitized solar cell with an amphiphilic ruthenium sensitizer and polymer gel electrolyte 2003;2:498.

[106] Papageorgiou N. An Iodine/Triiodide Reduction Electrocatalyst for Aqueous and Organic Media. J Electrochem Soc 1997;144:876. doi:10.1149/1.1837502.

[107] Tsekouras G, Mozer AJ, Wallace GG. Enhanced Performance of Dye Sensitized Solar Cells Utilizing Platinum Electrodeposit Counter Electrodes. J Electrochem Soc 2008;155:K124. doi:10.1149/1.2919107.

[108] Fang X, Ma T, Guan G, Akiyama M, Abe E. Performances characteristics of dye-sensitized solar cells based on counter electrodes with Pt films of different thickness. J Photochem Photobiol A Chem 2004;164:179–82. doi:10.1016/j.jphotochem.2003.12.024.

[109] Khelashvili G, Behrens S, Weidenthaler C, Vetter C, Hinsch A, Kern R, et al. Catalytic platinum layers for dye solar cells: A comparative study. Thin Solid Films 2006;511-512:342–8. doi:10.1016/j.tsf.2005.12.059.

[110] Syrrokostas G, Siokou A, Leftheriotis G, Yianoulis P. Degradation mechanisms of Pt counter electrodes for dye sensitized solar cells. Sol Energy Mater Sol Cells 2012;103:119–27. doi:10.1016/j.solmat.2012.04.021.

. CHAPTER 3

NOVEL 1,3,4-OXADIAZOL BASED PHOTOSENSITIZERS FOR DYE SENSITIZED SOLAR CELLS (DSSCS)

Umer Mehmood[1], Khalil Harrabi[2], M. B. Mekki[2], Shakeel Ahmed[3], Ibnelwaleed A. Hussein[1*]

[1] Department of Chemical Engineering, King Fahd University of Petroleum & Minerals (KFUPM), P. O. Box 5050, Dhahran 31261, Kingdom of Saudi Arabia

[2] Department of physics, (KFUPM), P. O. Box 5050, Dhahran 31261, Kingdom of Saudi Arabia

[3] Center for Refining & Petrochemicals, KFUPM, P.O. Box 5050, Dhahran 31261, Kingdom of Saudi Arabia

[*]Corresponding Author: Ibnelwaleed A. Hussein , E-mail address:

ihussein@kfupm.edu.sa

This chapter has been submitted in journal of "*Synthesis*"

Abstract

1,3,4-Oxadiazol based photosensitizers were synthesized for solar cell applications. In this work, four oxadiazol based photosensitizers were synthesized by introducing biphenyl, naphthalene, anthracene and triphenyl amin as electron-donating moieties. The electrochemical and optical properties of these sensitizers were investigated .These photosensitizers were then employed in solar cells. The UV-Visible absorption spectroscopy, photocurrent–voltage (*I–V*) characteristic and electrochemical impedance spectroscopy (EIS) measurements were carried out to characterize the solar cells. The results indicate that 1,3,4-Oxadiazo pi-spacer with anthracene moiety shows the highest efficiency of 2.58%. Density functional theory and time dependent density functional theory DFT/TD-DFT modeling techniques were used to compute the electronic and optical properties of sensitizers.

Keywords: 1,3,4-Oxadiazol, electron-donating moieties, efficiency, Density functional theory

3.1. Introduction

Inorganic silicon based solar cells are being currently used for the conversion of photo energy on a commercial scale because of their high efficiency [1]. However, the need of highly purified silicon, use of toxic chemicals in their manufacture, and the high cost has restricted their worldwide use. These constraints encouraged the search for low cost and environmentally friendly solar cells. In this context, dye-sensitized solar cells (DSSCs) have received widespread attention in recent years because of their ease of processing and the low cost [2-7].

Dye is the major component of DSSCs, which absorbs incoming sunlight and produce excitons [8, 9]. The photosensitizer, which is chemically bonded to the porous surface of the semiconductor, can be a metal complex or a metal-free organic sensitizer. But metal free organic photosensitizers are preferred over ruthenium based sensitizers because of their low cost and good transport properties. The basic structural unit of metal-free dyes is the donor-pi-spacer-acceptor (D-π-A) unit and the photovoltaic properties of such dyes can be fine tuned by selecting suitable groups within the D-π -A structure [10]. These results suggest that the donor groups to form efficient sensitizers should be selected from the electron rich aryl amines family including phenylamine, aminocoumarin, indoline, and (difluorenyl)triphenylamine [8]. Many organic groups have been used as pi-spacer to tune the electrical and optical properties of light sensitive materials [11]. The best known organic compounds for obtaining such properties are porphyrins [12], styrylarylenes [13], perylenes [14], benzofurans [15], indoles [16], thiazole [17, 18] and oxadiazole [19]. Among them, the oxadiazole derivatives are considered the most efficient electron transport materials owing to their good thermal and chemical stabilities and high quantum

yield [20]. Many studies have shown that 2-(4-biphenylyl)-5-(4-tertbutylphenyl)-(1, 3, 4) oxadiazole exhibits excellent charge transport properties [19, 21-24]. Tian and co-workers successfully synthesized the naphthalimide derivatives containing the oxadiazole moiety. They found that oxadiazole moiety increases the electron injection properties and minimizes the carrier recombination [21].

The density functional theory (DFT) and time-dependent DFT (TD-DFT) can provide a deeper understanding of the relationship between molecular structure and properties of compounds. Thus, theoretical calculations are important to design new and efficient dyes for DSSCs [25-32]. DFT is used because it is the only ab initio method able to do the calculation at a cost acceptable for routine use. Here, the aim is to study the theoretical and experimental studies of novel oxadiazole based organic dyes and establish their structure-performance relationship for application in DSSCs.

3.2. Computational Detail

All the DFT/TD-DFT calculations were executed using Amsterdam Density Functional (ADF) program (2013.01).BAND mode was used to simulate the anatase TiO_2 cluster. Here, we selected tetragonal anatase crystal structure with single layer (001) surface slab. Then, a 4×1 supercell was created from this slab. All atoms were maped within the unit cell. The ground state geometries of oxadiazole dyes were optimized by applying generalized gradient approximation (GGA) at OLYP. The $(TiO_2)_8$ nano-particle cluster was also simulated by considering GGA at Becke, parameter,Lee-Yang-Parr (BYLP) level with triple-ζ polarization basis function. In all the calculations, the relativistic effects were taken into account by the zero order regular approximation (ZORA) Hamiltonian in its scalar approximation.

3.3. Experimental and Characterization

3.3.1. Designed system

The structures and names of new class of dyes are shown in Fig. 1. In these structures, biphenyl, naphthalene, anthracene and triphenyl amin were used as the electron-donating moiety and carboxyl and cyano groups (-COOH and -CN) were introduced as the electron acceptor and the anchor group because of their high electron-withdrawing ability and strong bonding to the semiconductor. 1,3,4-Oxadiazole was used as the π-conjugation system, which bridges the donor-acceptor systems. A double bond and a thiophene unit were also introduced to the pi-conjugation system to fine tune the planar molecular configuration and to broaden the absorption spectra. The performance of the dyes was tested with different isomers of oxadizoles as the π-conjugated bridge.

3.3.2. Fabrication of DSSCs

A 2 mM solution of each dye was prepared in methanol. The composite electrodes were soaked in the dye solution for 24 hours. After sensitization, the samples were washed with ethanol to eliminate unanchored dye. Then, DSSCs were fabricated employing the sensitized hybrid anode, platinum deposited counter electrode (Plasticol T, Solaronix), 60 μm sealing spacer (Meltonix 1170, Solaronix) and I^-/I_3^- redox couple electrolyte prepared in methoxypropionitrile with a 50 mM redox concentration (Iodolyte Z-50, Solaronix).

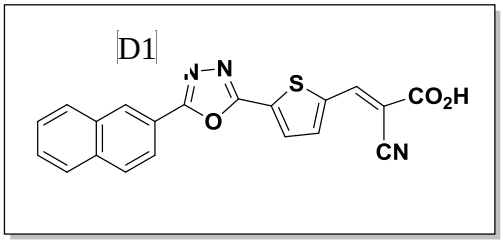

Moleclular Formula: $C_{20}H_{11}N_3O_3S$

MW: 373.5

(*E*)-2-Cyano-3-(5-(5-(naphthalen-2-yl)-1,3,4-oxadiazol-2-yl) thiophen-2-yl)acrylic acid

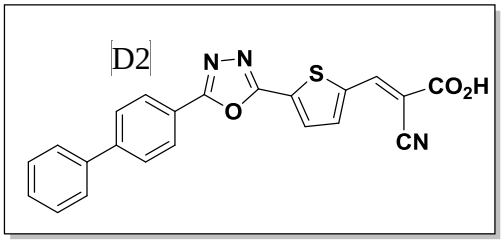

Moleclular Formula: $C_{22}H_{13}N_3O_3S$

MW: 399.07

(*E*)-3-(5-(5-([1,1'-Biphenyl]-4-yl)-1,3,4-oxadiazol-2-yl) thiophen-2-yl)-2-cyanoacrylic acid

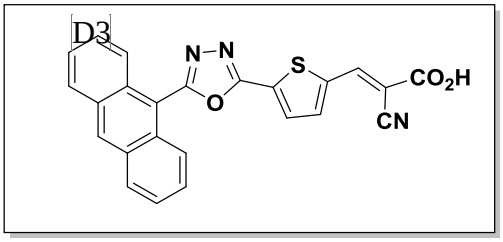

Moleclular Formula: $C_{24}H_{13}N_3O_3S$

MW: 423.07

(*E*)-3-(5-(5-(Anthracen-9-yl)-1,3,4-oxadiazol-2-yl)thiophen-2-yl)-2-cyanoacrylic acid

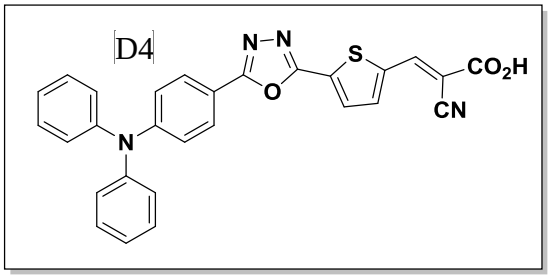

Moleclular Formula: $C_{28}H_{18}N_4O_3S$

MW: 490.5

(*E*)-2-Cyano-3-(5-(5-(4-(diphenylamino)phenyl)-1,3,4-oxadiazol-2-yl) thiophen-2-yl)acrylic acid

Fig 3-1: Structures of novel 1,3,4-Oxadiazol based photosensitizers

3.3.3. Characterization of DSSCs

The visible spectra of dyes in methanol and anchored to TiO_2 films at glass substrates were recorded with JASCO-670 UV/VIS spectrophotometer. Keithley 2400 Source Meter was used to measure the $I-V$ characteristics of the DSSCs using IV-5 solar simulator (Sr #83, PV Measurement, Inc) at AM1.5G (100 $mWcm^{-2}$). The silicon solar cell was used as a reference for calibration. The impedance spectroscopy (EIS) was measured in dark conditions of illumination via Bio-Logic SAS (VMP3, s/n:0373), with an AC signal of 10 mV in amplitude, in the frequency range between 10 Hz and 500KHz.

3.4. Results and Discussion

3.4.1. Energy levels of photosensitizers

The HOMOs, LUMOs, and the band gap energies of the photosensitizers play an important role in providing the thermodynamic driving force for the electron injection. For efficient charge transfer, the LUMOs of dyes must be more negative than the conduction band of the semiconductor while HOMO levels must be more positive than the redox potential of electrolyte. We used a DFT technique to find the band gap of TiO_2 and novel photosensitizers. The electron distribution of the HOMOs and LUMOs of D1, D2, D3 and D4 are shown in Fig.2. Clearly, the HOMOs of these compounds are the highest electron density located at donor moieties. The LUMOs are located in the anchoring group through the pi-bridge. Thus, the HOMO-LUMO excitation induced by light irradiation could move the electron distribution from the donor moieties to the anchoring unit through the pi-bridge segment. The interface between the sensitizer and TiO_2 plays an important role in the electron injection efficiency. Though $(TiO_2)_n$ clusters

(n = 4, 6, 8) were simulated, $(TiO_2)_8$ containing model was selected because of its balanced electronic properties (conduction band ~ -4.0 eV and band gap 3.18 eV).

Table-1 shows that the HOMO levels of the dyes are in the order of D3 (-4.689) >D4 (-5.180) >D1(-5.657)>D2 (-5.682). While, LUMOs energy levels are in the order of D3 (-3.694) > D4 (-3.840) > D2 (-3.867)>D1 (-3.956). The electron donating moitied significantly affect the HOMO and LUMO energy levels of the dyes. Similarly, the H-L_{gap} of the dyes are in the order of D3 (1.175) < D4 (1.340) <D1 (1.701) < D2 (1.815). These results suggest that dyes 1-4 can inject electrons to the conduction band of titanium oxide.

Table 3-1: The frontier molecular orbital (eV) and H-L $_{gap}$ (eV) energies of systems 1-4

Dyes	**LUMOs (eV)**	**HOMOs (eV)**	**Band Gap (eV)**
D1	-3.956	-5.657	1.701
D2	-3.867	-5.682	1.815
D3	-3.694	-4.869	1.175
D4	-3.840	-5.180	1.340

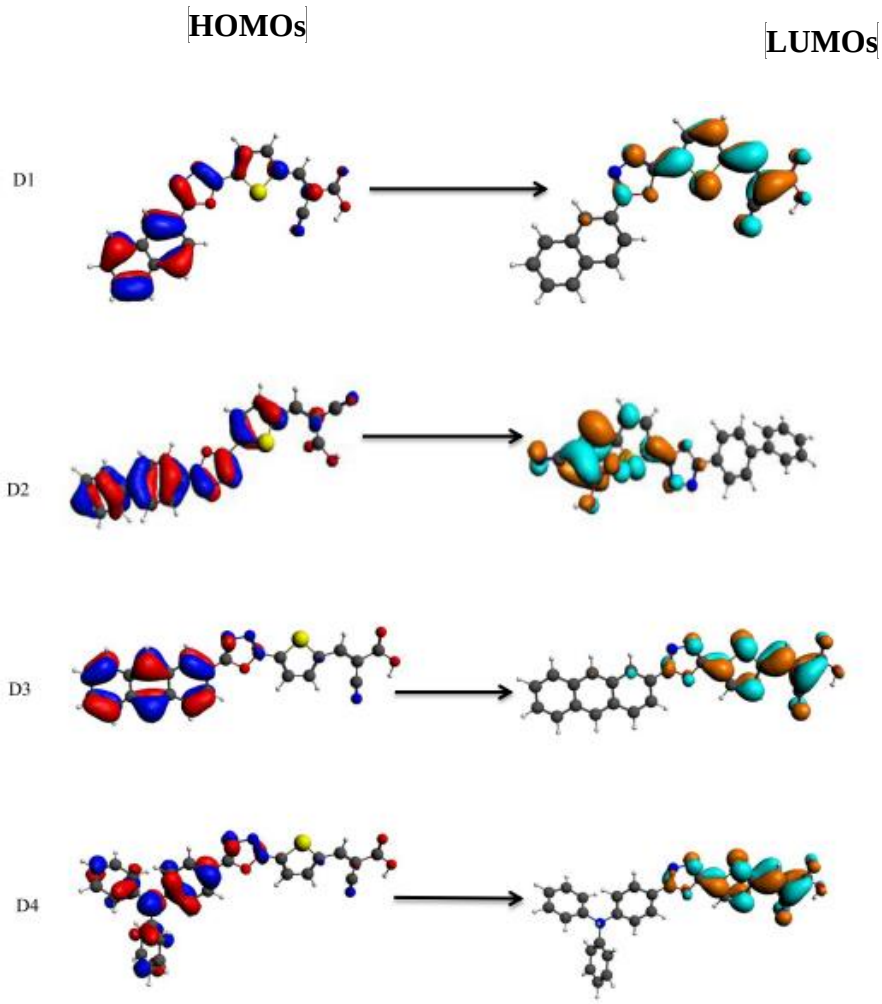

Fig 3-2: Simulated HOMOs and LUMOs of dyes

3.4.2. Optical properties

The UV-Vis absorption spectra of D3 in chloroform and adsorbed on TiO_2 are shown in Fig 3. Two distinct absorption bands of D3 in chloroform can be observed: one relatively weak bond is in the region (380-400 nm) corresponding to the π-π* electron transitions of the conjugated molecules and the other is around 430-460 nm that can be assigned to an intramolecular charge transfer (ICT) between electron-donor and electron acceptor anchoring moieties. However, the absorption shifts to lower energy values when anchored to TiO_2. This is due to the fact that on the electrode the carboxylate groups bind to the TiO_2 surface in which Ti^{4+} acts as proton. The interaction between the carboxylate group and the surface Ti^{4+} ions may lead to increased delocalization of the π* orbital. The energy of the π* level is decreased by this delocalization, which explains the red shift for the absorption spectra.

3.4.3. Photovoltaic performance

Typical solar cells, with an effective area of 0.35 cm^2 are fabricated using D1, D2 D3 and D4 dyes. Short-circuit current density (*Jsc*), open circuit voltage (Voc), fill factor (FF), and photovoltaic conversion efficiency (η) of DSSCs are listed in Table-2 and the corresponding photocurrent evoltage (*I-V*) curves are showed in Fig-4. Among the four dyes, the D3-sensitized cell exhibited the best photovoltaic performance. Based on these parameters, the electron-donating ability of the donor in a dye molecule plays a key role. The electron-donating ability of donor groups is indicated by the LUMOs energy levels. Higher HOMO and LUMO energy levels of D3 do not only generate charge separation, but also accelerate the dye regeneration via fast oxidation of tri-iodide by oxidized dyes,

to avoid charge recombination between oxidized dyes and photo-injected electrons in the TiO2 film, thus enhancing the sensitized cell performance.

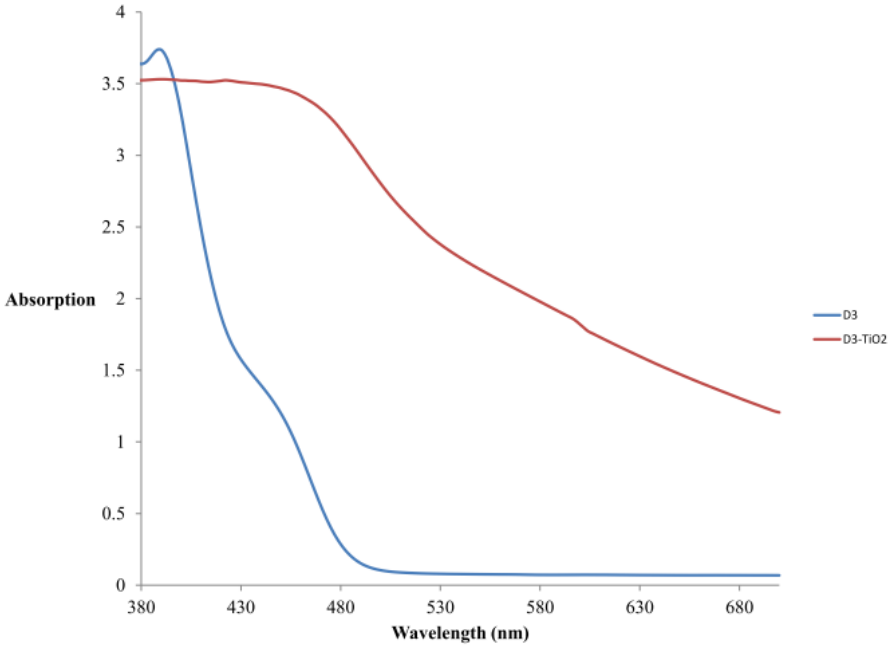

Fig 3-3: UV-Vis absorption spectrum of D3 in chloroform and anchored to TiO_2

Table 3-2: Photovolatic properties of DSSCs based on hybrid anodes

Dye	j_{sc} (mA/cm^2)	V_{oc} (mV)	FF(%)	η (%)
D1	0.479	448	50	0.11
D2	0.952	455	51	0.23
D3	8.178	632	50	2.58
D4	2.196	587	40	0.52

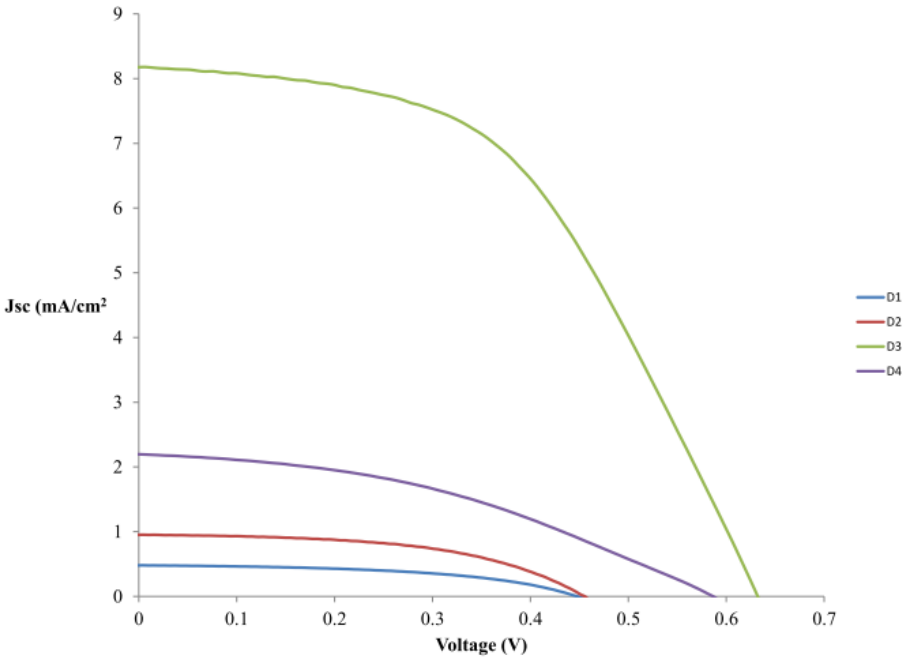

Fig 3-4: Current − voltage curves of DSSCs

3.4.4. Electrochemical impedance spectroscopy (EIS) analysis

EIS analysis is performed to further elucidate the photovoltaic properties. Figure 5 shows the Nyquist plot of DSSCs which were assembled with TiO_2-SQ2 and 0.06%MWCNTS-TiO_2-SQ2. Generally, a normal impedance spectrum of DSSCs is represented by three arcs (semicircles). The first semicircle represents the charge transport resistance at counter electrode/electrolyte (R_1), second signifies the charge transport resistance at the photoanode / electrolyte interface (R_2), and third indicates the diffusion process of I^-/I_3^- redox couple in electrolyte (*Zw)* [33, 34]. Only second arc comes out in the Nyquist plot in the Fig 5. It is probable that the other two arcs corresponding to R_1 and *Zw* are overshadowed by large semicircle reprenting R_2 [35, 36]. The R_2 is related to the charge recombination rate, e.g., a smaller R_2 indicates a faster charge recombination. The R_2 value for DSSC assembled with D3 is greater that of D1, D2 and D4. The higher R_2 of D3 relative to D1, D2 and D3 could be attributed to the steric hindrance of bulky antherence unit.

3.5. Conclusion

A series of novel dyes D1, D2, D3 and D4 have been prepared for dye sensitized solar cells (DSSCs). The results indicate that the donor moiety in organic dyes strongly influences the performance of DSSCs. The incorporation of antherence unit as a donor moiety improves the efficiency of DSSC as compared to other donor units i.e. biphenyl, naphthalene and triphenylamine. Among the four photosensitizers synthesized, maximum efficiency of 2.58% was obtained with a DSSCs based on D3 (J_{sc} = 8.178 mA/cm^2, V_{oc} =632 Mv , FF =0.5). These results advocates that the photosensitizers based on antherence unit are auspicious candidates for DSSCs.

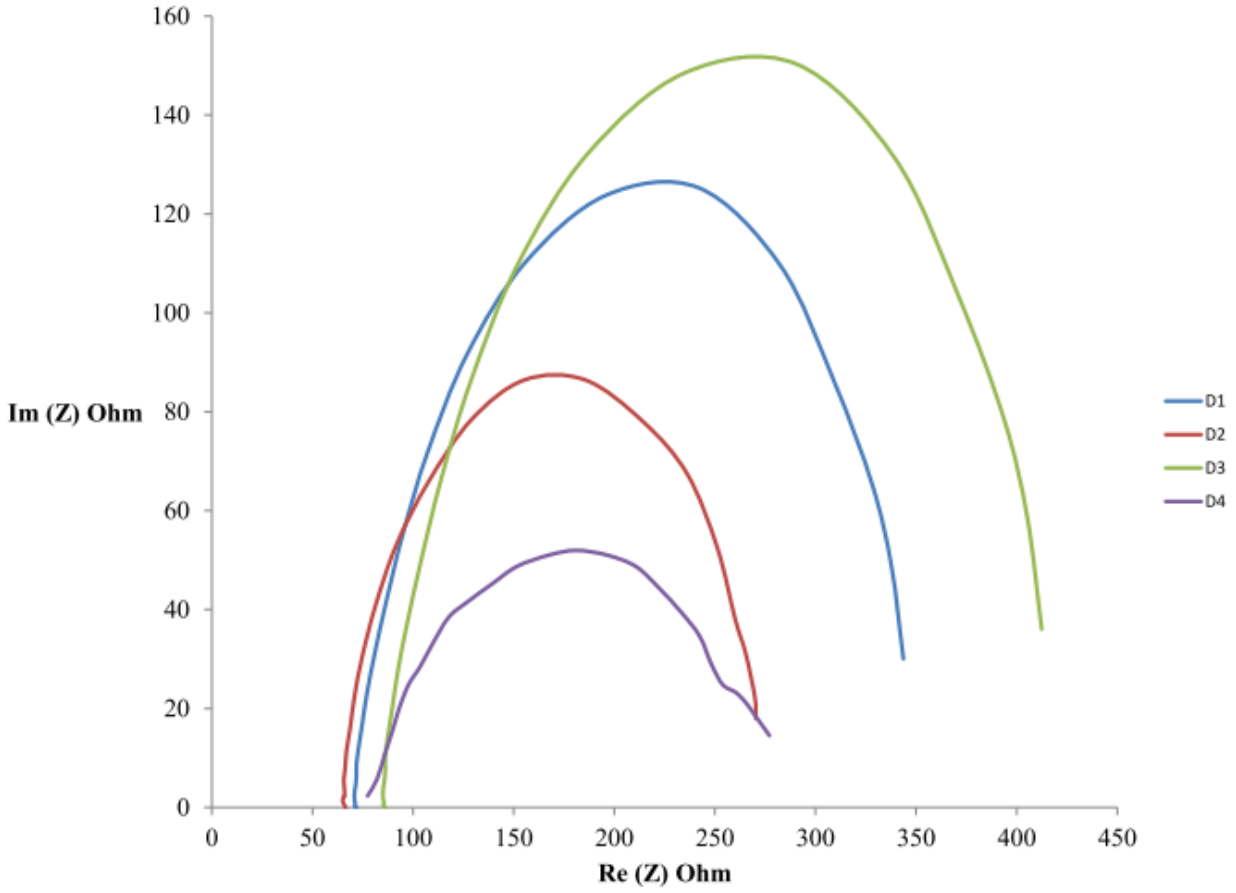

Fig 3-5: EIS investigation of DSSCs based on novel sensitizers

3.6. Acknowledgment

The authors would like to acknowledge the support provided by King Abdulaziz City for Science and Technology (KACST) through the Science & Technology Unit at King Fahd University of Petroleum & Minerals (KFUPM) for funding this work through project # 11-ENE1635-04 as part of the National Science, Technology and Innovation Plan. KFUPM is also acknowledged for supporting this research. The authors would like to acknowledge the Center of Research Excellence for Renewable Energy at KFUPM for its support.

3.7. References

[1] Perlin J. Silicon Solar Cell Turns 50 2004.

[2] Ha E-S, Yoo B, Baik H, Lee Y, Kim K-J. Photocurrent enhancement of dye-sensitized solar cells owing to increased dye-adsorption onto silicon-nanoparticle-coated titanium-dioxide films. Chem Asian J 2012;7:1624–9. doi:10.1002/asia.201101055.

[3] Lu X, Zhou G, Wang H, Feng Q, Wang Z-S. Near infrared thieno[3,4-b]pyrazine sensitizers for efficient quasi-solid-state dye-sensitized solar cells. Phys Chem Chem Phys 2012;14:4802–9. doi:10.1039/c2cp40441a.

[4] Agrawal S, English NJ, Thampi KR, MacElroy JMD. Perspectives on ab initio molecular simulation of excited-state properties of organic dye molecules in dye-sensitised solar cells. Phys Chem Chem Phys 2012;14:12044–56. doi:10.1039/c2cp42031g.

[5] O'Regan B, Grätzel M. A low-cost, high-efficiency solar cell based on dye-sensitized colloidal TiO2 films. Nature 1991;353:737–40. doi:10.1038/353737a0.

[6] Parisi ML, Maranghi S, Basosi R. The evolution of the dye sensitized solar cells from Grätzel prototype to up-scaled solar applications: A life cycle assessment approach. Renew Sustain Energy Rev 2014;39:124–38. doi:10.1016/j.rser.2014.07.079.

[7] Deepak TG, Anjusree GS, Thomas S, Arun TA, Nair S V., Sreekumaran Nair A. A review on materials for light scattering in dye-sensitized solar cells. RSC Adv 2014;4:17615. doi:10.1039/c4ra01308e.

[8] Umer Mehmood, Saleem-ur Rahman, Khalil Harrabi, Ibnelwaleed A. Hussein and BVSR. Recent Advances in Dye Sensitized Solar Cells. Adv Mater Sci Eng 2014;2014:12. doi:http://dx.doi.org/10.1155/2014/974782.

[9] Mehmood U, Hussein IA, Daud M, Ahmed S, Harrabi K. Theoretical study of benzene/thiophene based photosensitizers for dye sensitized solar cells (DSSCs). Dye Pigment 2015;118:152–8. doi:10.1016/j.dyepig.2015.03.003.

[10] Tian Z, Huang M, Zhao B, Huang H, Feng X, Nie Y, et al. Low-cost dyes based on methylthiophene for high-performance dye-sensitized solar cells. Dye Pigment 2010;87:181–7. doi:10.1016/j.dyepig.2010.03.029.

[11] SPIE | Journal of Photonics for Energy | Density functional theory study on dye-sensitized solar cells using oxadiazole-based dyes n.d. http://photonicsforenergy.spiedigitallibrary.org/mobile/article.aspx?articleid=2174548 (accessed April 07, 2015).

[12] Panda MK, Ladomenou K, Coutsolelos AG. Porphyrins in bio-inspired transformations: Light-harvesting to solar cell. Coord Chem Rev 2012;256:2601–27. doi:10.1016/j.ccr.2012.04.041.

[13] Hosokawa C, Higashi H, Nakamura H, Kusumoto T. Highly efficient blue electroluminescence from a distyrylarylene emitting layer with a new dopant. Appl Phys Lett 1995;67:3853. doi:10.1063/1.115295.

[14] Jacob J, Sax S, Piok T, List EJW, Grimsdale AC, Müllen K. Ladder-type pentaphenylenes and their polymers: efficient blue-light emitters and electron-accepting materials via a common intermediate. J Am Chem Soc 2004;126:6987–95. doi:10.1021/ja0398823.

[15] Anderson S, Taylor PN, Verschoor GLB. Benzofuran trimers for organic electroluminescence. Chemistry 2004;10:518–27. doi:10.1002/chem.200305284.

[16] High-Efficiency Poly(p-phenylenevinylene)-Based Copolymers Containing an Oxadiazole Pendant Group for Light-Emitting Diodes n.d. http://pubs.acs.org/doi/pdf/10.1021/ja036955+ (accessed December 31, 2014).

[17] Dessì A, Barozzino Consiglio G, Calamante M, Reginato G, Mordini A, Peruzzini M, et al. Organic Chromophores Based on a Fused Bis-Thiazole Core and Their Application in Dye-Sensitized Solar Cells. European J Org Chem 2013;2013:1916–28. doi:10.1002/ejoc.201201629.

[18] Dessì A, Calamante M, Mordini A, Peruzzini M, Sinicropi A, Basosi R, et al. Organic dyes with intense light absorption especially suitable for application in thin-layer dye-sensitized solar cells. Chem Commun (Camb) 2014;50:13952–5. doi:10.1039/c4cc06160h.

[19] Wang C, Jung G-Y, Hua Y, Pearson C, Bryce MR, Petty MC, et al. An Efficient Pyridine- and Oxadiazole-Containing Hole-Blocking Material for Organic Light-Emitting Diodes: Synthesis, Crystal Structure, and Device Performance. Chem Mater 2001;13:1167–73. doi:10.1021/cm0010250.

[20] Panchamukhi SI, Belavagi N, Rabinal MH, Khazi IA. Synthesis and optoelectronic properties of symmetrical thiophene based 2,5-disubstiuted 1,3,4-oxadiazoles: highly fluorescent materials for OLED applications. J Fluoresc 2011;21:1515–9. doi:10.1007/s10895-011-0838-y.

[21] Zhu W, Yao R, Tian H. Synthesis of novel electro-transporting emitting compounds. Dye Pigment 2002;54:147–54. doi:10.1016/S0143-7208(02)00039-6.

[22] New Series of Blue-Emitting and Electron-Transporting Copolymers Based on Fluorene n.d. http://pubs.acs.org/doi/pdf/10.1021/ma011593g (accessed December 31, 2014).

[23] Chung S-J, Kwon K-Y, Lee S-W, Jin J-I, Lee CH, Lee CE, et al. Highly Efficient Light-Emitting Diodes Based on an Organic-Soluble Poly(p-phenylenevinylene) Derivative Carrying the Electron-Transporting PBD Moiety. Adv Mater 1998;10:1112–6. doi:10.1002/(SICI)1521-4095(199810)10:14<1112::AID-ADMA1112>3.0.CO;2-P.

[24] Skene WG, Pérez Guarìn SA. Spectral characterization of thiophene acylhydrazides. J Fluoresc 2007;17:540–6. doi:10.1007/s10895-007-0209-x.

[25] Density functional theory characterization and design of high-performance diarylamine-fluorene dyes with different p spacers for dye-sensitized solar cells n.d. http://pubs.rsc.org/en/content/articlepdf/2012/jm/c1jm13028e (accessed December 31, 2014).

[26] Wang J, Bai F-Q, Xia B-H, Feng L, Zhang H-X, Pan Q-J. On the viability of cyclometalated Ru(II) complexes as dyes in DSSC regulated by COOH group, a DFT study. Phys Chem Chem Phys 2011;13:2206–13. doi:10.1039/c0cp01556c.

[27] Wang J, Li H, Ma N-N, Yan L-K, Su Z-M. Theoretical studies on organoimido-substituted hexamolybdates dyes for dye-sensitized solar cells (DSSC). Dye Pigment 2013;99:440–6. doi:10.1016/j.dyepig.2013.05.027.

[28] Fan W, Tan D, Deng W-Q. Acene-modified triphenylamine dyes for dye-sensitized solar cells: a computational study. Chemphyschem 2012;13:2051–60. doi:10.1002/cphc.201200064.

[29] Sang-aroon W, Saekow S, Amornkitbamrung V. Density functional theory study on the electronic structure of Monascus dyes as photosensitizer for dye-sensitized

solar cells. J Photochem Photobiol A Chem 2012;236:35–40. doi:10.1016/j.jphotochem.2012.03.014.

[30] Zarate X, Schott E, Gomez T, Arratia-Pérez R. Correction to "Theoretical Study of Sensitizer Candidates for Dye-Sensitized Solar Cells: Peripheral Substituted Dizinc Pyrazinoporphyrazine–Phthalocyanine Complexes." J Phys Chem A 2013;117:4996–4996. doi:10.1021/jp404833n.

[31] Zhang J, Kan Y-H, Li H-B, Geng Y, Wu Y, Su Z-M. How to design proper ?-spacer order of the D-?-A dyes for DSSCs? A density functional response. Dye Pigment 2012;95:313–21. doi:10.1016/j.dyepig.2012.05.020.

[32] Rocca D, Gebauer R, De Angelis F, Nazeeruddin MK, Baroni S. Time-dependent density functional theory study of squaraine dye-sensitized solar cells. Chem Phys Lett 2009;475:49–53. doi:10.1016/j.cplett.2009.05.019.

[33] LEE K, HU C, CHEN H, HO K. Incorporating carbon nanotube in a low-temperature fabrication process for dye-sensitized TiO2 solar cells☆. Sol Energy Mater Sol Cells 2008;92:1628–33. doi:10.1016/j.solmat.2008.07.012.

[34] Xie Y-L, Li Z-X, Xu Z-G, Zhang H-L. Preparation of coaxial TiO2/ZnO nanotube arrays for high-efficiency photo-energy conversion applications. Electrochem Commun 2011;13:788–91. doi:10.1016/j.elecom.2011.05.003.

[35] Li S, Lin Y, Tan W, Zhang J, Zhou X, Chen J, et al. Preparation and performance of dye-sensitized solar cells based on ZnO-modified TiO2 electrodes. Int J Miner Metall Mater 2010;17:92–7. doi:10.1007/s12613-010-0116-z.

[36] Nair AS, Jose R, Shengyuan Y, Ramakrishna S. A simple recipe for an efficient TiO2 nanofiber-based dye-sensitized solar cell. J Colloid Interface Sci 2011;353:39–45. doi:10.1016/j.jcis.2010.09.042.

CHAPTER 4

HYBRID TIO_2-MULTI WALL CARBON NANOTUBES (MWCNTS) PHOTOANODES FOR EFFICIENT DYE SENSITIZED SOLAR CELLS (DSSCS)

Umer Mehmood[1], Khalil Harrabi[2], M. B. Mekki[2], Shakeel Ahmed[3], Nouar tabet[4], Ibnelwaleed A. Hussein[1*]

[1] Department of Chemical Engineering, King Fahd University of Petroleum & Minerals (KFUPM), P. O. Box 5050, Dhahran 31261, Kingdom of Saudi Arabia

[2] Department of physics, (KFUPM), P. O. Box 5050, Dhahran 31261, Kingdom of Saudi Arabia

[3] Center for Refining & Petrochemicals, KFUPM, P.O. Box 5050, Dhahran 31261, Kingdom of Saudi Arabia

[4]Qatar Environment and Energy Research Institute, Qatar Foundation, Qatar

[*]Corresponding Author: Ibnelwaleed A. Hussein , E-mail address:

ihussein@kfupm.edu.sa

This chapter has been published in "Solar Energy Materials & Solar Cells " on 2 April, 2015

Abstract

Titanium oxide/multi-walled carbon nanotubes (TiO_2/MWCNTs) photoanodes were prepared using mixing technique. Dye sensitized solar cells (DSSCs) based on TiO_2/MWCNTs composite with different concentrations of CNTs (0, 0.03. 0.06, 0.09, 0.15, 0.21 wt. %) were fabricated using N_3 dye as a sensitizer. Transmission electron microscope (TEM) was used to confirm the dispersion of carbon nanotubes in TiO_2. The UV-Visible absorption spectroscopy, photocurrent–voltage (*I–V*) characteristic and electrochemical impedance spectroscopy (EIS) measurements were carried out to characterize device. The results show that the photo conversion efficiency is highly dependent on the concentration of CNTs in the photoanode. The solar cell based on photoanode containing 0.03 wt. % MWCNTs, has a power conversion efficiency, which is about 30% greater than that of the unmodified photoanode. We also used density functional theory (DFT) quantum modeling technique to investigate the thermodynamic aspects of the charge transport processes involved in DSSC. Our simulation outcomes support the experimental results.

Keywords: Hybrid, DSSC, MWCNTs, density functional theory

4.1. Introduction

The world energy demand is continually increasing and the world power consumption, which is 13 terawatts (TW) currently, is expected to reach about 28 TW in 2050 [1]. Fossil fuels, which are depleting rapidly, meet 80% of the energy requirement of the whole world [2]. Moreover, the burning of fossil fuels raises the amount of carbon dioxide in the atmosphere. Owing to growing energy demand, exhaustion of oil resources, and global warming issues, there is a need for clean and renewable energy technologies. Photovoltaic technology employing solar energy is regarded as the most efficient technology among all the sustainable energy technologies such as tidal power, solar thermal, hydropower, and biomass [3]. The solar radiation from the sun is approximately 3×10^{24} J per year, which is ten times the current energy demand [4]. Therefore, the conversion of photo energy into electrical energy is generally considered as the most potential way to resolve the world energy crisis, owing to its huge reserves.

DSSCs have got global attention in the past fifteen years owing to their easy processing and low production cost compared with inorganic solar cell. Meanwhile, the CNTs are also being extensively explored and employed due to their excellent morphological and electrical properties. These two apparently discrete inventions (DSSCs and CNTs) were fortuitously linked together in 1991. In this year, Grätzel devised dye sensitized solar cell [5] while Iijima discovered CNTs [6]. Fortunately, both innovations were reported by the top scientific journal *Nature*.

The major component of the DSSCs is a dye. Its function is to absorb incoming sunlight and produce excitons. It is chemically bonded to the porous surface of the semiconductor. Presently, ruthenium(II)-polypyridyl complexes based DSSCs have got overall power conversion efficiencies (PCE) over 11% under standard (Global Air Mass 1.5)

illumination [7–9]. The high efficiencies of the ruthenium (II) -polypyridyl DSSCs can be attributed to their wide absorption range, good spectroscopic and photostability in the final device. In addition, the carboxylate groups attached to the bipyridyl moiety lower the energy of the ligand π^* orbital. The general representation of carboxylic acid based sensitizers is [Ru ($dcbH_2$)$_2$LL′], while $dcbH_2$, and L and/or L′ represent anchoring ligands and ancillary ligands, respectively. An example of a high performance carboxylic acid based sensitizer is *cis*-[Ru($dcbH_2$)$_2$(NCS)$_2$], which is also known as the N_3 dye . Similarly, there are two crystalline forms of TiO_2, anatase and rutile, the former is preferred because the exciton mobility in rutile is less than in anatase due to the high packing density.

However, the efficiency of DSSC is still low compared with the silicon solar cells due to recombination of injected electrons with the electrolyte (dark current) and oxidized dye [10]. Therefore, in order to improve the PCE of DSSCs, there is need to reduce the charge recombination and accelerate the electron transport [11]. Since CNTs show outstanding electrical conductivity [12–14], their incorporation in photanode may enhance the PCE of DSSCs by reducing the charge recombination .

Here, we also employed DFT and time dependent DFT to investigate the thermodynamic aspects of charge transport processes involved in DSSC. It is an effective tool as compared to other high level quantum approaches because the computed orbitals are suitable for the typical MO-theoretical analyses and interpretations [15]. Many theoreticians have successfully applied this technique to calculate the electronic structure properties of photosensitizers [15–21].

4.2.Computer simulations

All the DFT/TD-DFT calculations were executed using Amsterdam Density Functional (ADF) program (2013.01).

4.2.1. TiO2 cluster Model

BAND mode was used to simulate the anatase TiO_2 cluster. Here, we selected tetragonal anatase crystal structure with single layer (001) surface slab. Then, we created 4×1 supercell from this slab. All atoms were maped within the unit cell.

4.2.2. Simulation Method

TiO_2 and carbon doped TiO_2 models were simulated by considering generalized gradient approximation (GAD) at BYLP level and triple-ζ polarization basis function. The ground state geometries of N_3, N_3-TiO_2 N_3-(TiO2-C) systems were optimized by applying a hybrid B3LYP level together with triple-ζ polarization basis function. UV-Vis spectra of N_3 was simulated in ethanol solvent. Here the conductor-like screening model (COSMO) was selected to take the solvent effects into account. While the excitation energies were examined using TD-DFT and statistical average of orbital potentials (SAOP) model including the salvation effects. Eighty singlet-singlet transitions were calculated, which are sufficient to fully define the whole absorption spectrum. In all the calculations, the relativistic effects were taken into account by the zero order regular approximation (ZORA) Hamiltonian in its scalar approximation.

Light harvesting efficiency (LHE) [22] and free energy of electron injection (ΔG^{inject}) [20] can be calculated by the following relations:

$$LHE = 1-10^{-A} \qquad (1)$$

"A" represents the absorption

$$\Delta G^{inject} = Eox^{dye*} - E_{CB} \quad (2)$$

E_{CB} is the conduction band of the semiconductor and Eox^{dye*} is the dye excited state potential, which is related as [17]:

$$Eox^{dye*} = Eox^{dye} - \Delta E \quad (3)$$

Similarly Eox^{dye} shows the dye ground state potential and ΔE is the minimum energy of absorption associated with λ_{max}, While [18]

$$Eox^{dye} = -HOMO \quad (4)$$

4.3.Experimental

4.3.1. Preparation of hybrid photoanodes

A suspension solution of ethanol and MWCNTs was prepared by dissolving 0.01g of MWCNTs in 20 ml ethanol solution. It was then sonicated for 4hr to attain a good dispersion of MWNTs in ethanol. An exact quantity of dispersed MWCNTs was mixed with known amount of anatase TiO_2 paste (T/SP **14451**, solaronix) to obtain a composite paste. Five different samples of TiO_2-MWCNTs were prepared by varying the composition of MWCNTs i.e. 0, 0.03. 0.06, 0.09, 0.15, 0.21 wt. %.The TiO_2-MWCNTs paste was then tape casted on FTO glass substrate (2 mm,7Ω/seq, solaronix). The coated glass substrate annealed at 450^{o}C for 30 min. Other photoanodes were prepared via the same process. The thickness of each photoanode was found by using cross sectional images obtained from SEM (JEOL, 6610LV). The average thickness of each film was 22 µm.

4.3.2. DSSCs Fabrication and characterization

0.5 mM solution of N_3 (Ruthenizer-535, solaronix) dye was prepared in methanol. The hybrid electrodes were soaked in the dye solution for 24 hours. After sensitization, the samples were washed with alchol to eliminate unanchored dye. Then, DSSCs were fabricated employing the sensitized hybrid anode, platinum deposited counter electrode (Plasticol T, solaronix), 60 μm sealing spacer (Meltonix 1170, solaronix) and I^-/I_3^- redox couple electrolyte prepared in methoxypropionitrile with a 50 mM redox concentration (Iodolyte Z-50, solaronix).

The UV-Vis spectra of N_3 in ethanol and adsorbed on TiO_2 films at glass substrates were recorded with an Ocean Optics ISS-UV/VIS spectrophotometer. Keithley 2400 Source Meter was used to measure the $I-V$ characteristics of the DSSCs using IV-5 solar simulator (Sr #83, PVmeasurement, Inc) at AM1.5G (100 $mWcm^{-2}$).The silicon solar cell was used as a reference for calibration. The impedance spectroscopy (EIS) was measured in dark conditions of illumination via Bio-Logic SAS (VMP3, s/n:0373), with an AC signal of 20 mV in amplitude, in the frequency range between 10 mHz and 1MHz. The applied bias was between 0 mV and 800 mV above the V_{oc} of the DSSC.

4.4.Results and Discussion

The dispersion of MWCNTs in TiO_2 was ensured by TEM (JEOL, JEM-2100F) analysis. TiO_2-MWCNT sample having 0.15% CNT was selected for TEM analysis. It was difficult to obtain TEM images of dispersed MWCNTs in TiO_2 from low concentration samples. Fig 4-1 (a) shows the anatase TiO2 nanoparticles, while, Fig 4-1 (b) shows that MWCNs randomly distributed in TiO_2. The interface connection between MWCNTs and TiO_2 can clearly be observed, indicating that TiO_2 nanoparticles were well attached on

the surface of the MWCNTs. The diameter of the coated MWCNTs significantly increases and consequently the inner core of MWCNTs is hardly visible, shown in Fig 4-1 (c, d).

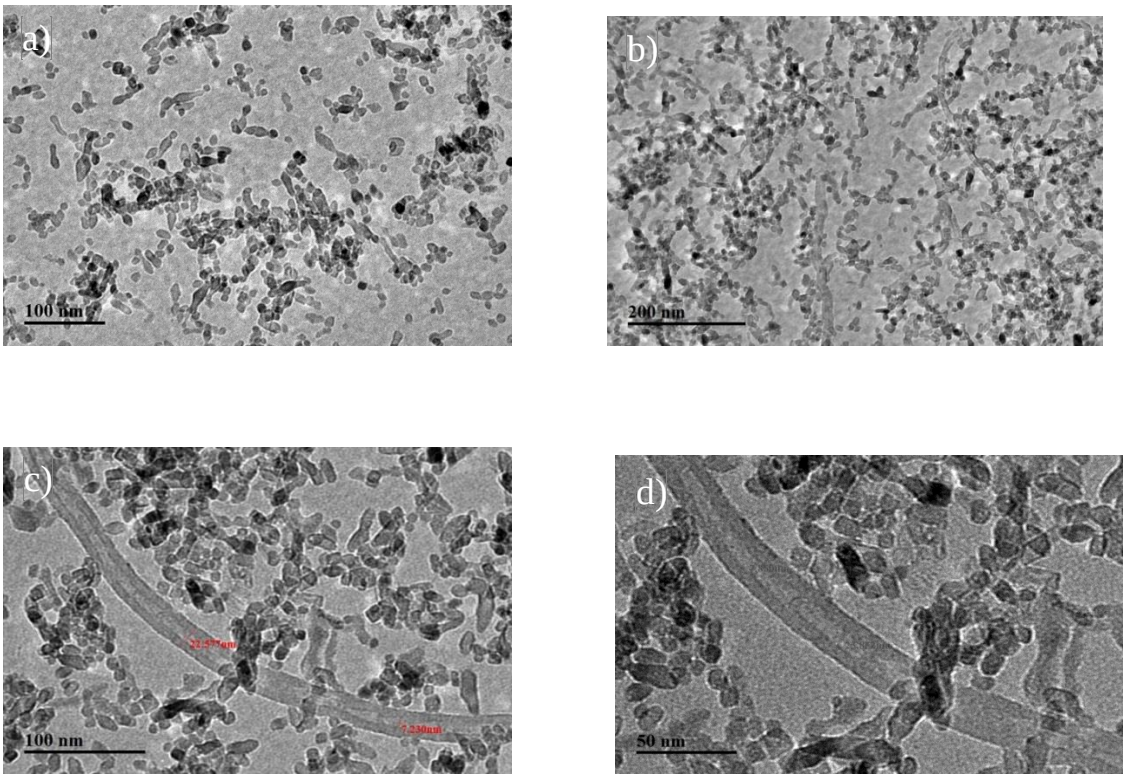

Fig 4-1: *Transmission electron microscope* images of a 0.15 % sample at various magnifications (a) Pure TiO_2 b) Dispersion of MWCNTs in TiO_2 c) Dispersion of single MWCNT in TiO_2 at 100 nm and d) 50 nm

The HOMOs, LUMOs and band gap energies of photosensitizers play an important role in providing the thermodynamic driving force for the electron injection to conduction band of TiO_2. For efficient charge transfer, the LUMOs of dyes must be more negative than the conduction band of the semiconductor while HOMO levels must be more positive than the redox potential of electrolyte.The simulated structures of N_3, TiO_2/N_3 and C-TiO_2/N_3 are shown in Fig 4-2. The simulated comduction band, valence band and band gap of TiO2 and C-TiO2 are shown in Table 4-1 (a), while HOMOs, LUMOs and band gap of photosensitizer are shown in table in Table 4-1 (b). These tabulated values are in good agreement with the experimental values [23,24]. The computed results show that the doping of MWCNTs (one of the allotropic form of carbon) on TiO_2 significantly reduces the band gap of TiO_2 cluster. This is because the CNTs possess lower value of E_{CB} (~0 eV vs. NHE) than that of TiO_2 (−0.5 eV vs. NHE) [13], the charge equilibrium between CNTs and TiO_2 would cause a shift of apparent Fermi level (*EF*) to more positive potential i.e. downward shift as shown in Fig 4-3. Moreover, the thermodynamic driving force for charge transfer (ΔG^{inject}) is defined as the energy difference between the excited state of photosensitizer and the conduction band edge of metal oxide. The downward positive shift due to MWCNTs can generate significant driving force to facilitate the charge transfer from the excited dye to the conduction band of the photoanode. The simulated ΔG^{inject} value for C-TiO_2/N_3 is greater than TiO_2/N_3 , as indicated in Table 4-1(b).

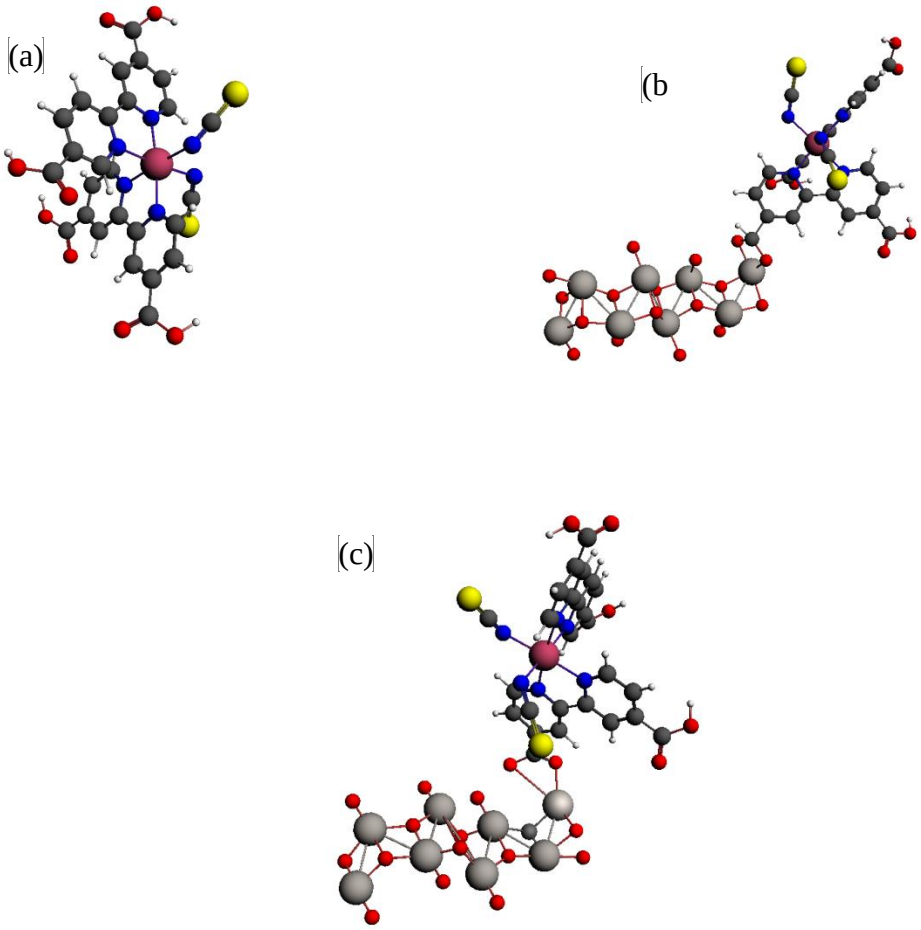

Fig 4-2: Simulated structures of (a) N_3, (b) TiO_2/N_3 and (c) C-TiO_2/N_3

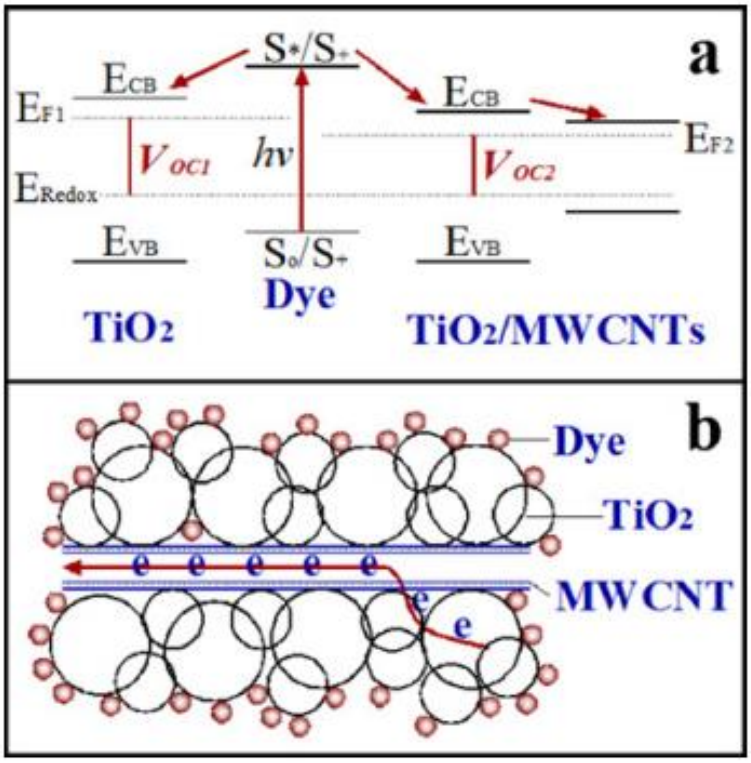

Fig 4-3: incorporation of MWCNTs in TiO2 causes a shift of energy level (a) and enhance the electrical conductivity (b)

Table 4-1(a). Simulated electronic structure properties of TiO_2 and carbon doped TiO_2

System	E_{CB} (eV)	V_B (eV)	Band gap (eV)
TiO_2	-7.2	- 4.1	3.1
C-TiO_2	-7.2	-4.4	2.7

Table 4-1 (b). Simulated electronic structure and optical properties of photosensitizer

Sysm	HOMO	LUMO	H-L_{gap}	λ_{max}	ΔE	Eox^{dye}	Eox^{dye*}	ΔG^{inject}	*A*	*LHE
N_3	-5.63	-3.67	1.96	542	2.29	5.63	3.34		0.9	87
TiO_2/N_3				567	2.18			-0.76	1.65	97
C-TiO2/N_3				581	2.13			-1.06	2.10	99

Units of HOMO, LUMO, H-L_{gap} , ΔE ,Eox^{dye} ,Eox^{dye*} and ΔG^{inject} are(eV)
Unit of λ_{max} is nm
*LHE, corresponding to maximum A

The UV-vis absorption spectra of N3 in methanol and anchored to TiO_2 and TiO_2-MWCNTs are shown in Fig 4-4(a). The two broad visible bands at 547 and 419 nm in N3 are assigned to metal-to-ligand charge-transfer (MLCT) origin. The bands in the UV at 322 nm are assigned as intra ligand (π-π*) charge-transfer transitions. However, the absorption shifts to lower energy values when anchored to TiO_2 and TiO_2-MWCNTs. This is due to the fact that on the electrode the carboxylate groups bind to the TiO_2 surface in which Ti^{4+}acts as proton. The interaction between the carboxylate group and the surface Ti^{4+}ions may lead to increased delocalization of the π* orbital.The energy of the π* level is decreased by this delocalization, which explains the red shift for the absorption spectra. But the TiO2-MWCNTs based photoanode has a greater red shift value as compared to pure TiO_2. This is because the CNTs may exhibit photosensitizing properties, thus extending photovoltaic properties into the visible spectrum [25]. *Similarly, th**e*** simulated absorption spectra of N_3, N_3-TiO2 and N_3-TiO2-MWCNTs are shown in Fig 4-4b are in good agreement with the experimental spectra. Thus, the COSMO solvation model with SOAP function is appropriate for computing the absorption spectra of systems.

The *I–V* curves of the DSSCs based on hybrid photoanodes are shown in Fig 4-5. While the device parameters, i.e. J_{sc}, V_{oc} and FF are shown in Table 4-2. The DSSC with the highest efficiency is achieved in the case of 0.03%MWCNTs-TiO_2 film and is characterized by photo conversion efficiency is as high as 0.85%, which presents about 30 % increase with respect to pure TiO_2 (0.65%). Insertion of MWCNTs in TiO_2 network significantly enhances the efficiency of DSSC. This is because the incorporation of MWCNTs increases the surface area of hybrid anode and thus more dye loading.

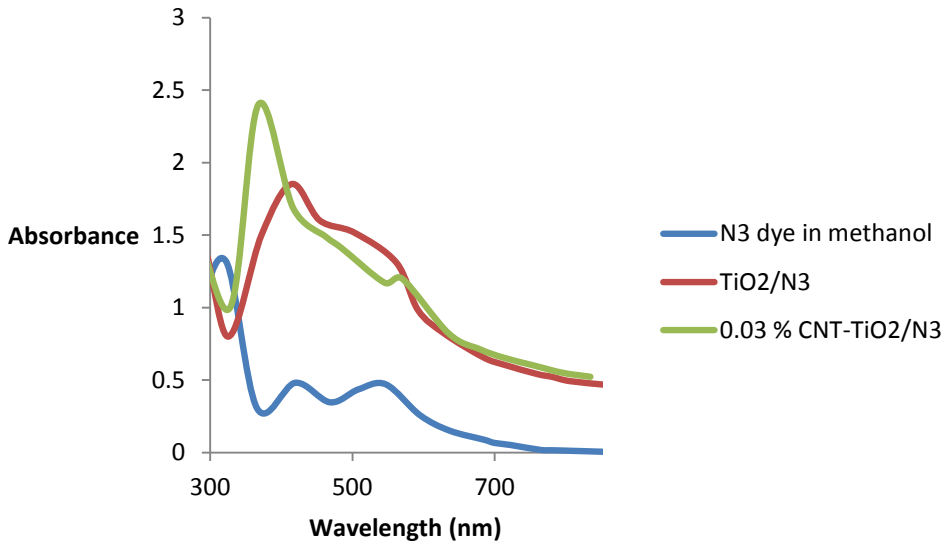

Fig 4-4(a). UV-Vis spectra of N_3, TiO_2/N_3 and CNTs-TiO_2/N_3

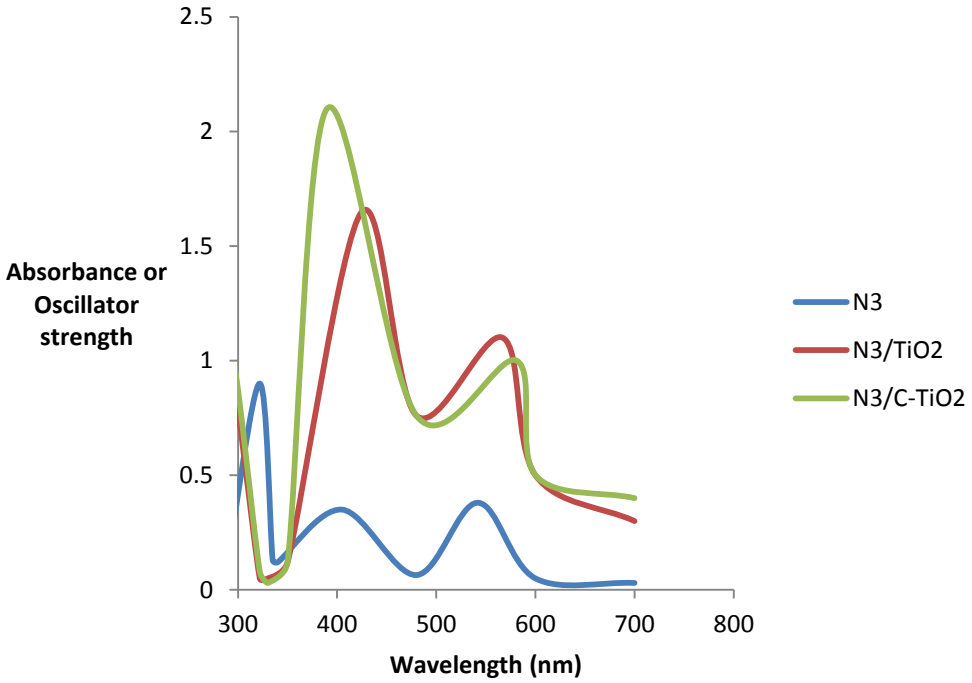

Fig 4-4(b). Simulated UV-Vis spectra of N_3, TiO_2/N_3 and CNTs-TiO_2/N_3

Moreover, the MWCNTs also improve the electron injection efficiency of the electrons due to increase positive potential (as described above). Simulation outcomes also favor these results. Table 4-1 (b) shows that absorptions (A) or oscillator strengths of N3, N3-TiO2 and N3-TiO2-MWCNTs increase in the order of N3-TiO2-MWCNTs > N3-TiO2> N3.Thus, LHE will be in the order of N3-TiO2-MWCNTs > N3-TiO2> N3. It demonstrates that higher the LHE greater will be the photo current and henec more efficiency. However, the decline in Voc at increasing CNTs contents could be attributed to the downshift of the potential band edge of the TiO_2. It can also be observed that increase in MWCNTs concentration from optimum level (0.03%) negatively affect the performance of DSSCs. This is because of the decrease in film transparency owing to increase MWCNTs contents. Another possibility of low efficiency at a high MWCNTs concentration could be attributed to the formation of CNT agglomerates inside the TiO_2 matrix acting as trapping sites that obstruct the fast charge collection at the electrodes. Such a poor charge collection at theelectrode, together with enhanced light loss due to CNT direct absorption, strongly reduces the efficiency of DSSCs at high CNTs contents.

Electrochemical impedance spectroscopy (EIS) analysis is performed to further elucidate the photovoltaic properties. Figure 4-6(a) shows the Nyquist plots of DSSCs which were assembled with TiO_2-N_3 and 0.03%MWCNTS-TiO_2-N_3. The large semicircle represents the interfacial charge transfer resistances (R_3) at the photoanode/electrolyte interface. The R_3 is related to the charge recombination rate, e.g., a smaller R_3 indicates a faster charge recombination.The R_3 value for DSSC assembled with pure TiO_2 is smaller than that of 0.03%MWCNTs-TiO_2 DSSC as shown in Fig 4-6 (a), proposing charge recombination is greatly reduced owing to the incorporation of CNTs. However, the CNTs concentration

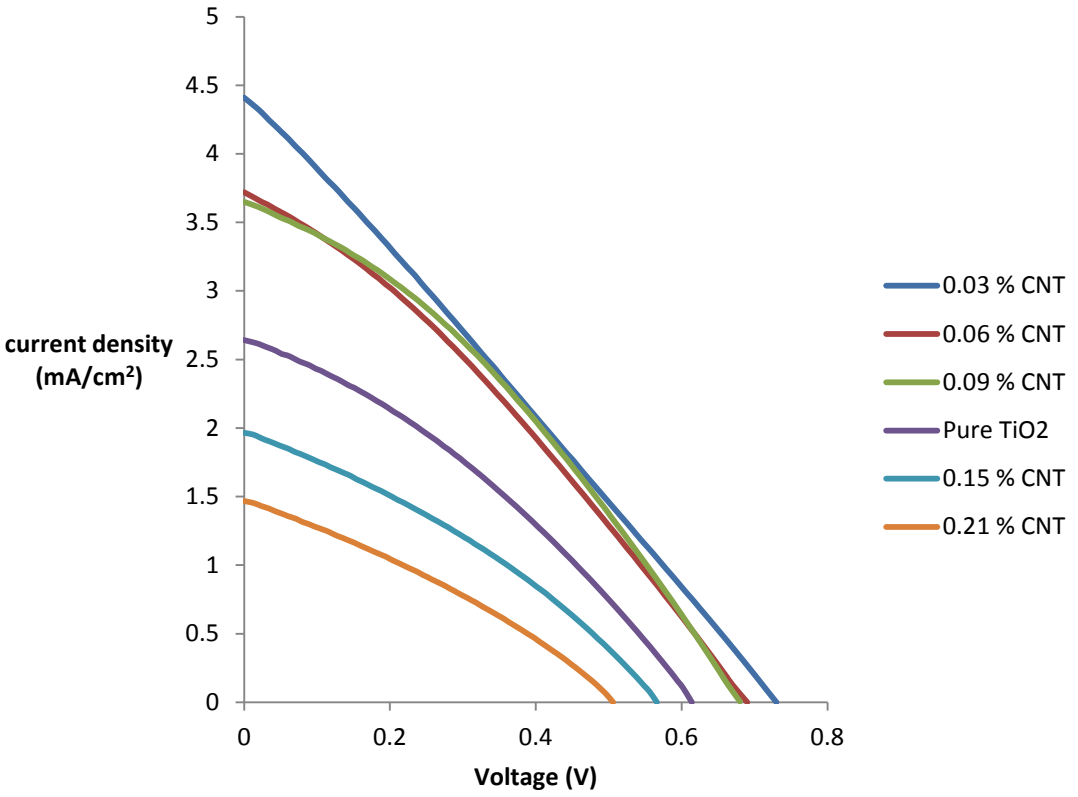

Fig 4-5. Current − voltage curves of DSSCs fabricated using different concentrations of CNTs

Table 4-2. Photovolatic properties of DSSCs based on hybrid anodes

No	Anode structure	j_{sc} (mA/cm^2)	V_{oc} (mV)	FF(%)	η (%)
1	TiO_2	2.651	617	33	0.64
2	TiO2 +0.03%MWCNT	4.415	730	27	0.85
3	TiO2 +0.06%MWCNT	3.715	686	31	0.78
4	TiO2 +0.09%MWCNT	3.652	679	34	0.83
5	TiO2 +0.15%MWCNT	1.974	569	32	0.37
6	TiO2 +0.21%MWCNT	1.475	506	31	0.23

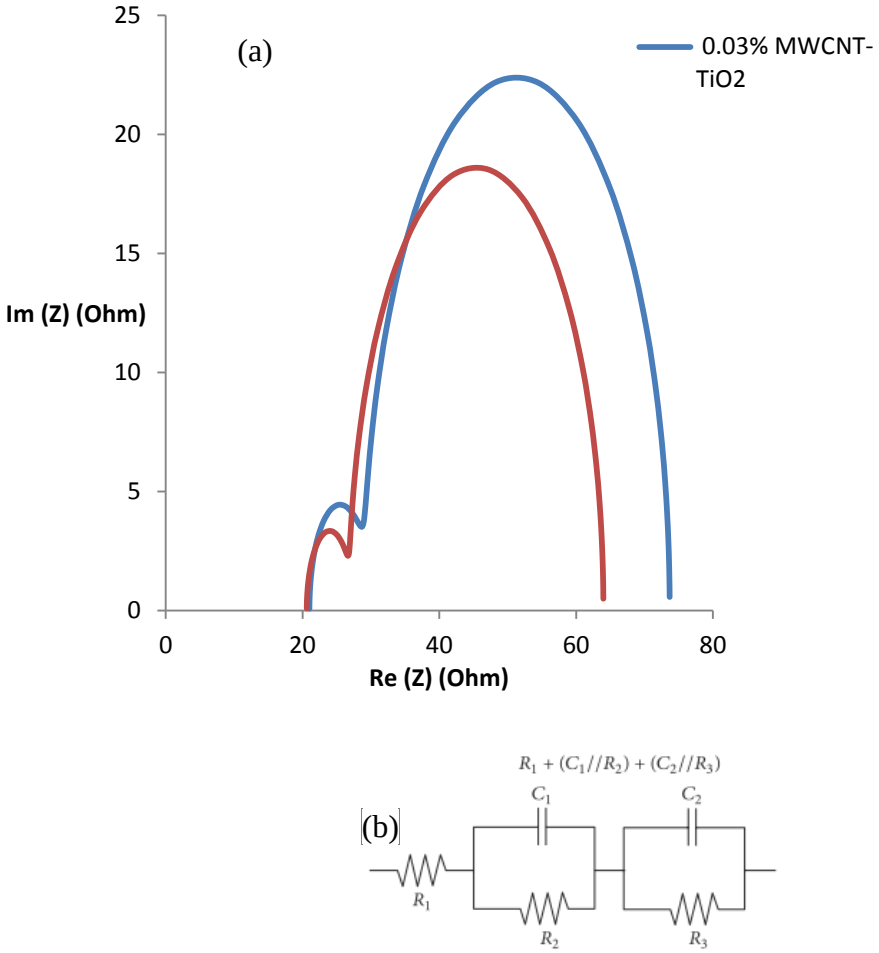

Fig 4-6. a) EIS investigation of the modified and unmodified DSSCs and b) The equivalent circuit model of DSSC in which R_1: Serial resistance of FTO glass. $C_1//R_2$: Impedance at Pt/electrolyte interface and $C_2//R_3$: Impedance at TiO_2/dye/electrolyte interface.

Table 4-3. The resistances and capacitance values of DSSC based on TiO2 and TiO2-MWCNTs

Photo anode	R1(Ω)	C_1 (mF)	R_2 (Ω)	C_2 (mF)	R_3 (Ω)
TiO2	20.62	20	6.235	0.57	37.15
TiO_2-0.03%MWCNT	21	23	8.023	0.45	44.65

greater than 0.03 wt.% leads to the smaller values of R_3 due to a shorter electron lifetime of the order of few tens of mili seconds [14]. Figure 4-6 (b) shows the equivalent circuit model of DSSCs. The equivalent circuit model can describe the junction impedance, and the EIS measurement system can compute the value of junction impedance. Table 3-3 shows all the values of the equivalent circuit model.

Regardless of the PCE gains a significant enhancement when 0.03 wt.% CNTs is dispersed into the TiO_2 paste, the absolute value (0.84%) is exceptionally lower than the highest efficiency hitherto achieved (∼12%) [5]. The reason is that the photoanode film is too thick (22μm). For an effective charge collection, the film thickness should be less than the electron diffusion length [26]. The reported diffusion length of electrons in TiO_2 film is about 9–11 μm based on electron transport studies [27–29]. A thick photoanode results in a long electron diffusion distance to the FTO substrate (electrode) which increases the probability of recombination and thus degrades the efficiencies [30].

4.5.Conclusion

In conclusion, we established that the dispersion of small of MWCNTs in TiO_2 can significantly improve the photo conversion efficiency of DSSCs. Optimum concentration (0.03%) of CNTs does not affect the transparency of the TiO_2 layer, while significantly increasing charge collection at the photoanode. The enhancement of electron lifetime, dye loading and the reduction of recombination phenomena lead to an increase in PCE of the DSSCs, with a maximum value of 0.84% (corresponding to the addition of 0.030 wt % MWCNTs). Here, our simulation outcomes using DFT/TD-DFT also support the

experimental result. Hence, we presented a fast, cheap, and an effective means to increase the PCE of DSSCs.

4.6.Acknowledgements

The authors would like to acknowledge the support provided by King Abdulaziz City for Science and Technology (KACST) through the Science & Technology Unit at King Fahd University of Petroleum & Minerals (KFUPM) for funding this work through project # **11-ENE1635-04** as part of the National Science, Technology and Innovation Plan. KFUPM is also acknowledged for supporting this research. The authors would like to acknowledge the Center of Research Excellence for Renewable Energy at KFUPM.

4.7.References

[1] A. Hagfeldt, G. Boschloo, L. Sun, L. Kloo, H. Pettersson, Dye-sensitized solar cells., Chem. Rev. 110 (2010) 6595–663. doi:10.1021/cr900356p.

[2] B. Li, L. Wang, B. Kang, P. Wang, Y. Qiu, Review of recent progress in solid-state dye-sensitized solar cells, Sol. Energy Mater. Sol. Cells. 90 (2006) 549–573. doi:10.1016/j.solmat.2005.04.039.

[3] J. Gong, J. Liang, K. Sumathy, Review on dye-sensitized solar cells (DSSCs): Fundamental concepts and novel materials, Renew. Sustain. Energy Rev. 16 (2012) 5848–5860. doi:10.1016/j.rser.2012.04.044.

[4] K.R. Millington, Encyclopedia of Electrochemical Power Sources, Elsevier, 2009. doi:10.1016/B978-044452745-5.00317-8.

[5] B. O'Regan, M. Grätzel, A low-cost, high-efficiency solar cell based on dye-sensitized colloidal TiO2 films, Nature. 353 (1991) 737–740. doi:10.1038/353737a0.

[6] S. Iijima, Helical microtubules of graphitic carbon, Nature. 354 (1991) 56–58. doi:10.1038/354056a0.

[7] O. Kohle, M. Gr  tzel, A.F. Meyer, T.B. Meyer, The photovoltaic stability of, bis(isothiocyanato)rlutheniurn(II)-bis-2, 2?bipyridine-4, 4?-dicarboxylic acid and

related sensitizers, Adv. Mater. 9 (1997) 904–906. doi:10.1002/adma.19970091111.

[8] P. Péchy, T. Renouard, S.M. Zakeeruddin, R. Humphry-Baker, P. Comte, P. Liska, et al., Engineering of Efficient Panchromatic Sensitizers for Nanocrystalline TiO 2 -Based Solar Cells, J. Am. Chem. Soc. 123 (2001) 1613–1624. doi:10.1021/ja003299u.

[9] M.K. Nazeeruddin, P. Péchy, M. Grätzel, Efficient panchromatic sensitization of nanocrystalline TiO2 films by a black dye based on a trithiocyanato–ruthenium complex, Chem. Commun. (1997) 1705–1706. doi:10.1039/a703277c.

[10] A. Kongkanand, R.M. Domínguez, P. V Kamat, Single wall carbon nanotube scaffolds for photoelectrochemical solar cells. Capture and transport of photogenerated electrons., Nano Lett. 7 (2007) 676–80. doi:10.1021/nl0627238.

[11] A. Hinsch, J.M. Kroon, R. Kern, I. Uhlendorf, J. Holzbock, A. Meyer, et al., Long-term stability of dye-sensitised solar cells, Prog. Photovoltaics Res. Appl. 9 (2001) 425–438. doi:10.1002/pip.397.

[12] A. Kongkanand, P. V Kamat, Electron storage in single wall carbon nanotubes. Fermi level equilibration in semiconductor-SWCNT suspensions., ACS Nano. 1 (2007) 13–21. doi:10.1021/nn700036f.

[13] P. Du, L. Song, J. Xiong, N. Li, L. Wang, Z. Xi, et al., Dye-sensitized solar cells based on anatase TiO2/multi-walled carbon nanotubes composite nanofibers photoanode, Electrochim. Acta. 87 (2013) 651–656. doi:10.1016/j.electacta.2012.09.096.

[14] K.T. Dembele, G.S. Selopal, C. Soldano, R. Nechache, J.C. Rimada, I. Concina, et al., Hybrid Carbon Nanotubes–TiO 2 Photoanodes for High Efficiency Dye-Sensitized Solar Cells, J. Phys. Chem. C. 117 (2013) 14510–14517. doi:10.1021/jp403553t.

[15] G. te Velde, F.M. Bickelhaupt, E.J. Baerends, C. Fonseca Guerra, S.J.A. van Gisbergen, J.G. Snijders, et al., Chemistry with ADF, J. Comput. Chem. 22 (2001) 931–967. doi:10.1002/jcc.1056.

[16] J. Wang, H. Li, N.-N. Ma, L.-K. Yan, Z.-M. Su, Theoretical studies on organoimido-substituted hexamolybdates dyes for dye-sensitized solar cells (DSSC), Dye. Pigment. 99 (2013) 440–446. doi:10.1016/j.dyepig.2013.05.027.

[17] W. Fan, D. Tan, W.-Q. Deng, Acene-modified triphenylamine dyes for dye-sensitized solar cells: a computational study., Chemphyschem. 13 (2012) 2051–60. doi:10.1002/cphc.201200064.

[18] W. Sang-aroon, S. Saekow, V. Amornkitbamrung, Density functional theory study on the electronic structure of Monascus dyes as photosensitizer for dye-sensitized solar cells, J. Photochem. Photobiol. A Chem. 236 (2012) 35–40. doi:10.1016/j.jphotochem.2012.03.014.

[19] X. Zarate, E. Schott, T. Gomez, R. Arratia-Pérez, Theoretical study of sensitizer candidates for dye-sensitized solar cells: peripheral substituted dizinc pyrazinoporphyrazine-phthalocyanine complexes., J. Phys. Chem. A. 117 (2013) 430–8. doi:10.1021/jp3067316.

[20] J. Zhang, Y.-H. Kan, H.-B. Li, Y. Geng, Y. Wu, Z.-M. Su, How to design proper ?-spacer order of the D-?-A dyes for DSSCs? A density functional response, Dye. Pigment. 95 (2012) 313–321. doi:10.1016/j.dyepig.2012.05.020.

[21] D. Rocca, R. Gebauer, F. De Angelis, M.K. Nazeeruddin, S. Baroni, Time-dependent density functional theory study of squaraine dye-sensitized solar cells, Chem. Phys. Lett. 475 (2009) 49–53. doi:10.1016/j.cplett.2009.05.019.

[22] F. Cervantes-Navarro, D. Glossman-Mitnik, Density functional theory study of indigo and its derivatives as photosensitizers for dye-sensitized solar cells, J. Photochem. Photobiol. A Chem. 255 (2013) 24–26. doi:10.1016/j.jphotochem.2013.01.011.

[23] R. Kavitha, L.G. Devi, Synergistic effect between carbon dopant in titania lattice and surface carbonaceous species for enhancing the visible light photocatalysis, J. Environ. Chem. Eng. 2 (2014) 857–867. doi:10.1016/j.jece.2014.02.016.

[24] A. Anthonysamy, Y. Lee, B. Karunagaran, V. Ganapathy, S.-W. Rhee, S. Karthikeyan, et al., Molecular design and synthesis of ruthenium(ii) sensitizers for highly efficient dye-sensitized solar cells, J. Mater. Chem. 21 (2011) 12389. doi:10.1039/c1jm11760b.

[25] K. Woan, G. Pyrgiotakis, W. Sigmund, Photocatalytic Carbon-Nanotube-TiO 2 Composites, Adv. Mater. 21 (2009) 2233–2239. doi:10.1002/adma.200802738.

[26] T.G. Deepak, G.S. Anjusree, S. Thomas, T.A. Arun, S. V. Nair, A. Sreekumaran Nair, A review on materials for light scattering in dye-sensitized solar cells, RSC Adv. 4 (2014) 17615. doi:10.1039/c4ra01308e.

[27] S. Nakade, M. Matsuda, S. Kambe, Y. Saito, T. Kitamura, T. Sakata, et al., Dependence of TiO 2 Nanoparticle Preparation Methods and Annealing Temperature on the Efficiency of Dye-Sensitized Solar Cells, J. Phys. Chem. B. 106 (2002) 10004–10010. doi:10.1021/jp020051d.

[28] S. Nakade, Y. Saito, W. Kubo, T. Kitamura, Y. Wada, S. Yanagida, Influence of TiO 2 Nanoparticle Size on Electron Diffusion and Recombination in Dye-

Sensitized TiO 2 Solar Cells, J. Phys. Chem. B. 107 (2003) 8607–8611. doi:10.1021/jp034773w.

[29] S. Nakade, W. Kubo, Y. Saito, T. Kanzaki, T. Kitamura, Y. Wada, et al., Influence of Measurement Conditions on Electron Diffusion in Nanoporous TiO 2 Films: Effects of Bias Light and Dye Adsorption, J. Phys. Chem. B. 107 (2003) 14244–14248. doi:10.1021/jp035483i.

[30] J.K. Tsai, W.D. Hsu, T.C. Wu, T.H. Meen, W.J. Chong, Effect of compressed TiO2 nanoparticle thin film thickness on the performance of dye-sensitized solar cells., Nanoscale Res. Lett. 8 (2013) 459. doi:10.1186/1556-276X-8-459.

CHAPTER 5

CO-SENSITIZATION OF MWCNTS-TIO_2 HYBRID ANODE BY N3 AND N719 RUTHENIZERS FOR EFFICIENT DYE-SENSITIZED SOLAR CELLS

Umer Mehmood[1], Shakeel Ahmed[2],Ibnelwaleed A. Hussein[1*,] Khalil Harrabi[3], M. B. Mekki[3]

[1] Department of Chemical Engineering, King Fahd University of Petroleum & Minerals (KFUPM), P. O. Box 5050, Dhahran 31261, Kingdom of Saudi Arabia

[2] Center for Refining & Petrochemicals, KFUPM, P.O. Box 5050, Dhahran 31261, Kingdom of Saudi Arabia

[3] Department of physics, (KFUPM), P. O. Box 5050, Dhahran 31261, Kingdom of Saudi Arabia

[*]Corresponding Author: Ibnelwaleed A. Hussein , E-mail address: ihussein@kfupm.edu.sa

This chapter has been published in "Electrochimica Acta " on May 22, 2015

Abstract

Co-sensitization of two or more dyes on hybrid TiO_2- MWCNTs photoanode is an effective approach to enhance the performance of a dye-sensitized solar cell (DSSC). In this work, N719 sensitizer is co-sensitized with N3. The co-sensitized device showed enhanced V_{OC} and J_{SC} in comparison to single-dye sensitized devices. Upon optimization, the device made of the 0.1Mm N_3 + 0.4mM N719 yielded J_{SC} = 12.5 mA cm^{-2}, V_{oc} =0.73V, FF= 0.45 and η = 4.1 %.This performance is superior to that of either of the individual DSSCs sensitized with N_3 (3.69%) and N719 (3.51 %) under the same conditions of fabrication. The efficiency of DSSCs was further improved to 4.46% by the incorporation of MWCNTs in TiO_2. The hybrid TiO_2/MWCNTs photoanodes with different concentrations of CNTs (0.04. 0.08, 0.12, 0.16 wt. %) were prepared using mixing technique. The optimized molar ratio of N3/N719 was used for the sensitization of hybrid photonodes. Density functional theory (DFT) was used to compute the band gaps of TiO_2 and C-TiO_2 clusters .

Keywords: Hybrid, multi-walled carbon nanotubes, co-sensitization, density functional theory

5.1.Introduction

Energy is the driving force for development, economic growth, automation, and modernization. Energy usage and demand are increasing globally and researchers have taken this seriously to fulfill future energy demands [1,2]. At present global energy sources are mainly dependent on fossil fuels and the use of fossil fuel is the main reason for global increases of CO_2 amount[3] . According to global carbon emissions sources [4], carbon dioxide emissions from coal, oil, natural gas, cement, and gas flaring were 43%, 33%, 18%, 5.3%, and 0.6%, respectively in 2012. Emissions of greenhouse gases grew 2.2% per year between 2000 and 2010, compared with 1.3% per year from 1970 to 2000 [5]. The world is not capable of absorbing large amounts of CO_2 at the rate it is produced by fossil fuels. As a result, increasing the volume of CO_2 in the environment has increased global warming and further climate change. Global warming and climate changes are challenging all over the world. The use of renewable energy provides benefits that reduce emissions of air pollutants as well as greenhouse gases .Therefore, alternative sources of energy are needed so that mankind can survive on the Earth without depending on fossil fuels . Solar energy is one of the renewable energy sources that will contribute to the security of future energy supplies [6,7]. Solar radiation from the sun is approximately 3×10^{24} J per year, which is ten times the current energy demands [8]. Light from the sun can be harvested by dye-sensitized solar cells (DSSCs). DSSCs have attracted considerable attention due to an ideal compromise between efficiency and cost-performance [9–11].The major component of the DSSCs is a dye. Its function is to absorb incoming sunlight and produce excitons. It is chemically bonded to the porous surface of the semiconductor.

However, the traditional dyes generally used in DSSCs suffer from narrow absorption spectra and/or low absorption intensity and therefore low efficiency of DSSCs [10]. To achieve higher cell efficiency, a certain sensitizer is needed so as to absorb incident light as much as possible., Currently, there is no single organic sensitizer which provides strong absorption in a wide range of wavelengths (400-900 nm) [12]. Therefore, the co - sensitization strategy is applied to the organic dyes with complementary absorption spectra to obtain a broader and a more intense absorption band, thus increasing the performance of the DSSC [13–15]. Many co-sensitization systems have been proposed and demonstrated improved photovoltaic performance, such as ruthenium complex co-sensitized with an organic dye [16–18], porphyrin[19–21] or phtalocyanine [22–24] co-sensitized with an organic dye, and organic dye co-sensitized with another organic dye [25,26]. Another major cause of low efficiency of DSSCs is the recombination of injected electrons with the electrolyte (dark current) [27]. The incorporation of CNTs in TiO_2 films may improve the electron transport in DSSCs [28–30], owing to the creation of complex interpenetrating networks and favorable electrical conductivity [31,32]. It is supposed that one-dimensional carbon nanostructures allow the photocurrent to flow more efficiently in DSSCs by increasing orientation orders.

In this work both approaches (co-sensitization and hybrid anode) were used simultaneously to improve the efficiency of DSSCs. Here, we also employed DFT and TD-DFT to find the band gaps and UV-Vis spectra of systems. It is an effective tool as compared to other high level quantum approaches because the computed orbitals are suitable for the typical MO-theoretical analyses and interpretations [33].

5.2.Computer simulations of TiO_2 and C-TiO_2

All the DFT/TD-DFT calculations were executed using Amsterdam Density Functional (ADF) program (2013.01). BAND mode was used to simulate the anatase TiO_2 clusters. The tetragonal anatase crystal structure was selected with single layer (001) surface slab. Then, we created 4×1 super cell from this slab. All atoms were mapped within the unit cell. Then, TiO_2 and carbon doped TiO_2 models were simulated by considering generalized gradient approximation (GAD) at Becke parameter, Lee-Yang-Parr (BYLP) level and triple-ζ polarization basis function. In all the calculations, the relativistic effects were taken into account by the zero order regular approximation (ZORA) Hamiltonian in its scalar approximation.

5.3.Experimentation

Seven different samples of N_3 ,N719 and N3 + N719 i.e. 0.5mM N_3, 0.4mM N3 +0.1 mM N719, 0.3mM N3 +0.2 mM N719, 0.25mM N3 +0.25 mM N719, 0.2mM N3 +0.3 mM N719, 0.1mM N3 +0.4 mM N719 and 0.5mM N719 were prepared in methanol. DSSCs (TiO_2 based) were first fabricated (in open atmosphere) using these co-sensitization systems and then characterized to find the best system. The best co-sensitization system was then employed in hybrid TiO_2-MWCNTs based DSSCs to further improve the efficiency/performance.

5.3.1. Preparation of composite anodes

A suspension of ethanol and MWCNTs was prepared by dissolving 30 mg of MWCNTs (OD 10-20μm, purity > 95%, Ash <1.5%) in 25 ml ethanol. It was then sonicated for 4hr to attain a good dispersion of MWNTs in ethanol. An exact quantity of dispersed MWCNTs was mixed with known amount of anatase TiO_2 paste (T/SP **14451**, Solaronix)

to obtain a composite paste. Five different samples of TiO_2-MWCNTs were prepared by varying the composition of MWCNTs i.e. 0, 0.04. 0.08, 0.12, 0.16wt. %. The TiO_2-MWCNTs paste was then tape casted on FTO glass substrate (2 mm, 7Ω/seq, Solaronix). The coated glass substrate was annealed at 450^{o}C for 30 min. Other photoanodes were prepared following the same procedure. The thickness of each photoanode was found by using cross sectional images obtained from SEM (JEOL, 6610LV). The average thickness of each film was 22 μm.

5.3.2. Fabrication of DSSCs

TiO_2 and TiO_2-MWCNTs electrodes were soaked in the dye solutions for 24 hours. After sensitization, the samples were washed with ethanol to eliminate unanchored dye. Then, DSSCs were fabricated employing the sensitized anode (TiO_2, MWCNTs-TiO_2), platinum deposited counter electrode (Plasticol T, Solaronix), 60 μm sealing spacer (Meltonix 1170, Solaronix) and I^{-}/I_3^{-} redox couple electrolyte prepared in methoxypropionitrile with a 50 mM redox concentration (Iodolyte Z-50, Solaronix). The active surface area of the solar cell was 0.35 cm^2.

5.3.3. Characterization of DSSCs

The UV-Vis spectra of dye solutions in methanol and adsorbed on TiO_2 and MWCNTs-TiO_2 films at glass substrates were recorded with JASCO-670 UV/VIS spectrophotometer. Keithley 2400 Source Meter was used to measure the $I-V$ characteristics of the DSSCs using IV-5 solar simulator (Sr #83, PV Measurement, Inc) at AM1.5G (100 $mWcm^{-2}$). The silicon solar cell was used as a reference for calibration. The impedance spectroscopy (EIS) was measured in dark conditions of illumination via

Bio-Logic SAS (VMP3, s/n:0373), with an AC signal of 10 mV in amplitude, in the frequency range between 10 Hz and 1MHz. The applied bias was between 0 and 750 mV above the V_{oc} of the DSSC.

5.4.Results and Discussion

5.4.1. Morphological properties of composite anode

The dispersion of MWCNTs in TiO_2 was observed by TEM (JEOL, JEM-2100F) analysis. TiO_2-MWCNT sample having 0.16% CNT was selected for TEM analysis, because it was difficult to obtain TEM images of dispersed MWCNTs in TiO_2 from low concentration samples. Fig 5-1 (b) shows that the CNTs are well dispersed in TiO_2, although a few tangles can be observed due to the length of the MWCNTs. The interface connection between MWCNTs and TiO_2 can clearly be observed, indicating that TiO_2 possesses good affinity with MWCNTs. The inner core is hardly visible, because the surface of MWCNT is well decorated with TiO_2 nanoparticles as shown in Fig 5-1 (c).

5.4.2. Electrochemical properties

The HOMOs, LUMOs and band gap energies of photosensitizers play an important role in providing the thermodynamic driving force for the electron injection to the conduction band of TiO_2. For efficient charge transfer, the LUMOs of dyes must be more negative than the conduction band of the semiconductor while HOMO levels must be more positive than the redox potential of electrolyte. The simulated structures of TiO_2 and C-TiO_2 are shown in Fig 5-2. The simulated conduction band, valence band and band gap of TiO_2 and C-TiO_2 are shown in Table 5-1. These tabulated values are in good agreement with the experimental values [34]. The computed results show that doping of MWCNTs (one of the allotropic form of carbon) on TiO_2 significantly reduces the band gap of TiO_2

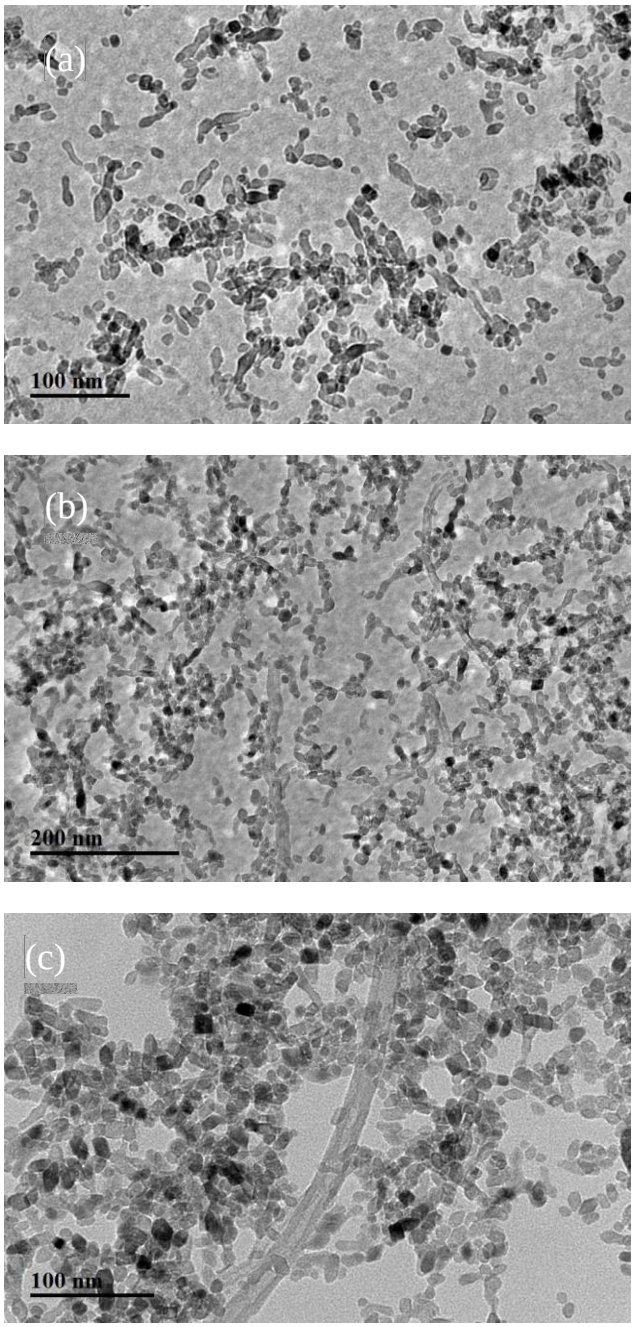

Fig 5-1: TEM images of a 0.16 % sample (a) Pure TiO_2 b) Dispersion of MWCNTs in TiO_2 and c) Dispersion of single MWCNT in TiO_2

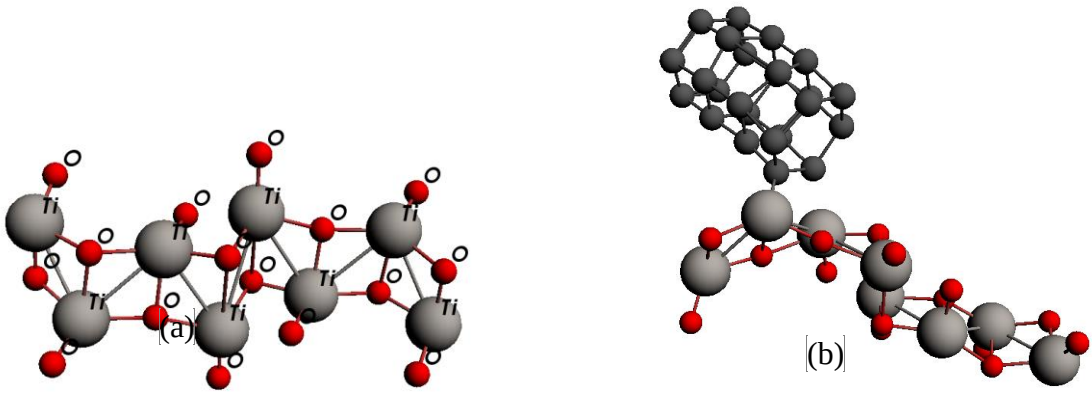

Fig 5-2: Simulated structures of TiO_2 (a) and CNT doped TiO_2

Table 5-1: Simulated electronic structure properties of TiO_2 and carbon doped TiO_2

System	E_{CB} (eV)	V_B (eV)	Band gap (eV)
TiO_2	-7.2	- 4.10	3.1
C-TiO_2	-7.2	-4. 30	2.9

cluster. This is because the CNTs possess the lower value of *the ECB* (~0 EV vs. NHE) than that of TiO_2 (−0.5 eV vs. NHE) [29]. The charge equilibrium between CNTs and TiO_2 would cause a shift of apparent Fermi level to more positive potential i.e.downward potential. The downward positive shift due to MWCNTs (carbon, in the case of simulation) can cause a significant driving force to expedite the charge transport from the dye to the photoanode.

5.4.3. Optical properties

UV-Vis spectra of N719, N3 and N719+N3 are shown in Fig 5-4 (a). N3 and N719 share similar absorption spectra as well as molecular structures. The broad visible peaks at 528, 526 and 382, 384 nm in N719 and N3 respectively, are assigned to metal-to-ligand charge transfer (MLCT) origin. The bands in the UV at 314,312 nm are assigned as intra ligand (π-π*) charge-transfer transitions. High absorption is observed for overall wavelengths in the absorption spectrum of 0.1mM N3 + 0.4mM N719 due to the synergistic effect of the two dyes. But *less* pronounced enhancement in the absorption peak hight indicates lower probability of hydrogen bond formation between the two dyes . However, the absorption spectrum of 0.1mM N3 + 0.4mM N719 shifts to lower energy values when anchored to TiO_2, shown in Fig 5-4 (b). It is due to the binding of the carboxylate groups (from both dyes) to the TiO_2 surface in which Ti^{4+}acts as proton . The interaction between the carboxylate groups and the surface Ti^{4+}ions may lead to increased delocalization of the π* orbital. The energy of the π* level is decreased by this delocalization, which explains the red shift for the absorption spectrum. Moreover, the

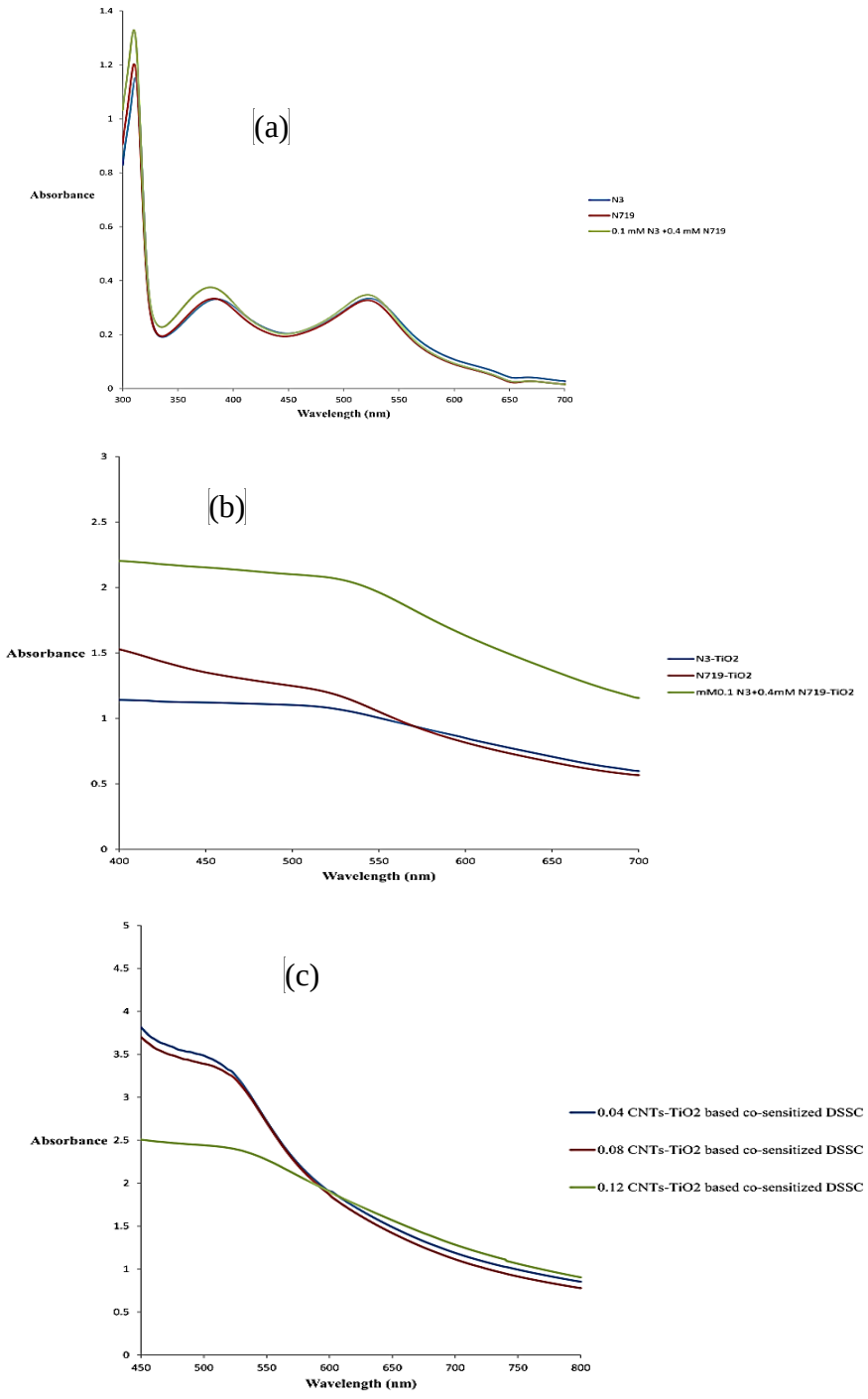

Fig 5-3 :(a) UV-Vis spectra of a) pure dyes in solvent b) Dyes anchored to TiO_2 film and c) dye anchored to MWCNTs-TiO2 hybrid composite film.

absorption spectrum of TiO_2/N3+N719 is more intense and broader as compared to individual dyes anchored to TiO_2. It means that the proposed co-sensitized thin films can absorb more photons than the individual sensitized TiO_2 films. Similarly, the co-sensitized based MWCNTs-TiO_2 thin films show high absorption as compared to TiO_2 co-sensitized film, shown in Fig5-4(c). This is because the CNTs may exhibit photosensitizing properties, thus extending photovoltaic properties into the visible spectrum [35]. However, the further increase in CNTs contents from an optimum level (0.04%) decreases the absorption of co-sensitized films (0.08% and 0.12%) due to diminution in film transparency.

5.4.4. Photovoltaic performance

Fig 5-4 (a) shows the current-voltage (*I-V*) characteristics of the TiO2 based DSSCs, sensitized/co-sensitized by N719,N_3 and N_3+N719. While Fig 5-4 (b) shows the (*I-V*) characteristics of the hybrid photoanode MWCNTs-TiO_2 based DSSCs, co-sensitized by 0.1mM N3+0.4mM N719. The photovoltaic parameters of DSSCs, i.e. J_{sc}, V_{oc} and FF are shown in Table 2. Under a standard AM 1.5G simulated sunlight irradiation, the N719 sensitized DSSC gave a J_{sc} of 11.31 mA·cm^{-2}, a V_{oc} of 739 mV, and a FF of 41.98%, resulted in an efficiency of 3.51%. Moreover, the N3 sensitized DSSC yielded a J_{sc} of 12 mA·cm^{-2}, a V_{oc} of 741 mV, a FF of 42%, and a efficiency of 3.7%. Encouragingly, compared with the devices sensitized by N3 or N719 alone, the co-sensitized (N3+N719) DSSC exhibited a significantly improved efficiency of 4.10%. The improvement in the efficiency is mainly due to the enhancement of the J_{SC} values (14.2 mA·cm^{-2}), which are highly related to the range and the intensity of the absorption spectrum. The overall efficiency of DSSCs was further improved to 4.46% by the

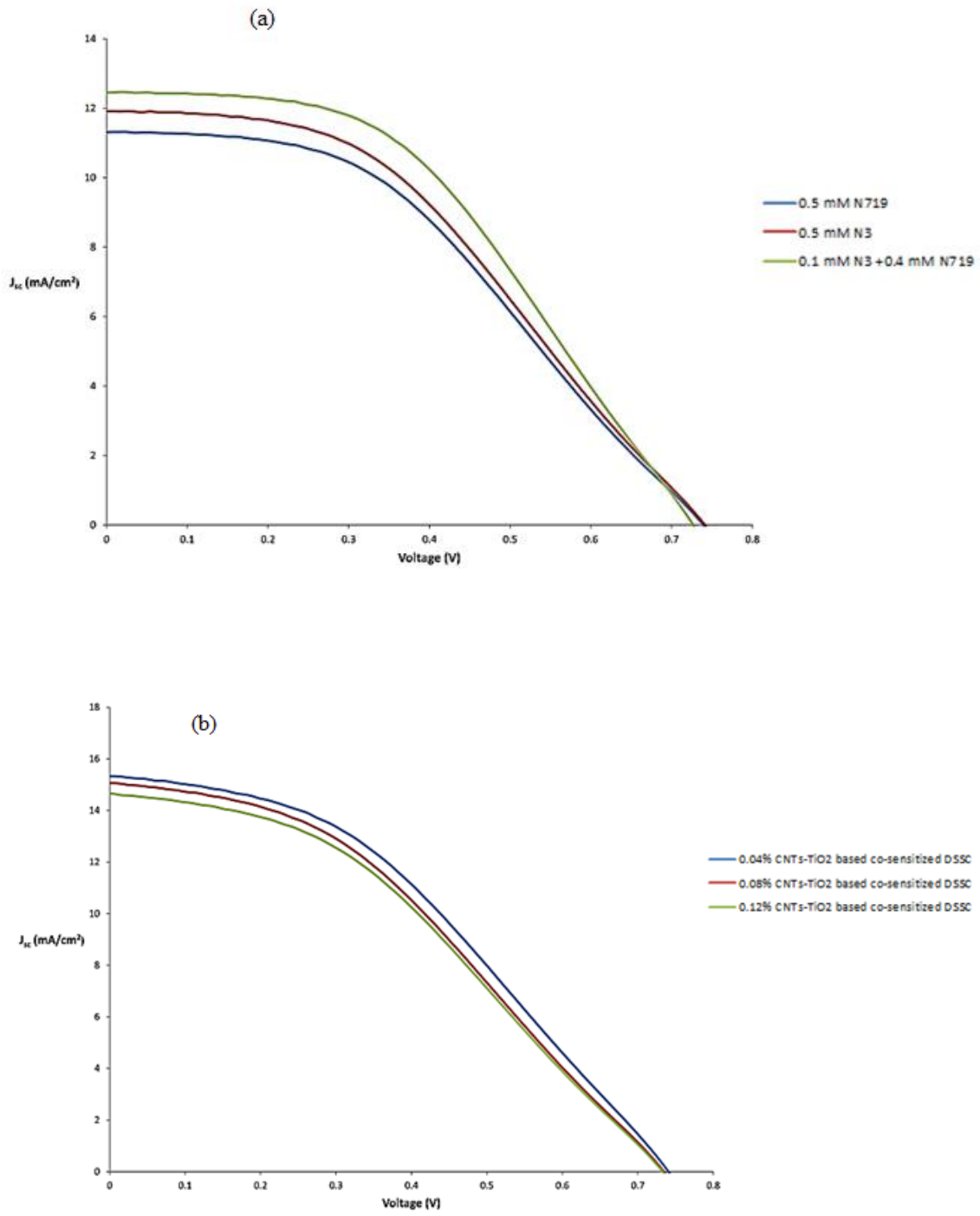

Fig 5-4: Current − voltage characteristics of DSSCs fabricated using a) TiO_2 and b) MWCNTs-TiO_2.

Table 5-2 :Photovolatic properties of DSSCs

DSSCs	j_{sc} **(mA/cm^2)**	V_{oc} **(mV)**	**FF(%)**	η **(%)**
TiO_2/0.5mM N719	11.312	739	42.00	3.51
TiO_2/0.5mM N_3	11.970	741	41.77	3.69
TiO_2/0.4mM N719+ 0.1mM N_3	12.500	727	45.30	4.10
TiO_2/0.3mM N719+ 0.2mM N_3	13.700	742	39.70	4.00
TiO_2/0.25mM N719+ 0.25mM N_3	12.219	750	41.65	3.81
TiO_2/0.2mM N719+ 0.3mM N_3	12.731	760	40.50	3.90
TiO_2/0.1mM N719+ 0.4mM N_3	12.801	744	38.30	3.65
0.04%CNTS-TiO_2/0.4mM N719+ 0.1mM N_3	15.331	741	39.25	4.46
0.08%CNTS-TiO_2/0.4mM N719+ 0.1mM N_3	15.059	734	38.10	4.21
0.12%CNTS-TiO_2/0.4mM N719+ 0.1mM N_3	14.700	731	38.25	4.12

Incorporation of MWCNTs in TiO_2. Insertion of MWCNTs in TiO_2 network significantly enhances the efficiency of DSSC. This is because the incorporation of MWCNTs : a) increases the surface area of hybrid anode and thus more dye loading, b) enhances light harvesting efficiency and thus more photo current and henec more efficiency and c) improve the electron injection efficiency of the electrons due to increase positive potential (as described above in sec 5-4.2). The little decline in V_{oc} at increasing CNTs contents could be attributed to the downshift of the potential band edge of the TiO_2. However an increase in MWCNTs concentration from an optimum level (0.04%) negatively affects the performance of DSSCs owing to decrease in film transparency. Another possibility of low efficiency at a high MWCNTs concentration could be attributed to the formation of CNT agglomerates inside the TiO_2 matrix acting as trapping sites that obstruct the fast charge collection at the electrodes. Therefore, the poor charge collection at the photoanode and light losses due to CNT direct absorption, diminish the efficiency of DSSCs at high CNTs contents.

5.4.5. Electrochemical impedance spectroscopy (EIS) analysis

EIS analysis is performed to further elucidate the photovoltaic properties. Fig 5-5 shows the Nyquist plot of DSSCs which were assembled with N719,N3, 0.1mM N3 + 0.4mM N719 and hybrid CNTs-TiO_2 co-sensitized. Generally, a normal impedance spectra of DSSCs is represented by three arcs (semicircles). The first semicircle represents the inter face resistance of electrons at counter electrode/electrolyte (R_1), second signifies the interface resistance at the photoanode / electrolyte (R_2), and the third indicates the diffusion process of I^-/I_3^- redox couple in electrolyte (Zw) [36,37]. Only second arc comes out in the Nyquist plot in the Fig 5-5. It is probable that the other two arcs corresponding

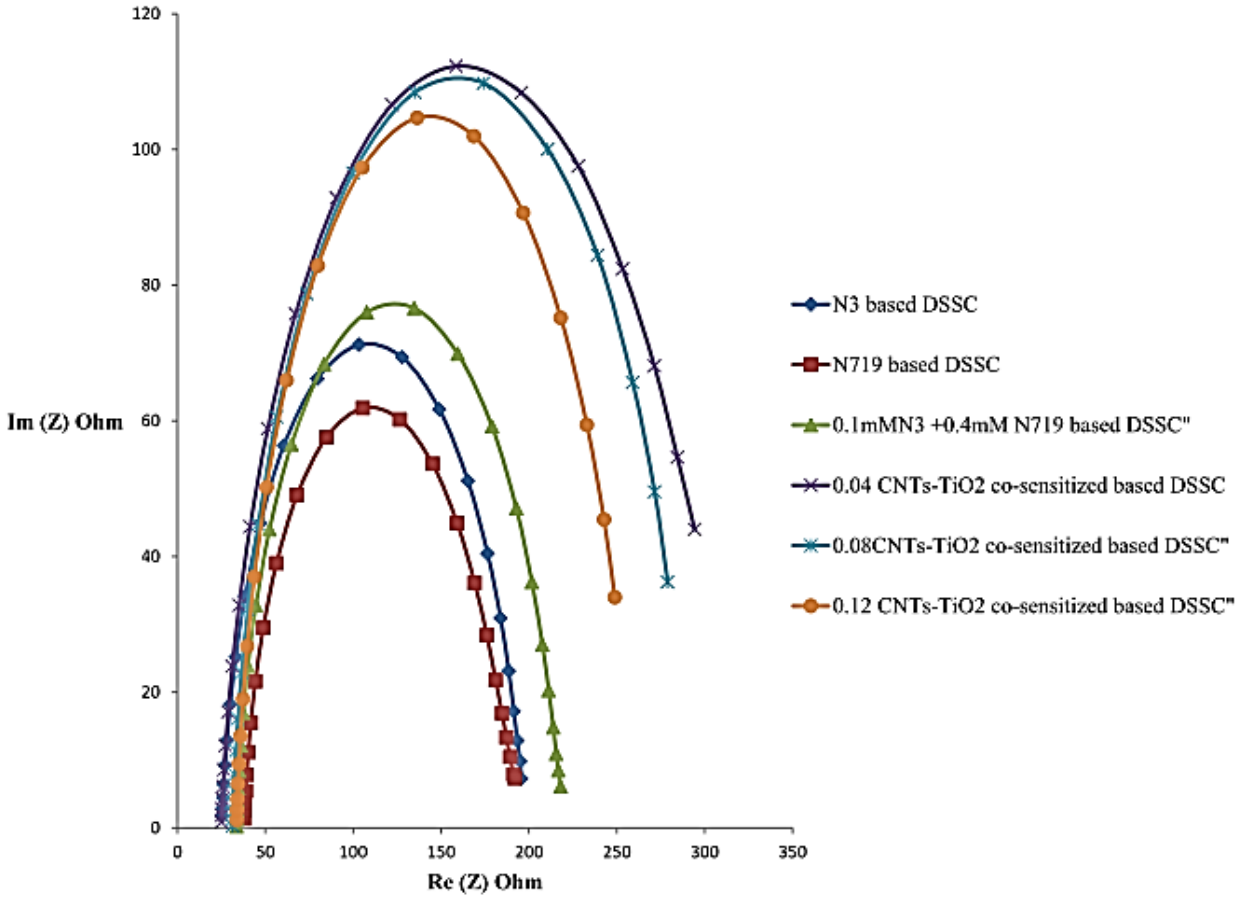

Fig 5-5 :EIS investigation of TiO_2 and TiO_2-MWCNTs based DSSCs

to R_1 and Zw are overshadowed by large semicircle reprenting R_2 [38,39]. The R_2 is related to the charge recombination rate, e.g., a smaller R_2 indicates a faster charge recombination. It can be clearly seen in Fig 5-5 that the radius of the semicircle for 0.1mM N3+0.4mM N719 based DSSC is greater than the based on the single dye and therefore possess high electron life time. The longer electron lifetime for DSSC based on cosensitization may be either due to a higher surface coverage of dye on the TiO_2 surface after cosensitization that block the approach of I_3^- to the free TiO_2 surface and decrease the recombination of injected electron with I_3^- ions, or due to the less aggregation of individual dyes in cosensitized conditions that improves the electron injections. Reduction in charge recombination and electron life time were further improved by the incorporation of MWCNTs in TiO_2. The R_2 value for TiO_2/0.1Mm N_3 + 0.4mM N719 is smaller than that of 0.04% MWCNTs-TiO_2/0.1Mm N_3 + 0.4mM N719 DSSC, proposing charge recombination is greatly reduced owing by incorporation of CNTs. However, the CNTs concentration greater than 0.04 wt.% will lead to the smaller values of R_3 due to a shorter electron lifetime of electrons [30].

5.5.Conclusion

The mixed solution of N719 and N3 in methanol was used for the co-sensitization of the photoanodes of DSSCs. The absorption spectrum of the co-sensitized TiO_2 films becomes more intense and broader than the absorption spectra of the individual N719 and N_3 dyes. The results indicate that the power conversion efficiency of DSSC based on 0.4N719+0.1N_3 is 17% and 11% higher than based on the individual dyes N719 and N3 respectively. Moreover, the cell efficiency of the DSSC with a molar ratio of N3/N719 = 0.1/0.4 was further improved to 4.46% by the incorporation of MWCNTs in TiO_2.

Optimum concentration (0.04%) of CNTs in photoanode does not affect the transparency of TiO_2 layer, while significantly increases the PCE of DSSC. Thus, we established a fast and highly effective technique to enhance the light conversion efficiency of DSSCs.

5.6.Acknowledgement

The authors would like to acknowledge the support provided by King Abdulaziz City for Science and Technology (KACST) through the Science & Technology Unit at King Fahd University of Petroleum & Minerals (KFUPM) for funding this work through project # 11-ENE1635-04 as part of the National Science, Technology and Innovation Plan. KFUPM is also acknowledged for supporting this research. The authors would like to acknowledge the Center of Research Excellence for Renewable Energy at KFUPM.

6. References

1 M. Hasanuzzaman, N. A. Rahim, R. Saidur and S. N. Kazi, *Energy*, 2011, **36**, 233–240.

2 M. Hasanuzzaman, N. A. Rahim, M. Hosenuzzaman, R. Saidur, I. M. Mahbubul and M. M. Rashid, *Renew. Sustain. Energy Rev.*, 2012, **16**, 4527–4536.

3 G. R. Timilsina, S. Csordás and S. Mevel, *Ecol. Econ.*, 2011, **70**, 2400–2415.

4 J. G. Canadell, C. Le Quéré, M. R. Raupach, C. B. Field, E. T. Buitenhuis, P. Ciais, T. J. Conway, N. P. Gillett, R. A. Houghton and G. Marland, *Proc. Natl. Acad. Sci. U. S. A.*, 2007, **104**, 18866–70.

5 M. Hosenuzzaman, N. A. Rahim, J. Selvaraj, M. Hasanuzzaman, A. B. M. A. Malek and A. Nahar, *Renew. Sustain. Energy Rev.*, 2015, **41**, 284–297.

6 K. W. J. Barnham, M. Mazzer and B. Clive, *Nat. Mater.*, 2006, **5**, 161–164.

7 J.-L. Bredas and J. R. Durrant, *Acc. Chem. Res.*, 2009, **42**, 1689–90.

8 K. R. Millington, *Encyclopedia of Electrochemical Power Sources*, Elsevier, 2009.

9 N. Robertson, *Angew. Chem. Int. Ed. Engl.*, 2006, **45**, 2338–45.

10 A. Hagfeldt, G. Boschloo, L. Sun, L. Kloo and H. Pettersson, *Chem. Rev.*, 2010, **110**, 6595–663.

11 C. Klein, M. K. Nazeeruddin, P. Liska, D. Di Censo, N. Hirata, E. Palomares, J. R. Durrant and M. Grätzel, *Inorg. Chem.*, 2005, **44**, 178–80.

12 J.-H. Yum, S.-R. Jang, P. Walter, T. Geiger, F. Nüesch, S. Kim, J. Ko, M. Grätzel and M. K. Nazeeruddin, *Chem. Commun. (Camb).*, 2007, 4680–2.

13 S.-Q. Fan, C. Kim, B. Fang, K.-X. Liao, G.-J. Yang, C.-J. Li, J.-J. Kim and J. Ko, *J. Phys. Chem. C*, 2011, **115**, 7747–7754.

14 L. Wei, Y. Yang, R. Fan, Y. Na, P. Wang, Y. Dong, B. Yang and W. Cao, *Dalton Trans.*, 2014, **43**, 11361–70.

15 Y. Ogomi, S. S. Pandey, S. Kimura and S. Hayase, *Thin Solid Films*, 2010, **519**, 1087–1092.

16 H. Ozawa, R. Shimizu and H. Arakawa, *RSC Adv.*, 2012, **2**, 3198.

17 L. Wei, Y. Yang, R. Fan, P. Wang, L. Li, J. Yu, B. Yang and W. Cao, *RSC Adv.*, 2013, **3**, 25908.

18 S. P. Singh, M. Chandrasekharam, K. S. V. Gupta, A. Islam, L. Han and G. D. Sharma, *Org. Electron.*, 2013, **14**, 1237–1241.

19 A. Yella, H.-W. Lee, H. N. Tsao, C. Yi, A. K. Chandiran, M. K. Nazeeruddin, E. W.-G. Diau, C.-Y. Yeh, S. M. Zakeeruddin and M. Grätzel, *Science*, 2011, **334**, 629–34.

20 C.-M. Lan, H.-P. Wu, T.-Y. Pan, C.-W. Chang, W.-S. Chao, C.-T. Chen, C.-L. Wang, C.-Y. Lin and E. W.-G. Diau, *Energy Environ. Sci.*, 2012, **5**, 6460.

21 H.-P. Wu, Z.-W. Ou, T.-Y. Pan, C.-M. Lan, W.-K. Huang, H.-W. Lee, N. M. Reddy, C.-T. Chen, W.-S. Chao, C.-Y. Yeh and E. W.-G. Diau, *Energy Environ. Sci.*, 2012, **5**, 9843.

22 J. N. Clifford, A. Forneli, H. Chen, T. Torres, S. Tan and E. Palomares, *J. Mater. Chem.*, 2011, **21**, 1693.

23 M. Kimura, H. Nomoto, N. Masaki and S. Mori, *Angew. Chem. Int. Ed. Engl.*, 2012, **51**, 4371–4.

24 L. Jin, Z. L. Ding and D. J. Chen, *J. Mater. Sci.*, 2013, **48**, 4883–4891.

25 D. Kuang, P. Walter, F. Nüesch, S. Kim, J. Ko, P. Comte, S. M. Zakeeruddin, M. K. Nazeeruddin and M. Grätzel, *Langmuir*, 2007, **23**, 10906–9.

26 J.-H. Yum, S.-R. Jang, P. Walter, T. Geiger, F. Nüesch, S. Kim, J. Ko, M. Grätzel and M. K. Nazeeruddin, *Chem. Commun. (Camb).*, 2007, 4680–2.

27 A. Kongkanand, R. M. Domínguez and P. V Kamat, *Nano Lett.*, 2007, **7**, 676–80.

28 A. Kongkanand and P. V Kamat, *ACS Nano*, 2007, **1**, 13–21.

29 P. Du, L. Song, J. Xiong, N. Li, L. Wang, Z. Xi, N. Wang, L. Gao and H. Zhu, *Electrochim. Acta*, 2013, **87**, 651–656.

30 K. T. Dembele, G. S. Selopal, C. Soldano, R. Nechache, J. C. Rimada, I. Concina, G. Sberveglieri, F. Rosei and A. Vomiero, *J. Phys. Chem. C*, 2013, **117**, 14510–14517.

31 J. Liu, Y.-T. Kuo, K. J. Klabunde, C. Rochford, J. Wu and J. Li, *ACS Appl. Mater. Interfaces*, 2009, **1**, 1645–9.

32 S.-R. Jang, R. Vittal and K.-J. Kim, *Langmuir*, 2004, **20**, 9807–10.

33 G. te Velde, F. M. Bickelhaupt, E. J. Baerends, C. Fonseca Guerra, S. J. A. van Gisbergen, J. G. Snijders and T. Ziegler, *J. Comput. Chem.*, 2001, **22**, 931–967.

34 R. Kavitha and L. G. Devi, *J. Environ. Chem. Eng.*, 2014, **2**, 857–867.

35 K. Woan, G. Pyrgiotakis and W. Sigmund, *Adv. Mater.*, 2009, **21**, 2233–2239.

36 K. LEE, C. HU, H. CHEN and K. HO, *Sol. Energy Mater. Sol. Cells*, 2008, **92**, 1628–1633.

37 Y.-L. Xie, Z.-X. Li, Z.-G. Xu and H.-L. Zhang, *Electrochem. commun.*, 2011, **13**, 788–791.

38 S. Li, Y. Lin, W. Tan, J. Zhang, X. Zhou, J. Chen and Z. Chen, *Int. J. Miner. Metall. Mater.*, 2010, **17**, 92–97.

39 A. S. Nair, R. Jose, Y. Shengyuan and S. Ramakrishna, *J. Colloid Interface Sci.*, 2011, **353**, 39–45.

40 T. G. Deepak, G. S. Anjusree, S. Thomas, T. A. Arun, S. V. Nair and A. Sreekumaran Nair, *RSC Adv.*, 2014, **4**, 17615.

41 S. Nakade, M. Matsuda, S. Kambe, Y. Saito, T. Kitamura, T. Sakata, Y. Wada, H. Mori and S. Yanagida, *J. Phys. Chem. B*, 2002, **106**, 10004–10010.

42 S. Nakade, Y. Saito, W. Kubo, T. Kitamura, Y. Wada and S. Yanagida, *J. Phys. Chem. B*, 2003, **107**, 8607–8611.

43 S. Nakade, W. Kubo, Y. Saito, T. Kanzaki, T. Kitamura, Y. Wada and S. Yanagida, *J. Phys. Chem. B*, 2003, **107**, 14244–14248.

44 J. K. Tsai, W. D. Hsu, T. C. Wu, T. H. Meen and W. J. Chong, *Nanoscale Res. Lett.*, 2013, **8**, 459.

CHAPTER 6

DYE SENSITIZED SOLAR CELLS BASED ON TIO_2 – GRAPHENE NANOCOMPOSITE PHOTOANODE

Umer Mehmood[1], Shakeel Ahmed[2],Ibnelwaleed A. Hussein[1*,] Khalil Harrabi[3]

[1]Department of Chemical Engineering, King Fahd University of Petroleum & Minerals, P. O. Box 5050, Dhahran 31261, Kingdom of Saudi Arabia

[2] Center for Refining & Petrochemicals, King Fahd University of Petroleum & Minerals, Dhahran 31261, Kingdom of Saudi Arabia

Department of physics, KFUPM, P. O. Box 5050, Dhahran 31261, Kingdom of Saudi Arabia

[*]Corresponding Author: Ibnelwaleed A. Hussein , E-mail address: ihussein@kfupm.edu.sa

This chapter has been submitted in "Solar Energy Material and Solar Cells " on June 01, 2015

Abstract

Composite photoanodes for dye sensitized solar cells (DSSCs) were prepared by simple addition of graphene (GR) micro-platelets to TiO_2 nanoparticulate paste. Transmission electron microscopy (TEM) was used to confirm the presence of graphene in composite films after heating at 450 C for 30 minutes. TiO_2/graphene based DSSCs with different concentrations of gaphene (0, 0.03. 0.06, 0.09, 0.15, 0.21 wt. %) were fabricated using N749 photosensitizer. The UV-Visible absorption spectroscopy, photocurrent–voltage (*I–V*) characteristic and electrochemical impedance spectroscopy (EIS) measurements were carried out to characterize the cells. The results indicate that graphene/TiO2 photoanode improves the performance of of solar cell. This is because the graphene/titania electrode accelerates electronic transportation and suppresses the charge recombination. Under an optimal conditions, solar cell based on graphene/TiO2 shows power conversion efficiency (PCE) of 4.1 %, which is about 30% greater than the cell based on pristine TiO_2 electrode (3.16%). The objective of this study is to develop a fast, cheap, and an effective means to increase the photo conversion efficiency (PCE) of DSSCs.

Keywords: Nanocomposite photoanodes, dye sensitized solar cell, graphene, Titania, power conversion efficiency.

6.1.Introduction

The use of renewable energy provides benefits that reduce emissions of air pollutants as well as greenhouse gases. Therefore, alternative sources of energy are needed so that mankind can survive on the Earth without depending on fossil fuels. Solar energy is one of the renewable energy sources that will contribute to the security of future energy supplies [1,2] Solar radiation from the sun is approximately 3×10^{24} J per year, which is ten times the current energy demands [3]. Light from the sun can be harvested by dye-sensitized solar cells (DSSCs).DSSCs have attracted considerable attention during the last decade due to an ideal compromise between efficiency and cost-performance [4–6]. DSSCs comprise of a sensitized semiconductor (Photoelectrode) and a catalytic electrode (counter electrode) with an electrolyte sandwiched between them.The major component of the DSSCs is a dye. Its function is to absorb incoming sunlight and produce excitons. It is chemically bonded to the porous surface of a metal oxide semiconductor. So far, polypyridyl ruthenium sensitizers based solar cells have attained up to 11% conversion efficiency [7–9] . But it is still low for commercial applications.

The major cause of low efficiency of DSSCs is the recombination of injected electrons (from the dye to the conduction band of the semiconductor) with the electrolyte (dark current) [10,11]. Photoanode of DSSCs plays an important role in the separation and transportation of electrons. Carbon-based materials CNTs) [12–14] and more recently graphene [15,16] have been proposed as an additive material for TiO_2 photoanode to increase the electron mobility, owing to their outstanding electronic properties. But the enhancement of PCE due to CNTs is limited by poor contact between CNTs and TiO_2 [17]. Two dimenssional Graphene nano carbon material was also introduced to prepare

the hybrid film. It has an excellent mobility of charge carrier (200 000 cm^2 V^{-1} s^{-1}) [18] and large specific surface area (2630 m^2/g) [19]. Jihuai Wu et al [17] introduced graphene into TiO_2 by one step hydrothermal reaction and reported a 17.7 % increase in PCE of DSSC. Tang et al [20] embedded graphene sheets in TiO_2 paste via molecular grafting and showed 1.68% efficiency, which is five times higher than that without graphene (0.32%). Sun et al [21] fabricated graphene/TiO_2 nanocomposites electrode through heterogeneous coagulation method and reported 4.28% efficiency, which is 59% greater than that without graphene. However the efficiency of these cells is still lower; and the fabrication method of graphing/TiO_2 nanocompostie is relatively complex. Here, we presented a fast, cheap, and one-step process to prepare the graphene/TiO2 photoanode. It is expected that the incorporation of graphene in photanode may enhance the PCE of DSSCs by reducing the charge recombination .

6.2.Computer simulations

The objective of the simulation is just to see the effect of carbon based materials on the band gap of TiO_2. All the DFT calculations were executed using Amsterdam Density Functional (ADF) program (2013.01). BAND mode was used to simulate the anatase TiO_2 clusters. The tetragonal anatase crystal structure was selected with single layer (001) surface slab. Then, we created 4×1 super cell from this slab. All atoms were mapped within the unit cell. Graphene is an allotrope of carbon in the form of a two-dimensional sheet. It is impossible to dope the 2D grapahne sheet on TiO_2 cluster in the ADF environment. Therefore, we only doped the single carbon atom on TiO_2 cluster to find/simulate a band gap of C-TiO_2. TiO_2 and carbon doped TiO_2 models were simulated by considering hybrid Becke parameter, Lee-Yang-Parr (B1YLP) level and triple-ζ

polarization basis function. In all the calculations, the relativistic effects were taken into account by the zero order regular approximation (ZORA) Hamiltonian in its scalar approximation.

6.3.Experimental

6.3.1. Preparation of composite anodes

A suspension of ethanol and graphene was prepared by dissolving 15 mg of graphenein 20 ml ethanol. It was then sonicated for 5hr to attain a good dispersion of graphene in ethanol. An exact quantity of dispersed graphene was mixed with known amount of anatase TiO_2 paste (T/SP **14451**, Solaronix) to obtain a composite paste. Five different samples of TiO_2-graphene were prepared by varying the composition of graphenes i.e. 0, 0.03. 0.06, 0.09, 0.12, 0.15 wt. %. The composite paste paste was then tape casted on FTO glass substrate (2 mm,7Ω/seq, Solaronix). The coated glass substrate annealed at 450^{o}C for 30 min. Other photoanodes were prepared following the same procedure. The thickness of each photoanode was found by using cross sectional images obtained from SEM (JEOL, 6610LV). The average thickness of each film was 20 µm.

6.3.2. Fabrication of DSSCs

A 0.5 mM solution of N749 was prepared in methanol. The composite electrodes were soaked in the dye solution for 24 hours. After sensitization, the samples were washed with ethanol to eliminate unanchored dye. Then, DSSCs were fabricated employing the sensitized hybrid anode, platinum deposited counter electrode (Plasticol T, Solaronix), 60 µm sealing spacer (Meltonix 1170, Solaronix) and I^{-}/I_3^{-} redox couple electrolyte prepared in methoxypropionitrile with a 50 mM redox concentration (Iodolyte Z-50, Solaronix).

6.3.3. Characterization of DSSCs

The visible spectra of N719 in methanol and adsorbed on TiO_2 films at glass substrates were recorded with JASCO-670 UV/VIS spectrophotometer. Keithley 2400 Source Meter was used to measure the $I-V$ characteristics of the DSSCs using IV-5 solar simulator (Sr #83, PV Measurement, Inc) at AM1.5G (100 $mWcm^{-2}$). The silicon solar cell was used as a reference for calibration. The impedance spectroscopy (EIS) was measured in dark conditions of illumination via Bio-Logic SAS (VMP3, s/n:0373), with an AC signal of 10 mV in amplitude, in the frequency range between 10 mHz and 1MHz.

6.4.Results and Discussion

6.4.1. Morphological properties of composite anode

The dispersion of graphene in TiO_2 was observed by TEM (JEOL, JEM-2100F) analysis. TiO_2-graphene sample having 0.15% graphene was selected for TEM analysis, because it was difficult to obtain TEM images (of dispersed graphene in $TiO_{2)}$ from low concentration samples.Fig 6-1(a) shows the TEM image of titania. Fig 6-1 (b) clearly demonstrates the crystalline nature of the graphene sheet. HRTEM was used to measure the graphene layer spacing in its crystalline lattice. The lattice spacing in graphene prepared by our method is 0.348 nm. While, Fig 6-1(c) shows the naanocomposit of Graphen-TiO_2. Fig 6-1(c) also shows that graphene nanosheets tend to congregate together to form multilayer agglomerates.

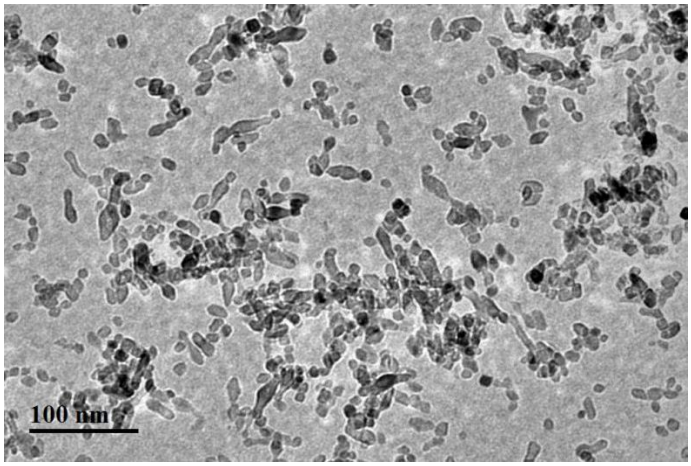

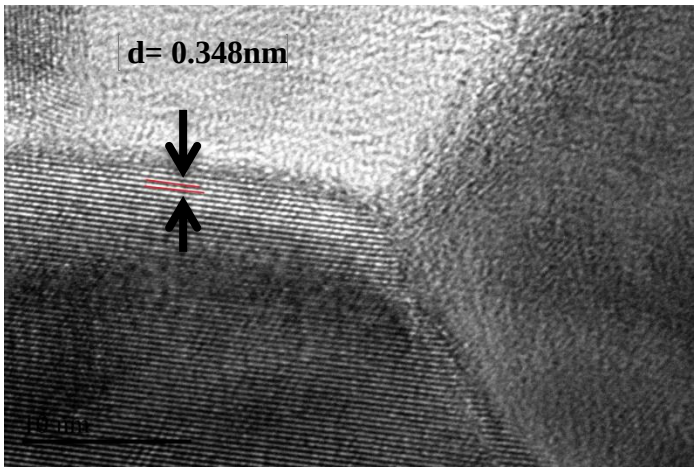

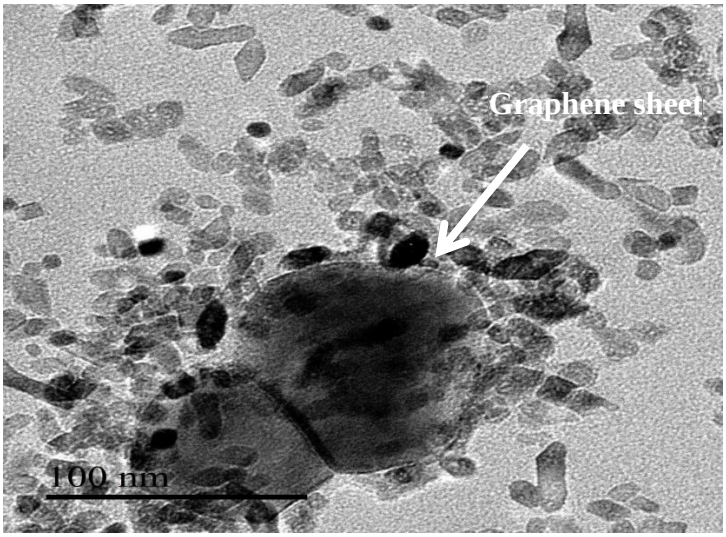

Fig 6-1:TEM images of a) TiO2 nanoparticles b) lattice spacing in graphene and c) TiO2-Graphene nanocomposites

The dispersion of graphene in TiO_2 was observed by TEM (JEOL, JEM-2100F) analysis. TiO_2-graphene sample having 0.15% graphene was selected for TEM analysis, because it was difficult to obtain TEM images (of dispersed graphene in $TiO_{2)}$ from low concentration samples.Fig -1(a) shows the TEM image of titania. Fig 6-1 (b) clearly demonstrates the crystalline nature of the graphene sheet. HRTEM was used to measure the graphene layer spacing in its crystalline lattice. The lattice spacing in graphene prepared by our method is 0.348 nm. While, Fig 6-1(c) shows the naanocomposit of Graphen-TiO_2. Fig 6-1(c) also shows that graphene nanosheets tend to congregate together to form multilayer agglomerates.

6.4.2. Effect of graphene on the band gap of TiO_2

The HOMOs, LUMOs and band gap energies of photosensitizers play a vital role in providing the driving force for the electron injection to conduction band of TiO_2. For efficient charge transfer, the LUMOs of dyes must be more negative than the conduction band of the semiconductor while HOMO levels must be more positive than the redox potential of electrolyte. We used a DFT technique to find the band gap of TiO_2 and C-TiO_2. The simulated structures of TiO_2 and C-TiO_2 are shown in Fig 6-2. While, the simulated conduction band, valence band and band gap of TiO_2 and C-TiO_2 are shown in Table-1. The computed results show that impregnation of graphene (one of the allotropic form of carbon) on TiO_2 significantly reduces the band gap of TiO_2 cluster. This is because the graphene possesses the lower value of *the* E_{CB} (~0 EV vs. NHE) [22] than that of the titania (−0. 5 eV vs. NHE) [23]. The charge equilibrium between graphene and TiO_2 would cause a shift of apparent Fermi level (E_F) to more positive potential.

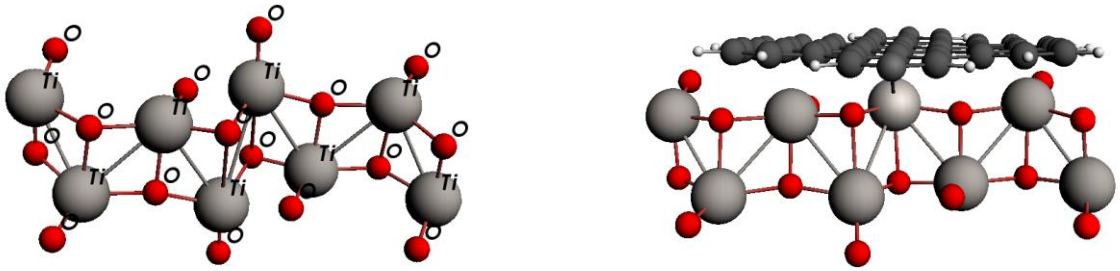

Fig 6-2. Simulated structures of a) TiO_2 and b) graphene doped TiO_2

Table 6-1: Simulated electronic structure properties of TiO_2 and carbon doped TiO_2

System	E_{CB} (eV)	V_B (eV)	Band gap (eV)
TiO_2	-7.2	- 4.10	3.1
C-TiO_2	-7.2	-4. 30	2.9

Moreover, the downward positive shift due to graphene can cause a significant driving force to expedite the electron transport from the sensitizer to the photoanode.

6.4.3. Photophysical properties

The visible spectra of N749 in methanol and anchored to TiO_2 and TiO_2-graphene, are shown in Fig 6-4 (a) and 4 (b) respectively. The two broad visible bands at 608 and 415 nm in N749 are assigned to metal-to-ligand charge-transfer (MLCT) origin. The bands in the UV at 322 nm are assigned as intra ligand (π-π*) charge-transfer transitions. However, the absorption shifts to lower energy values when anchored to TiO_2 and TiO_2-graphene. This is due to the fact that on the electrode the carboxylate groups bind to the TiO_2 surface in which Ti^{4+}acts as proton. The interaction between the carboxylate group and the surface Ti^{4+}ions may lead to increased delocalization of the π* orbital.The energy of the π* level is decreased by this delocalization, which explains the red shift for the absorption spectra. But the TiO2-graphene based photoanode has a greater red shift value as compared to pure TiO_2. This is because the graphene may exhibit photosensitizing properties, thus extending photovoltaic properties into the visible spectrum [24][25].

6.4.4. Photovoltaic properties of DSSCs based composite anode

Hybrid graphene/ TiO_2 based DSSCs were prepared with an effective area of 0.35 cm^2. The photovoltaic parameters, short-circuit current density (*Jsc*), open circuit voltage (Voc), fill factor (FF), and photovoltaic conversion efficiency (η), are summarized in Table 2 and the corresponding *I-V*curves are showed in Fig 4. The DSSC with the highest efficiency is achieved in the case of 0.09%MWCNTs-TiO_2,which is about 30 % greater than the unmodified TiO_2 (3.16). This is because the incorporation of graphene increases the surface area of hybrid anode and thus more dye loading. However, the little decline in

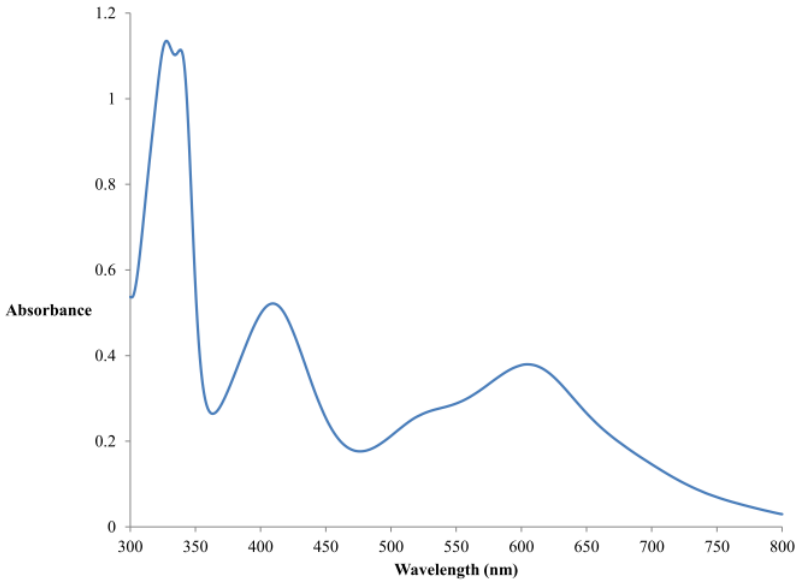

Fig 6-3 (a). UV-Vis spectra of N749 in methanol

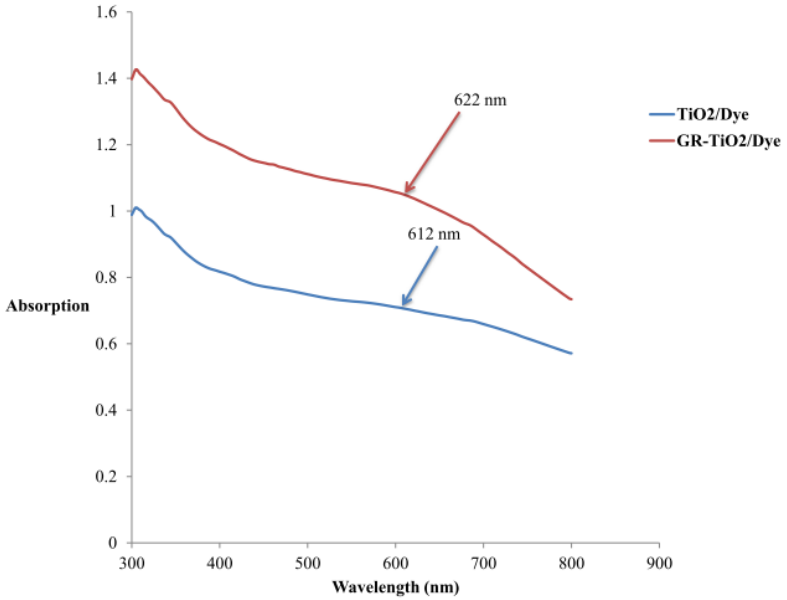

Fig 6-3 (b). UV-Vis spectra of TiO_2/N749 and 0.09%GR+TiO2/N749

Voc at increasing graphene contents could be attributed to the downshift of the potential band edge of the TiO_2 conduction band. It can also be observed that increase in graphene concentration from optimum level (0.09%) negatively affects the performance of DSSCs. This is because of the decrease in film transparency owing to increase graphene contents. Another possibility of low efficiency at a high graphene concentration could be attributed to the formation of graphene agglomerates inside the TiO_2 matrix acting as trapping sites that obstruct the fast charge collection at the electrodes. The less charge collection together with light loss owing to graphene direct absorption, strongly declines the efficiency of DSSCs at high graphene contents.

Table 6-2 :Photovolatic properties of DSSCs

DSSCs	j_{sc} (mA/cm^2)	V_{oc} (mV)	FF(%)	η (%)
Pure TiO_2	10.310	703.994	43.50	3.16
0.03%GR+TiO2	12.089	705.088	42.31	3.61
0.06%GR+TiO2	14.181	706.786	38.84	3.89
0.09%GR+TiO2	13.037	705.022	43.90	4.03
0.12%GR+TiO2	12.195	696.490	40.02	3.40
0.15%GR+TiO2	9.185	690.836	47.52	3.02

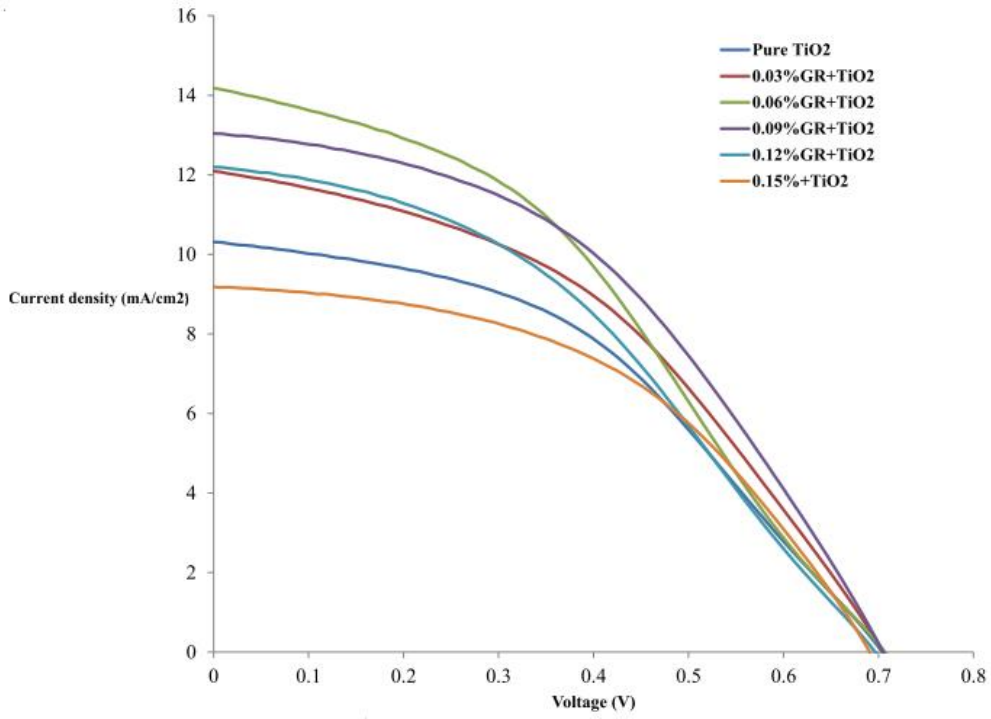

Fig 6-4: Current − voltage characteristics of DSSCs fabricated using different contents of graphene

6.4.5. Electrochemical impedance spectroscopy

EIS analysis is performed to further explain the photovoltaic properties of DSSCs. Fig 6-5 shows the Nyquist plot of DSSCs which were assembled with TiO_2-N749 and graphene-TiO_2-N749. Generally, a normal impedance spectrum of DSSCs is represented by three arcs (semicircles). The first semicircle represents the charge transport resistance at counter electrode/electrolyte (R_1), second signifies the charge transport resistance at the photoanode / electrolyte interface (R_2), and the third indicates the diffusion process of redox couple in electrolyte (*Zw)* [23,26]. Only second arc comes out in the Nyquist plot in the Fig 6-5. It is probable that the other two arcs corresponding to R_1 and *Zw* are overshadowed by larger semicircle reprinting R_2 [27,28]. The R_2 is related to the charge recombination rate, e.g., a high R_2 value shows a lower charge recombination and vise versa. The R_2 value for DSSC assembled with pure TiO_2 is smaller than that of 0.09%graphene-TiO_2, proposing charge recombination is greatly reduced owing to the incorporation of graphene. However, the graphene concentration greater than 0.09 wt.% will lead to the smaller values of R_2 due to a shorter electron lifetime of the order of few tens of mili seconds [29].

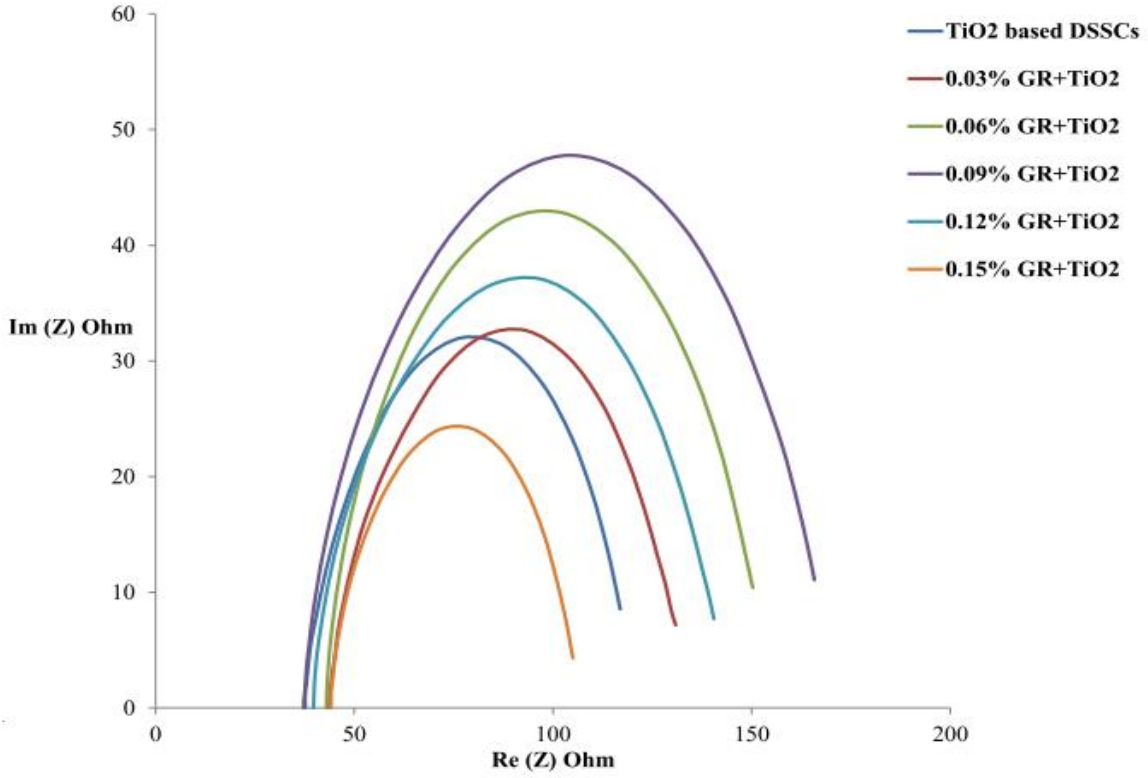

Fig 6-5. EIS investigation of TiO_2 and GR+TiO2 based DSSCs

6.5.Conclusion

We established a fast and highly reproducible methodology to fabricate DSSCs by simple addition of graphene sheets into a l TiO_2. The incorporation of graphene in TiO_2 slowing the recombination of photogenerated electrons, extending the excitation wavelength and increasing the surface-adsorbed amount of dye. We established that the dispersion of small amounts of graphenes in TiO_2 can significantly improve the photo conversion efficiency of DSSCs. Optimum concentration (0.09%) of graphene in photoanode does not affect the transparency of TiO_2 layer, while significantly increases the PCE of DSSC, with a maximum value of 4.12%. Thus, we established a profligate, economical, and highly effective technique to enhance the light conversion efficiency of DSSCs.

6.6.Acknowledgement

The authors would like to acknowledge the support provided by King Abdulaziz City for Science and Technology (KACST) through the Science & Technology Unit at King Fahd University of Petroleum & Minerals (KFUPM) for funding this work through project # 11-ENE1635-04 as part of the National Science, Technology and Innovation Plan. KFUPM is also acknowledged for supporting this research. The authors would like to acknowledge the Center of Research Excellence for Renewable Energy at KFUPM.

6.7.References

[1] K.W.J. Barnham, M. Mazzer, B. Clive, Resolving the energy crisis: nuclear or photovoltaics?, Nat. Mater. 5 (2006) 161–164. doi:10.1038/nmat1604.

[2] J.-L. Bredas, J.R. Durrant, Organic photovoltaics., Acc. Chem. Res. 42 (2009) 1689–90. doi:10.1021/ar900238j.

[3] K.R. Millington, Encyclopedia of Electrochemical Power Sources, Elsevier, 2009. doi:10.1016/B978-044452745-5.00317-8.

[4] A. Hagfeldt, G. Boschloo, L. Sun, L. Kloo, H. Pettersson, Dye-sensitized solar cells., Chem. Rev. 110 (2010) 6595–663. doi:10.1021/cr900356p.

[5] N. Robertson, Optimizing dyes for dye-sensitized solar cells., Angew. Chem. Int. Ed. Engl. 45 (2006) 2338–45. doi:10.1002/anie.200503083.

[6] C. Klein, M.K. Nazeeruddin, P. Liska, D. Di Censo, N. Hirata, E. Palomares, et al., Engineering of a novel ruthenium sensitizer and its application in dye-sensitized solar cells for conversion of sunlight into electricity., Inorg. Chem. 44 (2005) 178–80. doi:10.1021/ic048810p.

[7] M.K. Nazeeruddin, F. De Angelis, S. Fantacci, A. Selloni, G. Viscardi, P. Liska, et al., Combined experimental and DFT-TDDFT computational study of photoelectrochemical cell ruthenium sensitizers., J. Am. Chem. Soc. 127 (2005) 16835–47. doi:10.1021/ja052467l.

[8] F. Gao, Y. Wang, D. Shi, J. Zhang, M. Wang, X. Jing, et al., Enhance the optical absorptivity of nanocrystalline TiO2 film with high molar extinction coefficient ruthenium sensitizers for high performance dye-sensitized solar cells., J. Am. Chem. Soc. 130 (2008) 10720–8. doi:10.1021/ja801942j.

[9] C.-Y. Chen, M. Wang, J.-Y. Li, N. Pootrakulchote, L. Alibabaei, C.-H. Ngoc-le, et al., Highly efficient light-harvesting ruthenium sensitizer for thin-film dye-sensitized solar cells., ACS Nano. 3 (2009) 3103–9. doi:10.1021/nn900756s.

[10] A. Kongkanand, R.M. Domínguez, P. V Kamat, Single wall carbon nanotube scaffolds for photoelectrochemical solar cells. Capture and transport of photogenerated electrons., Nano Lett. 7 (2007) 676–80. doi:10.1021/nl0627238.

[11] K.T. Dembele, G.S. Selopal, R. Milan, C. Trudeau, D. Benetti, A. Soudi, et al., Graphene below the percolation threshold in TiO 2 for dye-sensitized solar cells, J. Mater. Chem. A. 3 (2015) 2580–2588. doi:10.1039/C4TA04395B.

[12] T. Sawatsuk, A. Chindaduang, C. Sae-kung, S. Pratontep, G. Tumcharern, Dye-sensitized solar cells based on TiO2–MWCNTs composite electrodes: Performance improvement and their mechanisms, Diam. Relat. Mater. 18 (2009) 524–527. doi:10.1016/j.diamond.2008.10.052.

[13] K.T. Dembele, R. Nechache, L. Nikolova, A. Vomiero, C. Santato, S. Licoccia, et al., Effect of multi-walled carbon nanotubes on the stability of dye sensitized solar cells, J. Power Sources. 233 (2013) 93–97. doi:10.1016/j.jpowsour.2013.01.075.

[14] C.-Y. Yen, Y.-F. Lin, S.-H. Liao, C.-C. Weng, C.-C. Huang, Y.-H. Hsiao, et al., Preparation and properties of a carbon nanotube-based nanocomposite photoanode for dye-sensitized solar cells., Nanotechnology. 19 (2008) 375305. doi:10.1088/0957-4484/19/37/375305.

[15] J. Durantini, P.P. Boix, M. Gervaldo, G.M. Morales, L. Otero, J. Bisquert, et al., Photocurrent enhancement in dye-sensitized photovoltaic devices with titania–graphene composite electrodes, J. Electroanal. Chem. 683 (2012) 43–46. doi:10.1016/j.jelechem.2012.07.032.

[16] N. Yang, J. Zhai, D. Wang, Y. Chen, L. Jiang, Two-dimensional graphene bridges enhanced photoinduced charge transport in dye-sensitized solar cells., ACS Nano. 4 (2010) 887–94. doi:10.1021/nn901660v.

[17] J. Zhao, J. Wu, M. Zheng, J. Huo, Y. Tu, Improving the photovoltaic performance of dye-sensitized solar cell by graphene/titania photoanode, Electrochim. Acta. 156 (2015) 261–266. doi:10.1016/j.electacta.2015.01.045.

[18] K.I. Bolotin, K.J. Sikes, Z. Jiang, M. Klima, G. Fudenberg, J. Hone, et al., Ultrahigh electron mobility in suspended graphene, Solid State Commun. 146 (2008) 351–355. doi:10.1016/j.ssc.2008.02.024.

[19] M.D. Stoller, S. Park, Y. Zhu, J. An, R.S. Ruoff, Graphene-based ultracapacitors., Nano Lett. 8 (2008) 3498–502. doi:10.1021/nl802558y.

[20] Y.-B. Tang, C.-S. Lee, J. Xu, Z.-T. Liu, Z.-H. Chen, Z. He, et al., Incorporation of graphenes in nanostructured TiO(2) films via molecular grafting for dye-sensitized solar cell application., ACS Nano. 4 (2010) 3482–8. doi:10.1021/nn100449w.

[21] S. Sun, L. Gao, Y. Liu, Enhanced dye-sensitized solar cell using graphene-TiO[sub 2] photoanode prepared by heterogeneous coagulation, Appl. Phys. Lett. 96 (2010) 083113. doi:10.1063/1.3318466.

[22] C.H. Tang, X.L. Dong, C. Ma, X.X. Zhang, H.C. Ma, X.F. Zhang, Constructing TiO2/Gr with Rapid Electrons Transfer for Efficiency Photocatalysis, in: Adv. Mater. Res., 2012: pp. 705–708. http://www.scientific.net/AMR.518-523.705 (accessed March 02, 2015).

[23] P. Du, L. Song, J. Xiong, N. Li, L. Wang, Z. Xi, et al., Dye-sensitized solar cells based on anatase TiO2/multi-walled carbon nanotubes composite nanofibers photoanode, Electrochim. Acta. 87 (2013) 651–656. doi:10.1016/j.electacta.2012.09.096.

[24] M.-Q. Yang, Y.-J. Xu, Basic Principles for Observing the Photosensitizer Role of Graphene in the Graphene–Semiconductor Composite Photocatalyst from a Case Study on Graphene–ZnO, J. Phys. Chem. C. 117 (2013) 21724–21734. doi:10.1021/jp408400c.

[25] Y. Zhang, N. Zhang, Z.-R. Tang, Y.-J. Xu, Graphene transforms wide band gap ZnS to a visible light photocatalyst. The new role of graphene as a macromolecular photosensitizer., ACS Nano. 6 (2012) 9777–89. doi:10.1021/nn304154s.

[26] K. LEE, C. HU, H. CHEN, K. HO, Incorporating carbon nanotube in a low-temperature fabrication process for dye-sensitized TiO2 solar cells☆, Sol. Energy Mater. Sol. Cells. 92 (2008) 1628–1633. doi:10.1016/j.solmat.2008.07.012.

[27] Y.-L. Xie, Z.-X. Li, Z.-G. Xu, H.-L. Zhang, Preparation of coaxial TiO2/ZnO nanotube arrays for high-efficiency photo-energy conversion applications, Electrochem. Commun. 13 (2011) 788–791. doi:10.1016/j.elecom.2011.05.003.

[28] S. Li, Y. Lin, W. Tan, J. Zhang, X. Zhou, J. Chen, et al., Preparation and performance of dye-sensitized solar cells based on ZnO-modified TiO2 electrodes, Int. J. Miner. Metall. Mater. 17 (2010) 92–97. doi:10.1007/s12613-010-0116-z.

[29] K.T. Dembele, G.S. Selopal, C. Soldano, R. Nechache, J.C. Rimada, I. Concina, et al., Hybrid Carbon Nanotubes–TiO 2 Photoanodes for High Efficiency Dye-Sensitized Solar Cells, J. Phys. Chem. C. 117 (2013) 14510–14517. doi:10.1021/jp403553t.

CHAPTER 7

THEORETICAL STUDY OF BENZENE/THIOPHENE BASED PHOTOSENSITIZERS FOR DYE SENSITIZED SOLAR CELLS (DSSCS).

Umer Mehmood[1], Ibnelwaleed A. Hussein[1*], Muhammad Daud[1] , Shakeel Ahmed[2], Khalil Harrabi [3]

[1] Department of Chemical Engineering, King Fahd University of Petroleum & Minerals (KFUPM), P. O. Box 5050, Dhahran 31261, Kingdom of Saudi Arabia

[2] Center for Refining & Petrochemicals, KFUPM, P.O. Box 5050, Dhahran 31261, Kingdom of Saudi Arabia

[3] Department of physics, KFUPM, P. O. Box 5050, Dhahran 31261, Kingdom of Saudi Arabia

[*]Corresponding Autho, E-mail address: ihussein@kfupm.edu.sa

This chapter has been published in “dyes and pigments” on 05 March 2015

Abstract

Complex organic compounds with benzene/thiophene as pi-segments are inspected as photosensitizers for applications in dye sensitized solar cells. To better understand the charge transport process involved in the dye sensitized solar cells, we used the results of Kohn–Sham density functional theory and time-dependent density functional theory (DFT) studies of benzene/thiophene based sensitizers as well as the dye bound to a TiO_2 nano cluster. We investigated the electronic structures and UV-Vis spectra of the sensitizers alone and linked to the cluster. We also showed energy level diagrams, the major transitions of molecular orbitals and free energy calculation of the electron transfer from the sensitizer to the conduction band of the TiO_2. The results show that LUMO of the dyes is greater than the conduction band of TiO_2 indicating that a full charge transfer from dyes to the conduction band of TiO_2 is thermodynamically allowed. The calculated results also indicate that D3 is the most plausible sensitizer due to the most negative ΔG_{inject} (0.91 eV) and a larger LHE value (0.95), which results in a higher IPCE.

Keywords: Density functional theory, benzene/thiophene, photosensitizers, free energy.

7.1.Introduction

The widespread commercialization of the photo voltaic (PV) cells is still limited mainly because of their high prices as compared to the amount of energy produced from them. Recent scientific research conducted for power conversion-efficiency reaches up to 24.2% [1], but is still non-competitive to the conventional electricity production sources. This relatively high cost is mainly due to the complex and expensive production process. Moreover, the need of highly purified silicon and use of toxic chemicals in their manufacturing, limits its use. These constraints encourage the scientists and researchers to divert their attention towards more efficient, economical and environment friendly solar cells. In this regard dye-sensitized solar cells (DSSCs) have received widespread attention in recent years because of their easy processing and low cost [2–5].

The major component of the DSSCs is a sensitizer. Its function is to adsorb an incoming sunlight and produce excitons. It is chemically bonded to the porous surface of the semiconductor. An efficient photosensitizer should: (i) possess intense absorption in the visible region (400 nm to 700 nm); (ii) adsorb strongly on the surface of the semiconductor; (iii) possess a high extinction coefficient; (iv) stable in its oxidized form, thus allows its reduction by an electrolyte; (v) stable enough to carry out ~108 turnovers, which typically correspond to 20 years of cell operation [6]. Photosensitizers are categorized into the metal complex and metal-free organic sensitizers. But metal free organic photosensitizers are preferred over ruthenium based sensitizers because of their low cost and good transport properties. The basic structural unit of metal-free dyes are donor-pi-spacer-acceptor (D-π-A). The photovoltaic properties of such dyes can be finely tuned by selecting suitable groups within the D-π-A structure [7] . This D-π-A dipolar

configuration creates an effective intramolecular charge transfer from donor to acceptor during electonexcitation. Instead of this charge transfer from donor to acceptor, the performance of DSSCs significantly depends on the conjugated bridging system [8]. Organic dyes based on thiophene, oligothiophene moiety [9], 3,4-ethylenedioxythiophene (EDOT) [10], thieno (3,2-b) thiophene (TT) [11] and dithieno (3,2-b:2`,3`-d) thiophene (DTT) [12] have been reported as efficient pi-bridging moities, exhibits high values of the solar conversion efficiency. Thiophene, has been appeared as an attractive pi-bridging segment for the development of PV materials due to its rigid conjugation structure and facile introduction of alkyl chains. Thiophene based photosensitizers are expected to improve the overall efficiency of DSSCs [13,14].

In this research work, DFT is used to calculate the structural and optical properties of three dyes. Eventually, we compared the theoretical results with the experimental data available [14]. Kohn–Sham DFT/TD-DFT is an effective tool to investigate the ground and excited state properties of photosensitizer complexes compared to other high level quantum approaches, since the computed orbitals are appropriate for typical molecular orbital-theoretical studies and elucidations. Many theoreticians have successfully applied this approach [15–20].

7.2.Theoretical Background

7.2.1. The Kohn–Sham molecular orbital (MO) model

The fundamental assumption in Kohn–Sham density functional theory (KS-DFT) is that we can use a single electron calculation to “n” interacting electrons. It can be done by applying appropriate local potential V_{XC} (r), external potentials Vext(r) and the Coulomb potential of the electron cloud V_C(r), then using Eq. (1)

$$\left(-\frac{1}{2}\nabla^2 + V_{ext}(r) + V_C(r) + V_{XC}(r)\right)\varphi_i(r) = \varepsilon_i\phi_i(r) \qquad (1)$$

The potential V_{XC} is the functional derivative with respect to the density (ρ) of the exchange–and–correlation energy functional E_{XC} [ρ]. The one-electron molecular orbitals (MOs) ϕ_i with corresponding orbital energies ε_i define the exact electronic charge density and give access to all properties. The (first) derivatives of the energy with respect to nuclear displacements at the end of the self consistent field (SCF) method are used to find stationary points in the energy surface, particularly for the geometry optimization of molecules [21].

According to Runge-Gross theorem [22] , the external potential individually finds out the density for a given interaction potential. While according to Kohn-Sham assumption the density of the non-interacting system is equal to the density of an interacting system. The benefit of this assumption is that, the wave function of a non-interacting system can be represented as a Slater determinant of single-particle orbitals, each of which are determined by a single partial differential equation in three variable. Then, the time-dependent (TD) Kohn–Sham equations are:

$$i\frac{\partial}{\partial t}\varphi_i(r,t) = \left(-\frac{\nabla^2}{2} + V[\rho](r,t)\right)\varphi_i(r,t) \qquad (2)$$

$$\rho(r,t) = \Sigma n_j|\varphi_i(r,t)|^2 \qquad (3)$$

The potential (V) includes the $V_C(r)$, the nuclear potential ,Vext(r) and (X_C), all are functions of time KS-TDDFT technique with solvent effect is used to calculate the excitation energies (E_{ex}) in DFT.

7.2.2. Computational Detail

In this work, all the DFT/TD-DFT calculations were executed using Amsterdam Density Functional (ADF) program (2013.01). The ground state geometries of dyes and dye/$(TiO_2)_8$ were optimized by applying a hybrid B3LYP level together with triple-ζ polarization basis function. $(TiO_2)_8$ nanoparticles anatase cluster was also simulated by considering a generalized gradient approximation (GAD) at BYLP level and triple-ζ polarization basis function. UV-Vis spectra of these dyes were simulated in chloromethane solvent. Here the conductor-like screening model (COSMO) was selected to consider the effect of solvent. While the E_{ex} were examined using the TD-DFT and statistical average of orbital potentials (SAOP) model including the salvation effects. Eighty singlet-singlet transitions were selected to define the whole absorption spectrum. In all the calculations, the relativistic effects were also considered by the zero order regular approximation (ZORA) Hamiltonian in its scalar approximation.

We employed GGA-BLYP, GGA-PW91, GGA-PB-86-D and hybrid-B1LYP with triple-ζ (zeta) polarization basis function to optimize the dye structures. But the calculated results with hybrid-B1LYP (along with triple-ζ) are good agreement with the experimental data [14].

7.2.3. Parameter estimation equations

The performance of DSSCs is evaluated by an incident photon to conversion efficiency (IPCE). It is associated with charge collection efficiency (η_c), electron injection efficiency (ϕ_{injc}) and light harvesting efficiency (LHE) as [15],

$$IPCE = LHE \times \phi_{injc} \times \eta_c \qquad (5)$$

LHE can be calculated in the following way [23]

$$LHE = 1 - 10^{f} \qquad (6)$$

Where "f" is the absorption of dye associated with maximum absorption also called oscillator strength and ϕ_{injc} is related to the free energy of electron injection as [15]

$$\phi_{inj} \alpha f(-\Delta G_{inject}) \qquad (7)$$

Eq-3 shows that the more negative ΔG_{inject} the greater will be electron injection efficiency. While ΔG_{inject} is the difference between the excited state oxidation potential e (E_{ox}^{dye*}) and the ground state reduction potential of the semiconductor conduction band (E_{CB}) [19],

$$\Delta G_{inject} = E_{ox}^{dye*} - E_{CB} \qquad (8)$$

TiO_2 cluster was also simulated and its E_{CB} was found to be -4.01 eV. Similarly, Eox^{dye*} can be calculated by using the following equation [19],

$$E_{ox}^{dye*} = E_{ox}^{dye} - \Delta E \qquad (9)$$

Where E_{ox}^{dye} (-HOMO) [17] is the dye's ground state oxidation potential and ΔE is the lowest absorption energy associated with λ_{max}.

7.3.Results and discussion

7.3.1. Designed systems

The structures and names of a new class of dyes are shown in Fig 7-1. In these structures, a 3,6-diiodocarbazole unit was used as the electron-donating moiety and carboxyl and cyano functional groups were inserted as the acceptor moiety and the anchor group owing to heir good electron-extracting capability and strong adhesion to metal oxide . benzene/thiophene or oligothiophene moiety was used as the π-conjugation spacers, which bridges the donor-acceptor systems. Benzene/thiophene as pi-bridge reduces the tendency to aggregate, but resistance to charge transfer between donor and acceptor increases. However, the insertion of thiophene moiety as a pi-bridge causes the red shift in absorption spectra. A double bond was also introduced to the pi-conjugation system to fine tune the planar molecular configuration and to broaden the absorption spectra.

7.3.2. Energy Levels

The HOMOs, LUMOs, and the band gap energies of the photosensitizers play an important role in providing the thermodynamic driving force for the electron injection. For efficient charge transfer, the LUMOs of dyes must be more negative than the conduction band of the semiconductor while HOMO levels must be more positive than the redox potential of electrolyte. The electron distribution of the HOMOs and LUMOs of D1, D2 and D3 are shown in Fig 7-2. Clearly, the HOMOs of these compounds are the highest electron density located at the nitrogen atoms of the carbazole. The LUMOs are located in the anchoring group through the pi-bridge.Thus, the HOMO-LUMO excitation induced by light irradiation could move the electron distribution from the carbazole segment to the anchoring unit through the pi-bridge segment. Table 7-1 shows that the

D1

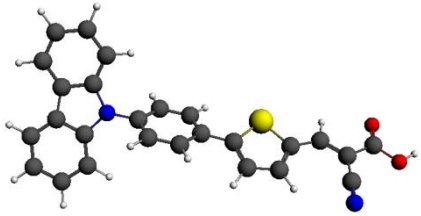

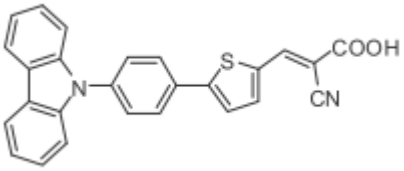

D2

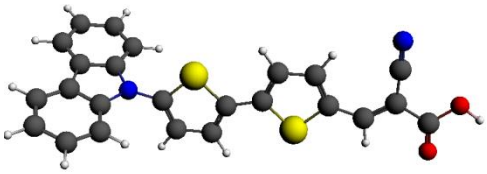

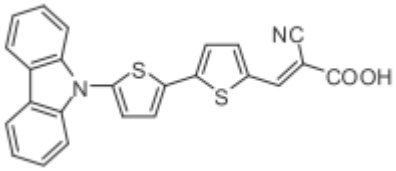

D3

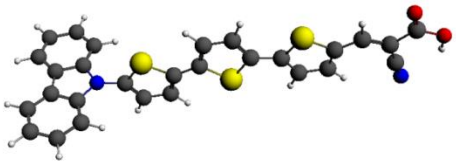

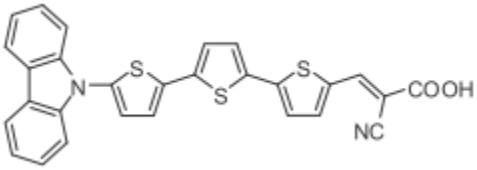

Fig 7-1:Chemical structures of organic dyes

HOMO levels of the dyes are in the order of D3 (-5.72) >D1 (-5.74) 1>D3(-5.81). While, LUMO energy levels are in the order of D1 (-2.97) > D2 (-3.07) > D3 (-3.18). The insertion of thiophene unit as the π-conjugation unit significantly affects the HOMO and LUMO energy levels of the dyes. Similarly, the H-L_{gap} of the dyes are in the order of D3 (2.54) < D2 (2.74) <D1 (2.77). These results suggest that dyes 1-3 can inject electrons to the conduction band of titanium oxide.

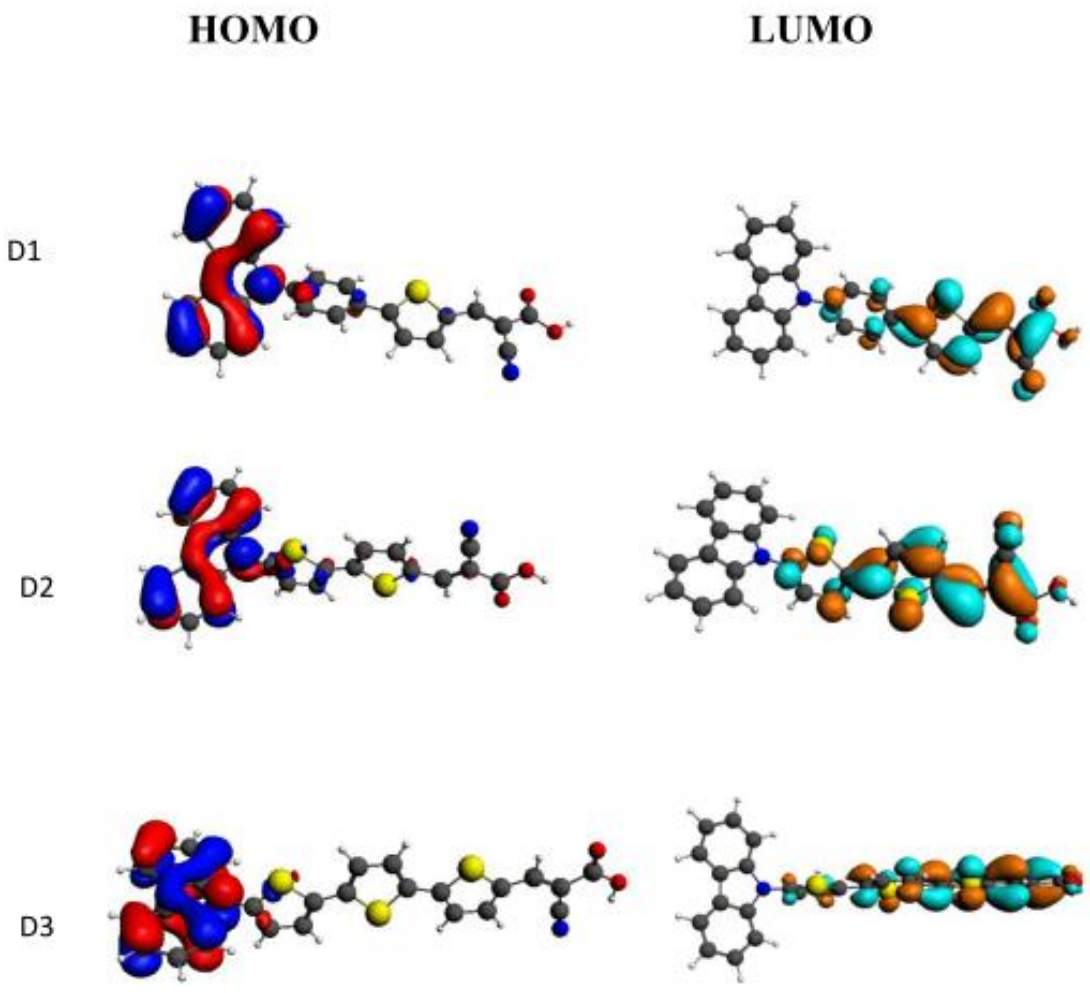

Fig 7-2 :Simulated HOMOs and LUMOs of dyes

Table 7-1: Simulated HOMOs (eV), LUMOs (eV) and H-L $_{gap}$ (eV) energies of dyes

Dyes	HOMO	LUMO	H-L$_{gap}$
D1	-5.74	-2.97	2.77
D2	-5.81	-3.07	2.74
D3	-5.72	-3.18	2.54

7.3.3. UV-Vis absorption spectra of dyes

An efficient photosensitizer should show a strong absorption in the visible region (400 nm to 700 nm). TDDFT calculations have been performed on D1, D2 and D3 to find out the optical properties. These calculated results of dyes (D, D2 and D3) are in good agreement with the experimental data [14], which shows that SAOP function with the COSMO model is accurate in finding the absorption spectra of dyes. The simulated spectra of systems 1-3 are shown in Fig 7-3. All the absorption spectra of dyes can be clearly divided into two sections, with the first peak occurring in the 300-400 nm region and second in the 400-700 nm region. The band in the UV- region is probably emerging from the transitions of electrons localized within the carbazole unit. The absorption occurring in the visible region is due to transfer of electrons from donor to acceptor, which is sensitive to the nature of the conjugation pathway and red-shifts onprogressive addition of thiophene units. The dye D2 with terthiophene as pi-bridge exhibits a significant red-shift as compared to D1 and D3. Also, the shorter peak position of the charge transfer transition for D1 (340 nm) is observed when compared with D2 (375 nm)

Table 7-2 :Optical, redox and energy level of photosensitizers

Dye	[a]λ_{max}	[b]λmax (Sim)	ΔE (eV)	E_{ox}^{dye} (eV)	E_{ox}^{dye*} (eV)	[c] f
D1	416	470	2.64	5.74	3.1	1.124
D2	440	477	2.60	5.81	3.2	0.73
D3	467	472	2.63	5.72	3.09	1.20

a: Experimenta Values [14]
b: Simulated Values
c: Oscillator strength

Table 7-3: Free energy of electron injection ΔG^{inject} (eV) and Light harvesting efficiency LHE

System	ΔG^{inject} (eV)	* LHE	Major Transitions
D1	-0.90	0.93	H-2$\longrightarrow$L (96%)
D2	-0.80	0.81	H-4 $\longrightarrow$ L (83%)
D3	-0.91	0.95	H $\longrightarrow$ L (98%)

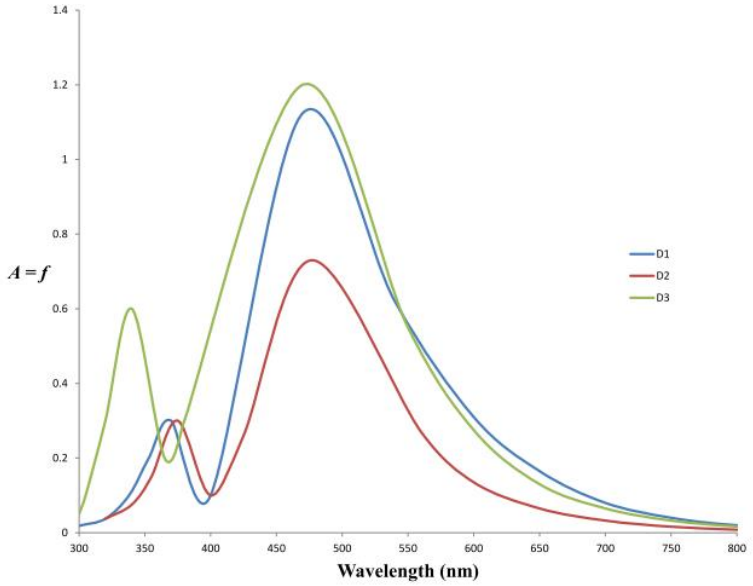

Fig 7-3: Simulated absorption spectra of systems 1-3

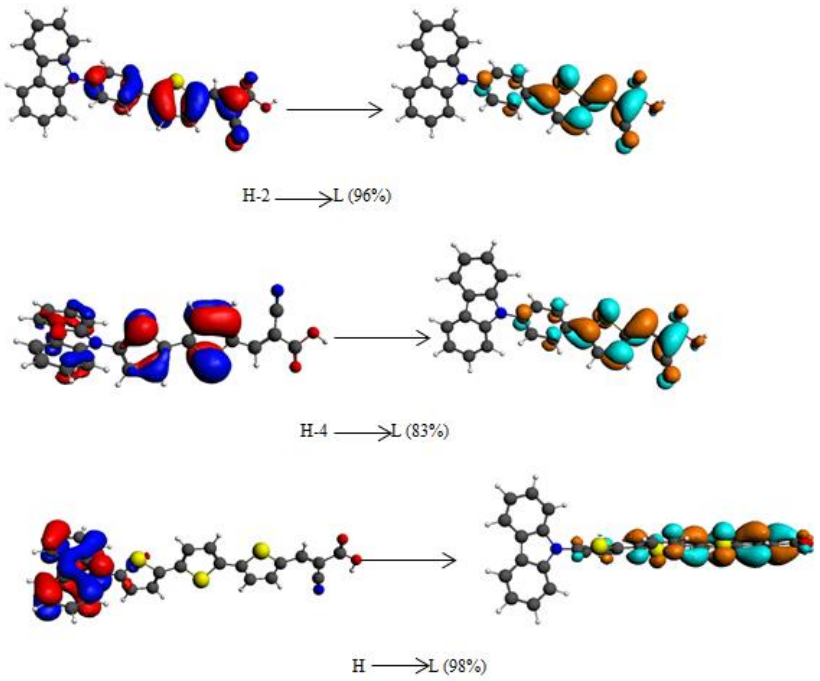

Fig 7-4: Major Transitions of system 1-3

and D3 (380), probably due to the deficiency of electrons in benzene relative to the thiophene unit.

Ground and excited state potential (Eox^{dye}), the maximum absorption (λmax), oscillation strength (*f*), and the main transitions are presented in the Table 7-2. The main molecular orbitals (MOs) involved in the dominant electron transitions of systems 1-3 are shown in Fig 7-4. The major transitions may be attributed to the transfer of charge from the carbazole group to -COOH and -CN through the benzene/thiophene unit.

7.3.4. Free energy of electron injection and light harvesting efficiency

LHE and ΔG_{inject} can be calculated using equation 6 and Equation 8, respectively, and the results are shown in the Table 7-3. All the calculated ΔG_{inject} values are negative, which indicates that the conduction band edge of TiO_2 lies, below the excited state of dyes, thus favoring electron injection. The ΔG_{inject} of the systems 1-3 increases in the order of D3 (-0.91) < D1 (-0.90) < D2 (-0.80) . Therefore, the order of the driving force of systems is D3 > D1 > D2. There is only a slight difference of the LHE for systems 1-3 indicating that all the photosensitizers will give comparable photocurrents. These results indicate that system-3 is the most plausible due to the most negative ΔG_{inject} (0.91 eV) and a larger LHE value (0.95), which results in a higher IPCE.

Table 7-4: ΔE (eV), λ_{max} (nm) , (*f*) major transitions dyes anchored to TiO_2

Dyes	λ_{max}	ΔE	*f*	Major Transitions
D1/TiO_2	493	2.520	0.75	H-3 ⟶ L+2 (92.8)
D2/TiO_2	510	2.434	0.80	H ⟶ L+1 (95%)
D3/TiO_2	497	2.490	0.86	L ⟶ H (96.2)

7.3.5. UV-Vis absorption spectra of dyes on the TiO_2 surface

The interface between the sensitizer and TiO_2 plays an important role in the electron injection efficiency. Though $(TiO_2)_n$ clusters (n = 4, 6, 8) were simulated, $(TiO_2)_8$ containing model was selected because of its balanced electronic properties (conduction band ~ -4.0 eV and band gap 3.18 eV). The models of dyes linked to $(TiO_2)_8$ are shown in Fig 7-5, while the simulated UV-Vis spectra of dyes/$(TiO_2)_8$ are shown in Fig 7-6. The spectra show a dramatic red-shift when compared to those in solution, with the red shift values of D1/$(TiO_2)_8$, D2/$(TiO_2)_8$ and D3/$(TiO_2)_8$ are 23, 33 and 25 nm, respectively. This may be due to the increased delocalization of the π^* orbital over the conjugated framework due to the interaction between the carboxylate group and Ti^{+4} ions, which decreases the energy of the π^* level. The band in the UV- region is probably emerging from the transitions of electrons. The major transitions in D1/TiO_2, D1/TiO_2 and D1/TiO_2 are shown in Fig 7-7. It can also be observed that dye D2/TiO_2 shows a higher red shift value when compared to other systems. The calculated excitation energies, oscillation strength and λ_{max}(nm) are shown in Table 7-4.

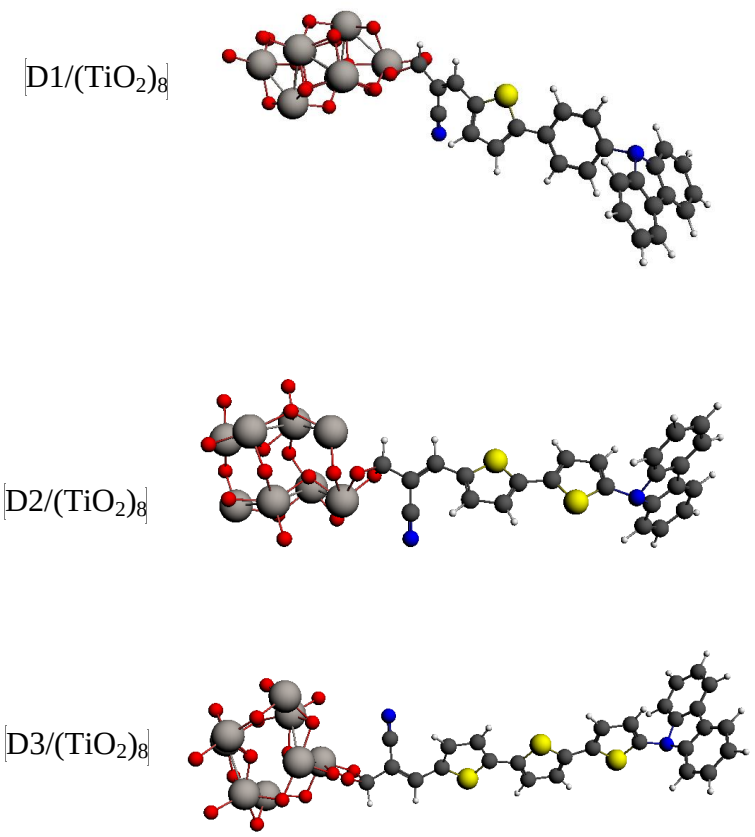

Fig 7-5. The model the of system 1-3 with $(TiO_2)_8$

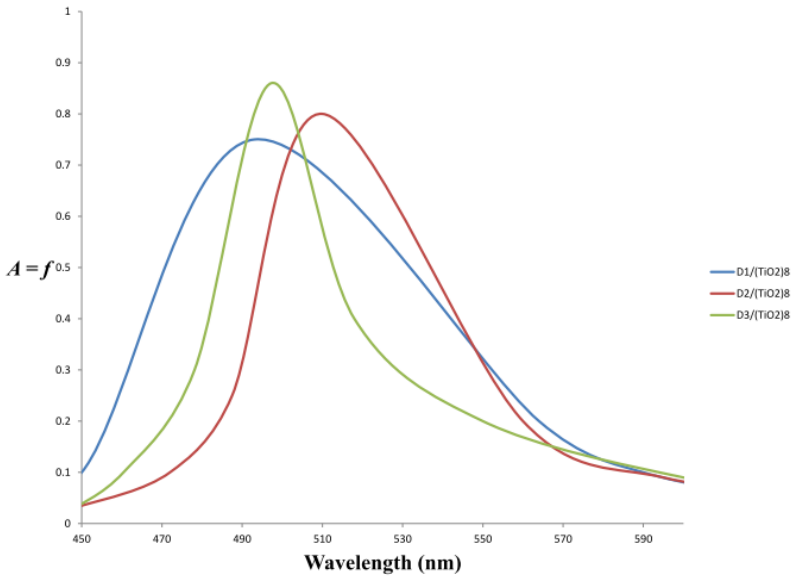

Fig 7-6 :The simulated absorption spectra of $(TiO_2)_8$/dyes 1-3

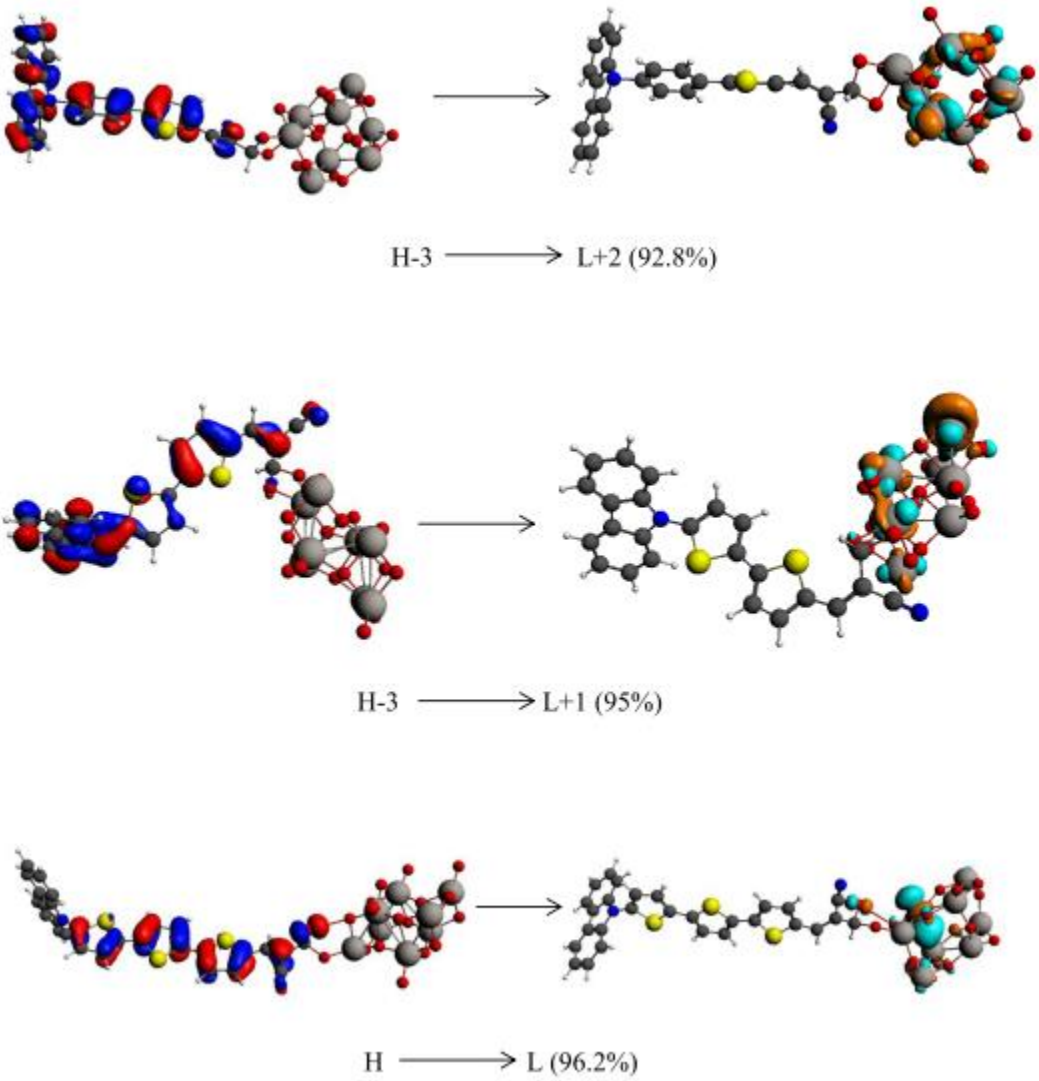

Fig 7-4: Major Transitions of D1/TiO_2, D2/TiO_2 and D3/TiO_2

7.4.Conclusion

DFT/TD-DFT modeling techniques has been used to conduct the computational study of the geometry and electronic structure of benzene/thiophene based photosensitizers. The calculated results of dyes (D, D2 and D3) are comparable with the experimental data, which shows that hybrid-B1LYP with triple-ζ (zeta) and SAOP are the right choices in calculating the electronic structure properties and optical properties of dyes respectively. The results also show that LUMO of the dyes is greater than the conduction band of TiO_2 indicating that a full charge transfer from these dyes to the conduction band of TiO_2 is thermodynamically allowed. It was also found that the absorption spectra of dyes/TiO_2 are red shifted owing to the increased delocalization of the π^* orbital of the conjugated framework.Moreover, the calculated results indicate that D3 is the most plausible due to the most negative ΔG_{inject} (0.91 eV) and a larger LHE value (0.95), which results in a higher IPCE. Therefore, it can be concluded from the above study that DFT/TD-DFT is an effective tool to design and computing the optical properties of photosensitizers for solar cell applications

7.5.Acknowledgment

The authors would like to acknowledge the support provided by King Abdulaziz City for Science and Technology (KACST) through the Science & Technology Unit at King Fahd University of Petroleum & Minerals (KFUPM) for funding this work through the project # 11-ENE1635-04 as part of National Science, Technology and Innovation Plan. KFUPM is also acknowledged for supporting this research. The authors would like to acknowledge the Center of Research Excellence for Renewable Energy at KFUPM for its support.

7.6.References

[1] M.A. Green, K. Emery, Y. Hishikawa, W. Warta, Solar cell efficiency tables (version 35), Prog. Photovoltaics Res. Appl. 18 (2010) 144–150. doi:10.1002/pip.974.

[2] E.-S. Ha, B. Yoo, H. Baik, Y. Lee, K.-J. Kim, Photocurrent enhancement of dye-sensitized solar cells owing to increased dye-adsorption onto silicon-nanoparticle-coated titanium-dioxide films., Chem. Asian J. 7 (2012) 1624–9. doi:10.1002/asia.201101055.

[3] X. Lu, G. Zhou, H. Wang, Q. Feng, Z.-S. Wang, Near infrared thieno[3,4-b]pyrazine sensitizers for efficient quasi-solid-state dye-sensitized solar cells., Phys. Chem. Chem. Phys. 14 (2012) 4802–9. doi:10.1039/c2cp40441a.

[4] S. Agrawal, N.J. English, K.R. Thampi, J.M.D. MacElroy, Perspectives on ab initio molecular simulation of excited-state properties of organic dye molecules in dye-sensitised solar cells., Phys. Chem. Chem. Phys. 14 (2012) 12044–56. doi:10.1039/c2cp42031g.

[5] B.O. Reagen, M. Gratzel, A Low-Cost , High-Efficiency Solar Cell Based on Dye-Sensitized Colloidal Ti02 Films, Lett. to Nat. 350 (1991) 737–739.

[6] Recent Advances in Dye Sensitized Solar Cells, (n.d.). file:///C:/Users/umer mehmood/Downloads/974782 (1).pdf (accessed January 09, 2015).

[7] S. Anderson, P.N. Taylor, G.L.B. Verschoor, Benzofuran trimers for organic electroluminescence., Chemistry. 10 (2004) 518–27. doi:10.1002/chem.200305284.

[8] D. Zhou, N. Cai, H. Long, M. Zhang, Y. Wang, P. Wang, An Energetic and Kinetic View on Cyclopentadithiophene Dye-Sensitized Solar Cells: The Influence of Fluorine vs Ethyl Substituent, J. Phys. Chem. C. 115 (2011) 3163–3171. doi:10.1021/jp110384n.

[9] Z.-S. Wang, N. Koumura, Y. Cui, M. Takahashi, H. Sekiguchi, A. Mori, et al., Hexylthiophene-Functionalized Carbazole Dyes for Efficient Molecular Photovoltaics: Tuning of Solar-Cell Performance by Structural Modification, Chem. Mater. 20 (2008) 3993–4003. doi:10.1021/cm8003276.

[10] W. Zeng, Y. Cao, Y. Bai, Y. Wang, Y. Shi, M. Zhang, et al., Efficient Dye-Sensitized Solar Cells with an Organic Photosensitizer Featuring Orderly Conjugated Ethylenedioxythiophene and Dithienosilole Blocks, Chem. Mater. 22 (2010) 1915–1925. doi:10.1021/cm9036988.

[11] G. Zhang, H. Bala, Y. Cheng, D. Shi, X. Lv, Q. Yu, et al., High efficiency and stable dye-sensitized solar cells with an organic chromophore featuring a binary pi-conjugated spacer., Chem. Commun. (Camb). (2009) 2198–200. doi:10.1039/b822325d.

[12] H. Qin, S. Wenger, M. Xu, F. Gao, X. Jing, P. Wang, et al., An organic sensitizer with a fused dithienothiophene unit for efficient and stable dye-sensitized solar cells., J. Am. Chem. Soc. 130 (2008) 9202–3. doi:10.1021/ja8024438.

[13] S. Qu, B. Wang, F. Guo, J. Li, W. Wu, C. Kong, et al., New diketo-pyrrolo-pyrrole (DPP) sensitizer containing a furan moiety for efficient and stable dye-sensitized solar cells, Dye. Pigment. 92 (2012) 1384–1393. doi:10.1016/j.dyepig.2011.09.009.

[14] L.-L. Tan, L.-J. Xie, Y. Shen, J.-M. Liu, L.-M. Xiao, D.-B. Kuang, et al., Novel organic dyes incorporating a carbazole or dendritic 3,6-diiodocarbazole unit for efficient dye-sensitized solar cells, Dye. Pigment. 100 (2014) 269–277. doi:10.1016/j.dyepig.2013.09.025.

[15] J. Wang, H. Li, N.-N. Ma, L.-K. Yan, Z.-M. Su, Theoretical studies on organoimido-substituted hexamolybdates dyes for dye-sensitized solar cells (DSSC), Dye. Pigment. 99 (2013) 440–446. doi:10.1016/j.dyepig.2013.05.027.

[16] W. Fan, D. Tan, W.-Q. Deng, Acene-modified triphenylamine dyes for dye-sensitized solar cells: a computational study., Chemphyschem. 13 (2012) 2051–60. doi:10.1002/cphc.201200064.

[17] W. Sang-aroon, S. Saekow, V. Amornkitbamrung, Density functional theory study on the electronic structure of Monascus dyes as photosensitizer for dye-sensitized solar cells, J. Photochem. Photobiol. A Chem. 236 (2012) 35–40. doi:10.1016/j.jphotochem.2012.03.014.

[18] X. Zarate, E. Schott, T. Gomez, R. Arratia-Pérez, Theoretical study of sensitizer candidates for dye-sensitized solar cells: peripheral substituted dizinc pyrazinoporphyrazine-phthalocyanine complexes., J. Phys. Chem. A. 117 (2013) 430–8. doi:10.1021/jp3067316.

[19] J. Zhang, Y.-H. Kan, H.-B. Li, Y. Geng, Y. Wu, Z.-M. Su, How to design proper ?-spacer order of the D-?-A dyes for DSSCs? A density functional response, Dye. Pigment. 95 (2012) 313–321. doi:10.1016/j.dyepig.2012.05.020.

[20] D. Rocca, R. Gebauer, F. De Angelis, M.K. Nazeeruddin, S. Baroni, Time-dependent density functional theory study of squaraine dye-sensitized solar cells, Chem. Phys. Lett. 475 (2009) 49–53. doi:10.1016/j.cplett.2009.05.019.

[21] G. te Velde, F.M. Bickelhaupt, E.J. Baerends, C. Fonseca Guerra, S.J.A. van Gisbergen, J.G. Snijders, et al., Chemistry with ADF, J. Comput. Chem. 22 (2001) 931–967. doi:10.1002/jcc.1056.

[22] E. Runge, E.K.U. Gross, Density-Functional Theory for Time-Dependent Systems, Phys. Rev. Lett. 52 (1984) 997–1000. doi:10.1103/PhysRevLett.52.997.

[23] W. Fan, W. Deng, Incorporation of Thiadiazole Derivatives as π spacer to Construct Efficient Metal-free Organic Dye Sensitizers for Dye-sensitized Solar Cells: A Theoretical Study, Commun. Comput. Chem. 1 (2013) 152–170. doi:10.4208/cicc.2013.v1.n2.6.

CHAPTER 8

DENSITY FUNCTIONAL THEORY (DFT) STUDY ON DYE-SENSITIZED SOLAR CELLS USING NOVEL OXADIAZOLE BASED DYES

Umer Mehmood[1], Ibnelwaleed A. Hussein[1*], Khalil Harrabi [2], Belum V.S. Reddy[3]

[1]Department of Chemical Engineering, King Fahd University of Petroleum & Minerals (KFUPM), P. O. Box 5050, Dhahran 31261, Kingdom of Saudi Arabia

[2] Department of physics, KFUPM, P. O. Box 5050, Dhahran 31261, Kingdom of Saudi Arabia

[3] Indian Institute of Chemical Technology, Hyderabad, India

[*]Corresponding Author. Tel: +966532432097, E-mail address: ihussein@kfupm.edu.sa

This chapter has been published in "Photonics for Energy" on 27 Jan 2015

Abstract

Density functional theory and time dependent density functional theory DFT/TD-DFT modeling techniques are used to conduct a computational study of the geometry and electronic structure of novel oxadiazole based organic sensitizers. A DFT study on the thermodynamic aspects of the charge transport processes associated with dye-sensitized solar cells (DSSCs) suggests that the system with 1,2,4-oxadiazole has a balance among the different crucial factors and may result in the highest incident photon to charge carrier efficiency. The dye/$(TiO_2)_8$ anatase clusters were also simulated to illustrate the electron injection efficiency at the interface. This study provides basic understanding of the impact of molecular design on the performance of oxadiazole dyes in DSSCs.

Keywords: Density functional theory, oxadiazole, light harvesting efficiency, free energy

8.1.Introduction

The world energy demand is continuously increasing and the world power consumption, which is 13 terawatts (TW) currently, is expected to reach about 23 TW by 2050 [1]. Fossil fuels, which are depleting rapidly, meet 80% of the energy requirement of the whole world [2]. Moreover, the burning of fossil fuels raises the amount of carbon dioxide in the atmosphere. Owing to the growing energy demand, exhaustion of oil resources, and global warming issues, there is a need for clean and renewable energy technologies. Among all the renewable energy forms, solar energy has showed its advantages and potential for power generation.[3]The solar radiation from the sun is approximately 3×10^{24} J per year, which is ten times the current energy demand [4]. Therefore, owing to the availability of huge reserves, the conversion of photo energy into electrical energy is generally considered potentially the best way to resolve the world energy crisis.

Inorganic silicon based solar cells are being currently used for the conversion of photo energy on a commercial scale because of their high efficiency [5]. However, the need of highly purified silicon, use of toxic chemicals in their manufacture, and the high cost has restricted their worldwide use. These constraints encouraged the search for low cost and environmentally friendly solar cells. In this context, dye-sensitized solar cells (DSSCs) have received widespread attention in recent years because of their ease of processing and the low cost [6–11]

One of the most important components of the DSSCs is the dye, which absorbs incoming sunlight and produce excitons. The photosensitizer, which is chemically bonded to the porous surface of the semiconductor, can be a metal complex or a metal-free organic

sensitizer. But metal free organic photosensitizers are preferred over ruthenium based sensitizers because of their low cost and good transport properties. The basic structural unit of metal-free dyes is the donor-pi-spacer-acceptor (D-π-A) unit and the photovoltaic properties of such dyes can be fine tuned by selecting suitable groups within the D-π -A structure [12].

Many organic groups have been used to tune the electrical and optical properties of light sensitive materials. The best known organic compounds for obtaining such properties are porphyrins [13], styrylarylenes [14], perylenes [15], benzofurans [16], indoles [17], thiazole [18,19] and oxadiazole [20]. Among them, the oxadiazole derivatives are considered the most efficient electron transport materials owing to their good thermal and chemical stabilities and high quantum yield [21]. Many studies have shown that 2-(4-biphenylyl)-5-(4-tertbutylphenyl)-(1, 3, 4) oxadiazole exhibits excellent charge transport properties [20,22–25]. Tian and co-workers successfully synthesized the naphthalimide derivatives containing the oxadiazole moiety. They found that oxadiazole moiety increases the electron injection properties and minimizes the carrier recombination [22].

The density functional theory (DFT) and time-dependent DFT (TD-DFT) can provide a deeper understanding of the relationship between molecular structure and properties of compounds. Thus, theoretical calculations are important to design new and efficient dyes for DSSCs [26–33].

Here, the aim is to study the photophysical properties of oxadiazole based organic dyes and establish their structure-performance relationship for application in DSSCs. A series of D-π-A oxadiazole based organic dyes that possess different electron-rich fragments or electron-excessive π -bridges were designed. Their electronic properties, absorption

spectra and performances in DSSCs were theoretically studied. This work is expected to provide guidance for experimental synthesis.

8.2.Computational Detail

All the DFT/TD-DFT calculations were executed using Amsterdam Density Functional (ADF) program (2013.01).

8.2.1. TiO2 cluster Model

BAND mode was used to simulate the anatase TiO_2 cluster. Here, we selected tetragonal anatase crystal structure with single layer (001) surface slab. Then, a 4×1 supercell was created from this slab. All atoms were maped within the unit cell.

8.2.2. Simulation Method

The ground state geometries of oxadiazole dyes, dye/$(TiO_2)_8$ and standard dyes were optimized by applying hybrid Becke,3-parameter, Lee-Yang-Parr (B3LYP) level together with triple-ζ polarization basis function. The $(TiO_2)_8$ nano-particle cluster was also simulated by considering generalized gradient approximation (GGA) at Becke, parameter,Lee-Yang-Parr (BYLP) level with triple-ζ polarization basis function. UV-Vis spectra of oxadiazole dyes were simulated in ethanol solvent, where the conductor-like screening model (COSMO) was used to take the solvent effects into account[28]. The excitation energies and oscillator strengths for the 80 singlet–singlet transitions at the optimized geometry in the ground state were obtained by TD-DFT calculations using the same basis set as for the ground state and statistical average of orbital potentials (SAOP) model including the solvation effects. In all the calculations, the relativistic effects were taken into account by the zero order regular approximation (ZORA) Hamiltonian in its scalar approximation.

8.3.Theoretical background

The performance of DSSCs is evaluated by incident photon to conversion efficiency (IPCE). It is associated with charge collection efficiency (η_c), electron injection efficiency (ϕ_{injc}) and light harvesting efficiency (LHE), as [27],

$$IPCE = LHE \times \phi_{injc} \times \eta_c \quad (1)$$

LHE can be calculated as follows [28],

$$LHE = 1 - 10^{-f} \quad (2)$$

where "f" is the absorption of dye associated with the maximum absorption, also called the oscillator strength and ϕ_{injc} is related to the free energy of electron injection by [27],

$$\phi_{injc} \alpha f(-\Delta G^{inject}) \quad (3)$$

Eq-3 shows that more negative the ΔG^{inject}, the greater the electron injection efficiency. While ΔG^{inject} is the difference between oxidation potential energy of the excited state (Eox^{dye*}) and the reduction potential energy of TiO_2 conduction band (ECB), which can be described as [32]

$$\Delta G^{inject} = Eox^{dye*} - E_{CB} \quad (4)$$

TiO_2 cluster was also simulated and its ECB was found to be -4.01 eV. Similarly, Eox^{dye*} can be calculated using the following equation [29] ,

$$Eox^{dye*} = Eox^{dye} - \Delta E \quad (5)$$

where Eox^{dye} (-HOMO) [30] is the ground state oxidation potential of the dye and ΔE is the lowest absorption energy associated with λ_{max}.

8.4.Results and discussion

8.4.1. Designed system

The structures and names of new class of dyes are shown in Fig 8-1. In these structures, a naphthalene unit was used as the electron-donating moiety and carboxyl and cyano groups (-COOH and -CN) were introduced as the electron acceptor and the anchor group because of their high electron-withdrawing ability and strong bonding to the semiconductor. Oxadiazole isomers were used as the π-conjugation system, which bridges the donor-acceptor systems. A double bond and a thiophene unit were also introduced to the pi-conjugation system to fine tune the planar molecular configuration and to broaden the absorption spectra. The performance of the dyes was tested with different isomers of oxadizoles as the π-conjugated bridge.

8.4.2. Energy levels

The HOMOs, LUMOs, and the band gap energies of the photosensitizers play an important role in providing the thermodynamic driving force for the electron injection. For efficient charge transfer, the LUMOs of dyes must be more negative than the conduction band of the semiconductor while HOMO levels must be more positive than the redox potential of electrolyte. Table 7-1(b) shows the HOMOs, LUMOs, and HOMO-LUMO energy gaps of oxadiazole photosensitizers. The HOMO levels of the systems are in the order of system-4 (-5.827) < system-3 (-5.808) < system-1 (-5.657) < system-2 (-5.582). The LUMO energy levels are in the order of system-1 (-3.956) < system-4 (-3.802) < system-3 (-3.767) < system-2 (-3.625). The insertion of oxadiazole isomers as the π-conjugation unit significantly affects the HOMO and LUMO energy levels. Similarly, the H-L_{gap} of systems are in the order of system-1 (1.701) < system-2 (1.957) <

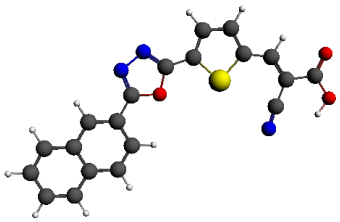

System-1

(E)-2-Cyano-3-(5-(5-(naphthalen-2-yl)- 1,3,4-oxadiazol-2-yl)-cyanoacrylic acid

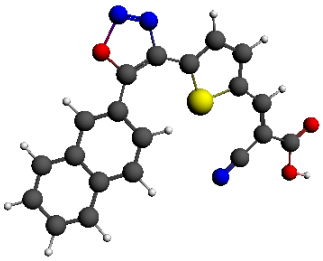

System-2

(E)-2-Cyano-3-(5-(5-(naphthalen-2-yl)- 1,2,3-oxadiazol-4-yl)-cyanoacrylic acid

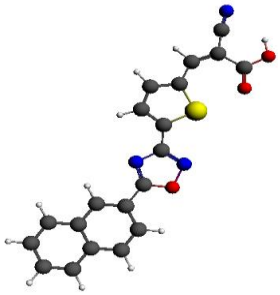

System-3

E)-2-Cyano-3-(5-(5-(naphthalen-2-yl)- 1,2,4-oxadiazol-3-yl)-cyanoacrylic acid

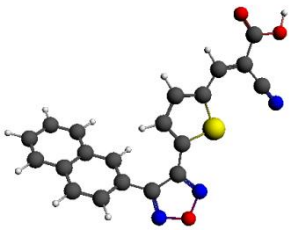

System-4

E)-2-Cyano-3-(5-(5-(naphthalen-2-yl)- 1,2,5-oxadiazol-3-yl)-cyanoacrylic acid

Fig 8-1: Chemical structures of organic dyes

system-4 (2.025) < system-3 (2.041). These results suggest that systems 1-4 should be capable of injecting electrons into the conduction bands of TiO_2.

Table 8-1b: The FMO (eV) and H-L $_{gap}$ (eV) energies of systems 1-4

Dyes	LUMO	HOMO	H-L_{GAP}
1	-3.956	-5.657	1.701
2	-3.625	-5.582	1.957
3	-3.767	-5.808	2.041
4	-3.802	-5.827	2.025

8.4.3. Absorption spectra of dyes

The simulated absorption spectra of systems 1-4 are shown in Fig 8-2. All the absorption spectra of dyes can be clearly divided into two regions, with the first major peak occurring in the 300-450 nm region and second in the 450-700 nm region. Ground and excited state potential (E_{ox}^{dye}), maximum absorption (λ_{max}), oscillation strength (f), and the main transitions are presented in Table 8-2. The main molecular orbitals (MOs) involved in the dominant electron transitions of systems 1-4 are shown in Fig 8-3. The major transitions may be attributed to the transfer of charge from the naphthalene group to -COOH and -CN through the thiophene unit and the π-conjugation system.

Table 8-2: Optical, redox and energy levels for oxadizol based photosensitizers

Dyes	E_{ox}^{dye}	E_{ox}^{dye*}	ΔE	λ_{max}	f	Main Transition
1	5.657	3.296	2.361	525	0.764	H-1 ⟶ L (82.4%)
2	5.583	3.133	2.450	507	0.722	H-1 ⟶ L (69%)
3	5.808	3.118	2.620	473	0.865	H-1 ⟶ L (57%)
4	5.827	3.258	2.569	483	0.780	H-1 ⟶ L (68%)

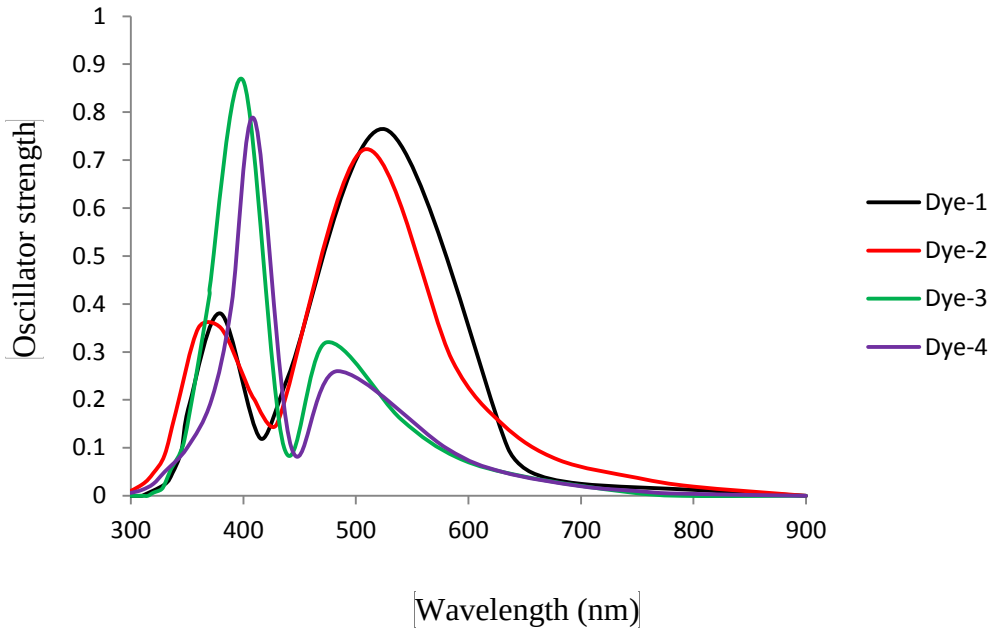

Fig 8-2: Simulated absorption spectra of systems 1-4

Table 8-3: Lowest absorption energy ΔE (eV), maximum absorption λ_{max} (nm) and oscillating strength (*f*)

System	λ_{max}	ΔE	*f*
1	542	2.290	0.52
2	520	2.387	0.48
3	492	2.523	0.58
4	495	2.507	0.50

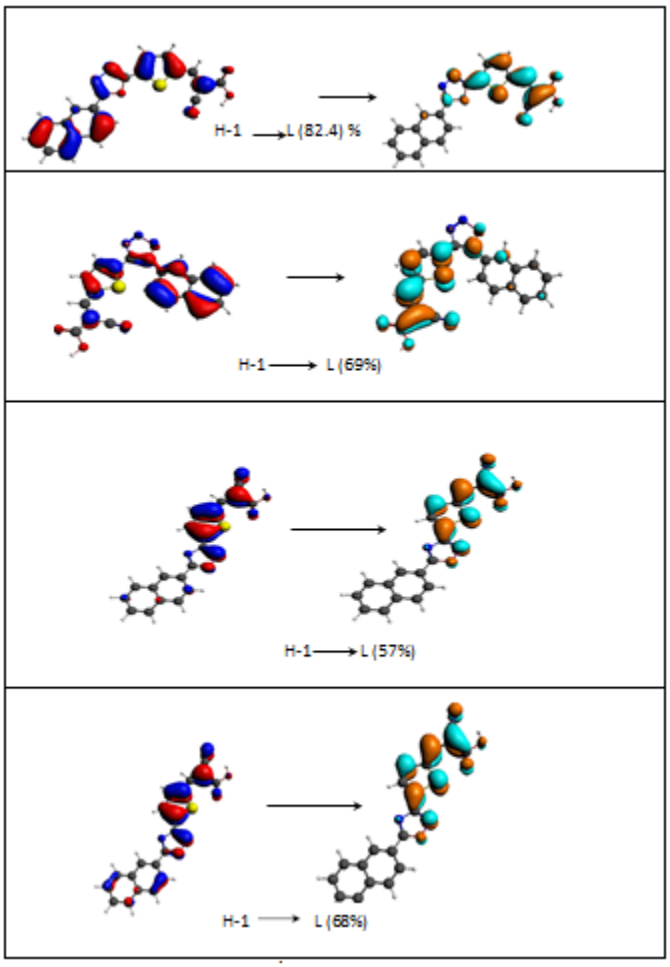

Fig 8-3. Major Transition of system 1-4

8.4.4. UV-Vis absorption spectra of dyes on the TiO_2 surface

The interface between the sensitizer and TiO_2 plays an important role in the electron injection efficiency. Though $(TiO_2)_n$ clusters (n = 4, 6, 8) were simulated, $(TiO_2)_8$ containing model was selected because of its balanced electronic properties (conduction band ~ -4.0 eV and band gap 3.18 eV). The models of dyes linked to $(TiO_2)_8$ are shown in Fig. 4, while the simulated UV-Vis spectra of dyes/$(TiO_2)_8$ are shown in Fig 8-5. The spectra show a red-shift when compared to those in solution, with the red shift values of system 1, system 2, system 3, and system 4 are 17, 13, 19, and 12 nm, respectively. This is due to the fact that the carboxylate group anchored to TiO_2 in which Ti^{4+} acts as a proton. The interaction between the carboxylate group and the Ti^{4+} ions may lead to the increased delocalization of the π^* orbital. The energy of the π^* level is decreased by this delocalization, which explains the red shift of the absorption spectra. It can also be observed that dye (3)/TiO_2 shows a higher red shift value when compared to other systems. The calculated excitation energies, oscillation strength, λ_{max}(nm) and the dominant transitions are shown in Table 8-3.

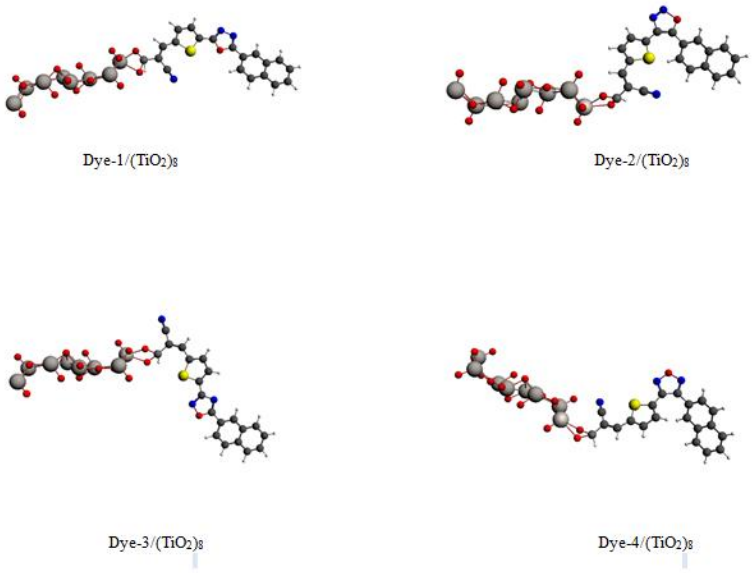

Fig 8-4: The models of system 1-4 with $(TiO_2)_8$

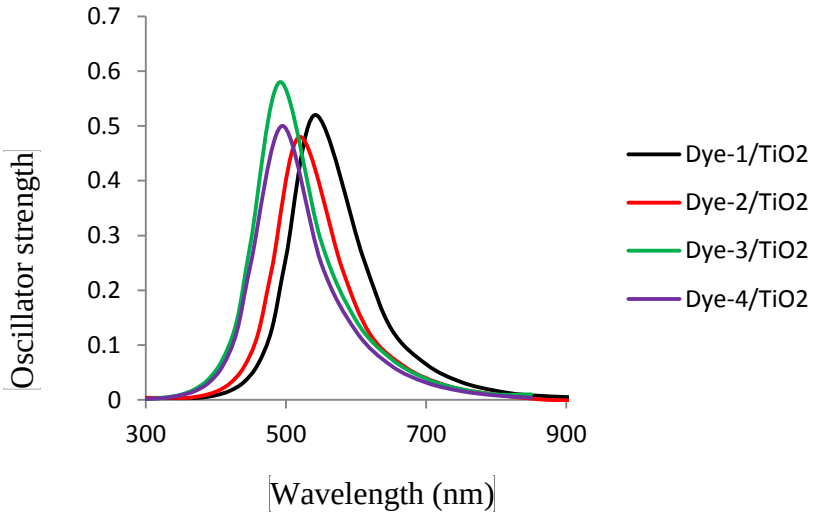

Fig 8-5:Simulated absorption spectra of $(TiO_2)_8$/systems 1-4

8.4.5. Free energy of electron injection and light harvesting efficiency

LHE and ΔG^{inject} can be calculated using Equation 2 and Equation 4, respectively, and the results are shown in Table 8-4. All the calculated ΔG^{inject} values are negative, which indicates that the conduction band edge of TiO_2 lies, blow the excited state of the dyes [28] , thus favoring electron injection . The ΔG^{inject} of the systems 1-4 increases in the order of system-3 (-0.882) < system-2 (-0.867) < system-4 (-0.742) < system-1 (-0.704) . Therefore, the order of the driving force of the systems is system-3 > system-2 > system-4 > system-1. There is only a slight difference of the LHE for systems 1-4, indicating that all the photosensitizers will give comparable photocurrents. These results indicate that system-3 is the most plausible due to the most negative ΔG^{inject} (0.882 eV) and a larger LHE value (0.86), which results in a higher IPCE.

Table 8-4: Free energy of electron injection ΔG^{inject} (eV) and light harvesting efficiency LHE

System	ΔG^{inject}	LHE
1	-0.704	82
2	-0.867	80
3	-0.882	86
4	-0.742	83

8.5.Conclusion

Four photosensitizers with oxadiazole isomers as the pi-conjugated spacer were designed and simulated using DFT/TD-DFT. The UV-Vis spectra as well as the driving force (ΔG^{inject}) of the systems 1-4 show that these dyes are potentially good photosensitizers. The results show that LUMO of the dyes is greater than the conduction band of TiO_2 indicating that a full charge transfer from these dyes into the conduction band of TiO_2 is thermodynamically allowed. It was also found that the absorption spectra of system-1 to system-4 are red shifted owing to the increased delocalization of the π^* orbital of the conjugated framework . Moreover, there is no significant difference between the LHE of systems 1-4. Therefore, it can be concluded that system-3 with 1,2,4-oxadiazol shows a balance among the different crucial parameters and is expected to be a promising sensitizer in the DSSC field.

8.6.Acknowledgment

The authors would like to acknowledge the support provided by King Abdulaziz City for Science and Technology (KACST) through the Science & Technology Unit at King Fahd University of Petroleum & Minerals (KFUPM) for funding this work through project # 11-ENE1635-04 as part of the National Science, Technology and Innovation Plan. KFUPM is also acknowledged for supporting this research. The authors would like to acknowledge the Center of Research Excellence for Renewable Energy at KFUPM for its support.

8.7.References

[1] Scott RA, editor. Encyclopedia of Inorganic and Bioinorganic Chemistry. Chichester, UK: John Wiley & Sons, Ltd; 2011. doi:10.1002/9781119951438.

[2] Li B, Wang L, Kang B, Wang P, Qiu Y. Review of recent progress in solid-state dye-sensitized solar cells. Sol Energy Mater Sol Cells 2006;90:549–73. doi:10.1016/j.solmat.2005.04.039.

[3] Gong J, Liang J, Sumathy K. Review on dye-sensitized solar cells (DSSCs): Fundamental concepts and novel materials. Renew Sustain Energy Rev 2012;16:5848–60. doi:10.1016/j.rser.2012.04.044.

[4] Millington KR. Encyclopedia of Electrochemical Power Sources. Elsevier; 2009. doi:10.1016/B978-044452745-5.00317-8.

[5] Perlin J. Silicon Solar Cell Turns 50 2004.

[6] Ha E-S, Yoo B, Baik H, Lee Y, Kim K-J. Photocurrent enhancement of dye-sensitized solar cells owing to increased dye-adsorption onto silicon-nanoparticle-coated titanium-dioxide films. Chem Asian J 2012;7:1624–9. doi:10.1002/asia.201101055.

[7] Lu X, Zhou G, Wang H, Feng Q, Wang Z-S. Near infrared thieno[3,4-b]pyrazine sensitizers for efficient quasi-solid-state dye-sensitized solar cells. Phys Chem Chem Phys 2012;14:4802–9. doi:10.1039/c2cp40441a.

[8] Agrawal S, English NJ, Thampi KR, MacElroy JMD. Perspectives on ab initio molecular simulation of excited-state properties of organic dye molecules in dye-sensitised solar cells. Phys Chem Chem Phys 2012;14:12044–56. doi:10.1039/c2cp42031g.

[9] O'Regan B, Grätzel M. A low-cost, high-efficiency solar cell based on dye-sensitized colloidal TiO2 films. Nature 1991;353:737–40. doi:10.1038/353737a0.

[10] Parisi ML, Maranghi S, Basosi R. The evolution of the dye sensitized solar cells from Grätzel prototype to up-scaled solar applications: A life cycle assessment approach. Renew Sustain Energy Rev 2014;39:124–38. doi:10.1016/j.rser.2014.07.079.

[11] Deepak TG, Anjusree GS, Thomas S, Arun TA, Nair S V., Sreekumaran Nair A. A review on materials for light scattering in dye-sensitized solar cells. RSC Adv 2014;4:17615. doi:10.1039/c4ra01308e.

[12] Tian Z, Huang M, Zhao B, Huang H, Feng X, Nie Y, et al. Low-cost dyes based on methylthiophene for high-performance dye-sensitized solar cells. Dye Pigment 2010;87:181–7. doi:10.1016/j.dyepig.2010.03.029.

[13] Panda MK, Ladomenou K, Coutsolelos AG. Porphyrins in bio-inspired transformations: Light-harvesting to solar cell. Coord Chem Rev 2012;256:2601–27. doi:10.1016/j.ccr.2012.04.041.

[14] Hosokawa C, Higashi H, Nakamura H, Kusumoto T. Highly efficient blue electroluminescence from a distyrylarylene emitting layer with a new dopant. Appl Phys Lett 1995;67:3853. doi:10.1063/1.115295.

[15] Jacob J, Sax S, Piok T, List EJW, Grimsdale AC, Müllen K. Ladder-type pentaphenylenes and their polymers: efficient blue-light emitters and electron-accepting materials via a common intermediate. J Am Chem Soc 2004;126:6987–95. doi:10.1021/ja0398823.

[16] Anderson S, Taylor PN, Verschoor GLB. Benzofuran trimers for organic electroluminescence. Chemistry 2004;10:518–27. doi:10.1002/chem.200305284.

[17] High-Efficiency Poly(p-phenylenevinylene)-Based Copolymers Containing an Oxadiazole Pendant Group for Light-Emitting Diodes n.d. http://pubs.acs.org/doi/pdf/10.1021/ja036955+ (accessed December 31, 2014).

[18] Dessì A, Barozzino Consiglio G, Calamante M, Reginato G, Mordini A, Peruzzini M, et al. Organic Chromophores Based on a Fused Bis-Thiazole Core and Their Application in Dye-Sensitized Solar Cells. European J Org Chem 2013;2013:1916–28. doi:10.1002/ejoc.201201629.

[19] Dessì A, Calamante M, Mordini A, Peruzzini M, Sinicropi A, Basosi R, et al. Organic dyes with intense light absorption especially suitable for application in thin-layer dye-sensitized solar cells. Chem Commun (Camb) 2014;50:13952–5. doi:10.1039/c4cc06160h.

[20] Wang C, Jung G-Y, Hua Y, Pearson C, Bryce MR, Petty MC, et al. An Efficient Pyridine- and Oxadiazole-Containing Hole-Blocking Material for Organic Light-Emitting Diodes: Synthesis, Crystal Structure, and Device Performance. Chem Mater 2001;13:1167–73. doi:10.1021/cm0010250.

[21] Panchamukhi SI, Belavagi N, Rabinal MH, Khazi IA. Synthesis and optoelectronic properties of symmetrical thiophene based 2,5-disubstiuted 1,3,4-oxadiazoles: highly fluorescent materials for OLED applications. J Fluoresc 2011;21:1515–9. doi:10.1007/s10895-011-0838-y.

[22] Zhu W, Yao R, Tian H. Synthesis of novel electro-transporting emitting compounds. Dye Pigment 2002;54:147–54. doi:10.1016/S0143-7208(02)00039-6.

[23] New Series of Blue-Emitting and Electron-Transporting Copolymers Based on Fluorene n.d. http://pubs.acs.org/doi/pdf/10.1021/ma011593g (accessed December 31, 2014).

[24] Chung S-J, Kwon K-Y, Lee S-W, Jin J-I, Lee CH, Lee CE, et al. Highly Efficient Light-Emitting Diodes Based on an Organic-Soluble Poly(p-phenylenevinylene) Derivative Carrying the Electron-Transporting PBD Moiety. Adv Mater 1998;10:1112–6. doi:10.1002/(SICI)1521-4095(199810)10:14<1112::AID-ADMA1112>3.0.CO;2-P.

[25] Skene WG, Pérez Guarìn SA. Spectral characterization of thiophene acylhydrazides. J Fluoresc 2007;17:540–6. doi:10.1007/s10895-007-0209-x.

[26] Density functional theory characterization and design of high-performance diarylamine-fluorene dyes with different p spacers for dye-sensitized solar cells n.d. http://pubs.rsc.org/en/content/articlepdf/2012/jm/c1jm13028e (accessed December 31, 2014).

[27] Wang J, Bai F-Q, Xia B-H, Feng L, Zhang H-X, Pan Q-J. On the viability of cyclometalated Ru(II) complexes as dyes in DSSC regulated by COOH group, a DFT study. Phys Chem Chem Phys 2011;13:2206–13. doi:10.1039/c0cp01556c.

[28] Wang J, Li H, Ma N-N, Yan L-K, Su Z-M. Theoretical studies on organoimido-substituted hexamolybdates dyes for dye-sensitized solar cells (DSSC). Dye Pigment 2013;99:440–6. doi:10.1016/j.dyepig.2013.05.027.

[29] Fan W, Tan D, Deng W-Q. Acene-modified triphenylamine dyes for dye-sensitized solar cells: a computational study. Chemphyschem 2012;13:2051–60. doi:10.1002/cphc.201200064.

[30] Sang-aroon W, Saekow S, Amornkitbamrung V. Density functional theory study on the electronic structure of Monascus dyes as photosensitizer for dye-sensitized solar cells. J Photochem Photobiol A Chem 2012;236:35–40. doi:10.1016/j.jphotochem.2012.03.014.

[31] Zarate X, Schott E, Gomez T, Arratia-Pérez R. Correction to “Theoretical Study of Sensitizer Candidates for Dye-Sensitized Solar Cells: Peripheral Substituted Dizinc Pyrazinoporphyrazine–Phthalocyanine Complexes.” J Phys Chem A 2013;117:4996–4996. doi:10.1021/jp404833n.

[32] Zhang J, Kan Y-H, Li H-B, Geng Y, Wu Y, Su Z-M. How to design proper ?-spacer order of the D-?-A dyes for DSSCs? A density functional response. Dye Pigment 2012;95:313–21. doi:10.1016/j.dyepig.2012.05.020.

[33] Rocca D, Gebauer R, De Angelis F, Nazeeruddin MK, Baroni S. Time-dependent density functional theory study of squaraine dye-sensitized solar cells. Chem Phys Lett 2009;475:49–53. doi:10.1016/j.cplett.2009.05.019.

CHAPTER 9

CONCLUSINS & RECOMMENDATIONS

9.1. Conclusion

Narrow absorption spectra and/or low absorption intensity of the sensitizers and the recombination of injected electrons with the electrolyte are the two major causes of the low conversion efficiency of DSSCs. In this work, the co-sensitization strategy was applied to obtain the broader and a more intense absorption band. While hybrid composites of MWCNTs and graphene micro-platelets with TiO_2 were used to reduce the dark current.

The mixed solution of N719 and N3 in methanol was used for the co-sensitization of the photoanodes of DSSCs. More intense and broader absorption spectrum of the co-sensitized TiO_2 film was observed than the absorption spectra of the individual N719 and N_3 dyes. This is because the CNTs may exhibit photosensitizing properties, thus extending photovoltaic properties into the visible spectrum. The results indicate that the power conversion efficiency of DSSC based on 0.4N719+0.1N_3 is 17% and 11% higher than based on the individual dyes N719 and N3 respectively. Moreover, the cell efficiency of the DSSC with a molar ratio of N3/N719 = 0.1/0.4 was further improved to 4.46% by the incorporation of MWCNTs in TiO_2. Optimum concentration (0.04%) of CNTs in photoanode does not affect the transparency of TiO_2 layer, while significantly increases the PCE of DSSC.

It has been observed that the enhancement of PCE due to CNTs is limited by poor contact between CNTs and TiO_2. Two dimensional Graphene nano carbon material was also introduced to prepare the hybrid film. The incorporation of graphene in TiO_2 slowing the recombination of photogenerated electrons, extending the excitation wavelength and increasing the surface-adsorbed amount of dye. It was examined that the dispersion of small amount of graphene in TiO_2 can significantly improve the photo conversion efficiency of DSSCs. Optimum concentration (0.09%) of graphene in photoanode does not affect the transparency of TiO_2 layer, while significantly increases the PCE of DSSC, with a maximum value of 4.12%.

DFT and time dependent TD-DFT were also employed to investigate the thermodynamic aspects of charge transport processes involved in DSSCs. Hybrid functions with triple-ζ polarization basis function were employed to simulate the geomatries of sensitizers. While, UV-Vis spectra of sensitizers and dye anchored to TiO_2 were simulated in different solvents. The conductor-like screening model (COSMO) was selected to take the solvent effects into account. The excitation energies were examined using TD-DFT and statistical average of orbital potentials (SAOP) model including the salvation effects. The simulated results were in good agreement with the experimental values. Thus, hybrid functions with triple-ζ polarization basis function and COSMO solvation model with SOAP function were appropriate for comuting the HOMOs, LUMOs, band gap, free energy of electron injection, absorption specta and LHE of photosensitizers.

The output of our research work is ten publications, four of them have been accepted and six are under review. We also have also filed two patents. The detail of manuscripts and patents are

1. **Umer Mehmood**, S Rahman, K Harrabi, IA Hussein, BVS Reddy, Recent Advances in Dye Sensitized Solar Cells, Advances in Materials Science and Engineering, Volume 2014 (2014),

2. **Umer Mehmood** ; Ibnelwaleed A. Hussein ; Khalil Harrabi ; Belum V. S. Reddy, Density functional theory study on dye-sensitized solar cells using oxadiazole-based dyes, *J. Photon. Energy*. 5(1), 053097 (Feb 24, 2015)

3. **Umer Mehmood**, Ibnelwaleed A Hussein, Muhammad Daud, Shakeel Ahmed, Khalil Harrabi, Theoretical study of benzene/thiophene based photosensitizers for dye sensitized solar cells (DSSCs), Dyes and Pigments, 2015

4. **Umer Mehmood**, Khalil Harrabi, M. B. Mekki, Shakeel Ahmed, Nouar tabet, Ibnelwaleed A. Hussein, Hybrid TiO2-multi wall carbon nanotubes (MWCNTs) photoanodes for efficient dye sensitized solar cells (DSSCs), Solar Energy Materials & Solar Cells

5. **Umer Mehmood**, Shakeel Ahmed**,**Ibnelwaleed A. Hussein, Khalil Harrabi, Dye sensitizedsolar cells based on TiO_2 – graphene nanocomposite photoanode, Organic Electronics (under review)

6. **Umer Mehmood**, Shakeel Ahmed,Ibnelwaleed A. Hussein, Khalil Harrabi, M. B. Mekki, Enhancing light conversion efficiency of dye-sensitized solar cells using TiO2- MWCNT nanocomposite photoanode, Electrochemica Acta (under review)

7. **Umer Mehmood**, Shakeel Ahmed,Ibnelwaleed A. Hussein, Khalil Harrabi, Co-sensitization of MWCNTs-TiO2 hybrid anode by N3 and N719 ruthenizers for efficient dye-sensitized solar cells, Organic Electronics (under review)

8. **Umer Mehmood** ; Ibnelwaleed A. Hussein ; Khalil Harrabi Shakeel Ahmed, Densityfunctional theory (DFT) study on the electronic structures of oxadiazole based dyes as photosensitizer for dye sensitized solar cells (DSSCs), Advances in Materials Science and Engineering (under review)

9. **Umer Mehmood**, Amir Al-Ahmed, Ibnelwaleed A. Hussein, Recent Advances in Polythiophene Based Photovoltaic Devices, Renewable & Sustainable Energy Reviews (under review)

10. **Umer Mehmood** ; Ibnelwaleed A. Hussein ; Khalil Harrabi Shakeel Ahmed Improving the efficiency of Dye sensitized solar cells by TiO 2 – graphene nanocomposite photoanode, Journal of Nanomaterials (Under Review)

Patents

1. Oxadiazole based photosensitizers for dye-sensitized solar cells (US14/720287)
2. Organic dyes incorporating the oxadiazole moiety for efficient dye-sensitized solar cells (US14/718040)

9.2. Recommendations

Low efficiency and low stability are the major challenges for the commercial growth of DSSCs. The following factors are responsible for the low efficiency and stability of DSSCs,

1) Non-optimized dark current
2) Poor performance of dyes in the NIR region
3) Poor contact between the electrodes
4) High volatility and high viscosity of electrolytes
5) Degradation of electrolyte properties due to UV absorption of light

Following steps can be recommended in order to further enhance the efficiency and stability of DSSCs,

1) Improvement in the morphology of semiconductors to reduce dark current
2) Improvement in the dye design to absorb light NIR region
3) Develop low volatile and less viscous electrolyte to improve the charge transfer rate.
4) Improvement in mechanical contact or adhesion between the two electrodes
5) Use of additives for dyes and electrolytes that enhance their properties.

Curriculum Vitae

Umer Mehmood

Department of Chemical Engineering,
King Fahd University of Petroleum & Minerals,
Dhahran, Kingdom of Saudi Arabia

Phone (M): +966 532432097
Phone (M): +92 3324707967
Nationality: Pakistani
Date of birth: 06-09-1984
Email: organicchemistry2@gmail.com

EDUCATION

***Ph.D* :** Chemical Engineering, 2011-2015
King Fahd University of Petroleum & Minerals, Saudi Arabia
Thesis: Synthesis and Characterization of Dye Sensitized Materials for Solar Cell Applications

***M.Sc* :** Polymer Engineering (First position holder in department), 2009-2011
University of Engineering & Technology, Lahore, Pakistan
Thesis: Recycling of mixed plastics waste

***B.Sc*:**.Chemical Engineering (Polymer) (Third position holder in department), 2004-2008
University of Engineering & Technology, Lahore, Pakistan

RESEARCH INTERESTS

- Solar cells
- Conductive polymers
- Qunatum Mechanical Modeling (DFT/TD-DFT)
- Process Simulation

TEACHING INTERESTS

- Transport Phenomena
- Heat Transfer
- Reaction Engineering
- Mass Transfer
- Poymer Material Testing and Characterization

WORK EXPERIENCE

King Fahd University of Petroleum & Minerals, Saudi Arabia
Lecturer-B Sep 2011-Present

- Teach Chemical Engineering Laboratory (CHE-409) to undergraduate students for two years
- Teach Chemical Engineering Laboratory (CHE-309) to undergraduate students for one year
- Write technical reports for the projects to be submitted to King Abdulaziz City fo Science and Technology (KACST)
- Work on the development of dye sensitized solar cells as part of my PhD thesis
- Teaching assistant in various undergraduate courses

University of Engineering & Technology, Lahore, Pakistan
Lecturer June 2009-Sep 2011

- Taught Various undergraduate courses,which include

- ✓ Transport Phenomena
- ✓ Heat Transfer
- ✓ Mass Transfer
- ✓ Reaction Engineering

- Testing of polymer materials

- Involved in developing different laboratories

INTERSHIPS and TRAINING

- BASF, Pakistan (4 weeks)
- Engro Poymer (1 week)
- Sui Northern Gas Pipelines Limited, Pakistan (4 weeks)

COMPUTER SKILLS

- MATLAB
- ADF (Amsterdam Density Functional program)
- Aspen HYSYS
- Aspen Plus
- MS office

LANGUAGE SKILLS

- English-Excellent oral and written skills
- Urdu-Excellent oral and written skills

JOURNAL PUBLICATIONS

1. **Umer Mehmood**, S Rahman, K Harrabi, IA Hussein, BVS Reddy, Recent Advances in Dye Sensitized Solar Cells, Advances in Materials Science and Engineering, Volume 2014 (2014),

2. **Umer Mehmood** ; Ibnelwaleed A. Hussein ; Khalil Harrabi ; Belum V. S. Reddy, Density functional theory study on dye-sensitized solar cells using oxadiazole-based dyes, *J. Photon. Energy*. 5(1), 053097 (Feb 24, 2015)

3. **Umer Mehmood**, Ibnelwaleed A Hussein, Muhammad Daud, Shakeel Ahmed, Khalil Harrabi, Theoretical study of benzene/thiophene based photosensitizers for dye sensitized solar cells (DSSCs), Dyes and Pigments, 2015

4. **Umer Mehmood**, Khalil Harrabi, M. B. Mekki, Shakeel Ahmed, Nouar tabet, Ibnelwaleed A. Hussein, Hybrid TiO2-multi wall carbon nanotubes (MWCNTs) photoanodes for efficient dye sensitized solar cells (DSSCs), Solar Energy Materials & Solar Cells

5. **Umer Mehmood**, Shakeel Ahmed**,**Ibnelwaleed A. Hussein, Khalil Harrabi, Dye sensitizedsolar cells based on TiO_2 – graphene nanocomposite photoanode, Organic Electronics (under review)

6. **Umer Mehmood**, Shakeel Ahmed,Ibnelwaleed A. Hussein, Khalil Harrabi, M. B. Mekki, Enhancing light conversion efficiency of dye-sensitized solar cells using TiO2- MWCNT nanocomposite photoanode, Journal of nanomaterials (under review)

7. **Umer Mehmood**, Shakeel Ahmed,Ibnelwaleed A. Hussein, Khalil Harrabi, Co-sensitization of MWCNTs-TiO2 hybrid anode by N3 and N719 ruthenizers for efficient dye-sensitized solar cells, Solar Energy (under review)

8. **Umer Mehmood** ; Ibnelwaleed A. Hussein ; Khalil Harrabi Shakeel Ahmed, Densityfunctional theory (DFT) study on the electronic structures of oxadiazole based dyes as photosensitizer for dye sensitized solar cells (DSSCs), Advances in Materials Science and Engineering (under review)

9. **Umer Mehmood**, Amir Al-Ahmed, Ibnelwaleed A. Hussein, Recent Advances in Polythiophene Based Photovoltaic Devices, Renewable & Sustainable Energy Reviews (under review)

10. M. Ramana Reddy, S. Gopal Reddy and B. V. Subba Reddy, **Umer Mehmood**,Ibnelwaleed A. Hussein, Khalil Harrabi , $Cu(OTf)_2$-catalyzed synthesis of 2,5-disubstituted oxazoles from α-diazoketones and its application to texamine and balsoxin alkaloids, Synthesis (under review)

11. G. Berdiyorov, K. Harrabi, **Umer Mehmood**, F. M. Peeters, N. Tabet, J. Zhang, I. A. Hussein, 3 and M. A. McLachlan , Derivatization and diffusive motion of molecular fullerenes: ab initio and atomistic simulations, Journal of Applied physics (Under Review)

12. GM Mamoor, N Qamar, **Umer Mehmood**, MS Kamal , Effect of Short Glass Fiber on Mechanical and Rheological Properties of PMMA/SBR Vulcanizate,Chemical Engineering Research Bulletin, 2009
13. **Umer Mehmood** ,GM Mamoor, Wahab Shahid, Amir Mushtaq, Umer Amjad, Recycling of Mixed Plastics Waste Containing Polyethylene, Polyvinylchloride and Polyethylene Terephthalate, Chemical Engineering Research Bulletin 16(2013) 25-32

Patents

1. Oxadiazole based photosensitizers for dye-sensitized solar cells (Docket No. 442623US)
2. Organic dyes incorporating the oxadiazole moiety for efficient dye-sensitized solar cells (Docket No. 442623US)